Architecture des réseaux de distribution en présence de production décentralisée. Planification sous incertitudes et modes d'exploitation décentralisés

Alireza Soroudi

UNIVERSITÉ DE GRENOBLE

THÈSE

Pour obtenir le grade de

DOCTEUR DE L'UNIVERSITÉ DE GRENOBLE

Spécialité : **Génie électrique**

Arrêté ministériel : 7 août 2006

Présentée par

« Alireza / SOROUDI»

Thèse dirigée par « **Nouredine, HADJSAID**» et « **Mehdi, EHSAN**»
Codirigée par « **Raphael/ CAIRE** »

préparée au sein du **Laboratoire G2elab**
dans **l'École Doctorale Electronique, Electrotechnique, Automatique & Traitement du Signal**

Architecture des réseaux de distribution en présence de production décentralisée - planification sous incertitudes et modes d'exploitation décentralisés

Thèse soutenue publiquement le **« 4 Oct 2011»**,
Devant le jury composé de :

Française, **Nouredine, HADJSAID**
Grenoble France, Grenoble INP, (Membre)
Française, **Raphael CAIRE**
Grenoble France, Grenoble INP, (Membre)
Iranien, Mehdi, EHSAN
Téhéran Iran, Sharif university of technology (Membre)
Iranien, Mahmoud, FOTUHI FIROUZABAD
Téhéran Iran, Sharif university of technology (Président)
Iranien, Mehdi, VAKILIAN
Téhéran Iran, Sharif university of technology (Rapporteur)
Iranien, Mehrdad , ABEDI
Téhéran Iran, Amirkabir university of technology (Membre)
Iranien, Ashkan , RAHIMIKIAN
Téhéran Iran, Tehran University (Membre)
Française, **Shahrokh SAADATE**
Vandoeuvre-Lès-Nancy cedex FRANCE Université Henri Poincaré Nancy1, (Rapporteur)

To my mother ,Simin, my father ,Shahryar and my sister ,Mona

Table of Contents

List of Figures

List of Tables

Acknowledgments

I would like to thank my advisor Dr. Mehdi Ehsan, for all of his help and guidance in the research and development of this thesis. I appreciate his skill and enthusiasm as a teacher and mentor; I also thank him for the opportunity to study and perform research at Sharif University of Technology. I would also like to thank Dr. Hadjsaid and Dr. Caire, my advisors in Grenoble- Institute National Polytechnique. My education at Grenoble-INP has encompassed much more than the field of power engineering. Their comments and suggestions throughout the development of this work have been invaluable and are greatly appreciated. I appreciate their time and commitment to my research activities and this work.

Vita

1981	July 5, Born, Tehran, Iran
2003	BSc., Electrical Engineering, Sharif University of Technology
2005	MSc., Electrical Engineering, Sharif University of Technology
2011	PhD., Electrical Engineering, Sharif University of Technology and Grenoble Institute National Polytechnique

Publications

1-Possibilistic Evaluation of Distributed Generations Impacts on Distribution Networks A. Soroudi, M. Ehsan, Raphael Caire, Nouredine Hadjsaid, IEEE Transactions on Power Systems

2- A Probabilistic Modeling of Photo Voltaic Modules and Wind Power Generation Impact on Distribution Networks A. Soroudi, M. Aien, M. Ehsan, IEEE Systems Journal special issue Integration of Intermittent Renewable Energy Resources into Power Grid.

3- Hybrid Immune-Genetic Algorithm Method for Benefit Maximization of DNOs and DG Owners in a Deregulated Environment A. Soroudi, M. Ehsan,Raphael Caire, Nouredine Hadjsaid IET Generation, Transmission & Distribution

4- A distribution network expansion planning model considering distributed generation options and techno-economical issues. A. Soroudi, M. Ehsan, Energy, Elsevier, Volume 77, Issue 8, June 2010, Pages 1038-1046.

5- A practical eco-environmental distribution network planning model including fuel cells and non-renewable distributed energy resources Alireza Soroudi, Mehdi Ehsan, Hamidreza

Zareipour, Renewable Energy, Elsevier, Volume 36, Issue 1, January 2011, Pages 179-188, ISSN 0960-1481

6- A possibilistic-probabilistic tool for evaluating the impact of stochastic renewable and controllable power generation on energy losses in distribution networks–A case study. A. Soroudi, M. Ehsan, Renewable and Sustainable Energy, Elsevier, Volume 77, Issue 8, June 2010, Pages 1038-1046.

7- Efficient immune-GA method for DNOs in sizing and placement of distributed generation units A. Soroudi, M. Ehsan, European Transactions on Electrical Power, Volume 21, Issue 3, pages 13611375, April 2011

8- Multi-Objective Planning Model for Integration of Distributed Generations in Deregulated Power Systems A. Soroudi, M. Ehsan, Iranian Journal of Science and Technology, Volume 34, No B3, PP. 307-324.

9- Imperialist Competition Algorithm for Distributed Generation Connections A. Soroudi, M. Ehsan, IET Generation, Transmission & Distribution

10- Probabilistic Dynamic Multi-objective Model for Renewable and Non-renewable DG Planning A. Soroudi, M. Ehsan, IET Generation, Transmission & Distribution

Abstract of the Dissertation

Multi Objective Distributed Generation Planning in a Flexible Environment

by

Alireza Soroudi

PhD candidate in Electrical Engineering

Sharif University of Technology, 2011

Supervised by :

Dr. Mehdi Ehsan

Dr. Nouredin Hadjsaid

Dr Raphael Caire

The process of deregulation that has involved electricity markets has introduced several new interesting research topics in power system area. This thesis addresses one of the fascinating issues among them: the study of distributed generation both renewable and conventional integration in distribution networks. From the distribution network operator (DNO)'s point of view, it is interesting to develop a comprehensive methodology which considers various distributed generation technologies as an option for supplying the demand. In this thesis, the planning problem has been multi-objectively modeled. This will help the planner in decision making while knowing the trade-offs between the objective functions. In order to find the Pareto optimal front of the problem a hybrid Genetic-Immune algorithm is proposed. The fuzzy satisfying method is used to find the final solution. Various objectives like cost, active losses, emission and the technical constraint satisfaction have been taken into account. The decision variables are the distribution network reinforcement strategies and also the investment decisions regarding DG units, in case where DNO can invest in DG units too. Another aspect which makes the proposed models more flexible, is considering the uncertainties of the input parameters. The uncertainties of input data have been treated in three different ways namely, probabilistic, possibilistic and finally mixed possibilistic-probabilistic methods.

In this thesis, two types of models have been developed: centralized and unbundled DG

planning model. In both models, the DNO is responsible to provide a reliable and efficient network for his costumers in its territory. In centrally controlled planning context, the DNO is authorized to make investment in DG units. In this model, the optimal size, number of DG units, location, DG technology and timing of investment in both DG units and network components are determined. The developed model will not only be useful in the centrally controlled planning context but also is applicable to other power markets that need to assess, monitor and guide the decisions of DG developers.

In unbundled DG planning model, the DNO is not authorized to make investment decisions in DG options. The decision variables of DNO are limited to feeder/substation expansion/reinforcement, capacitor placement, network reconfiguration and smart grid technologies.

Abbreviations

AHP	**A**nalytical **H**ierarchy **P**rocess
CHP	**C**ombined **H**eat and **P**ower
DGIC	**D**istributed **G**eneration **I**nvestment **C**ost
DGOC	**D**istributed **G**eneration **O**perating **C**ost
DNO	**D**istribution **N**etwork **O**perator
DG	**D**istributed **G**eneration
DGO	**D**istributed **O**perator/**O**wner
ESU	**E**nergy **S**torage **U**nit
FTN	**F**uzzy **T**rapezoidal **N**umber
FRC	**F**eeder **R**einforcement **C**ost
FC	**F**uel **C**ell
GA	**G**enetic **A**lgorithm
IA	**I**mmune **A**lgorithm
MCS	**M**onte **C**arlo **S**imulation
MT	**M**icro **T**urbine
MCDM	**M**ulti **C**riteria **D**ecision **M**aking
MODM	**M**ulti **O**bjective **D**ecision **M**aking
MADM	**M**ulti **A**ttribute **D**ecision **M**aking
NSGA	**N**one dominated **S**orting **G**enetic **A**lgorithm
NPV	**N**et **P**resent **V**alue
PDF	**P**robability **D**ensity **F**unction
PEM	**P**oint **E**stimate **M**ethod
PV	**P**hoto **V**oltaic cell
SRC	**S**ubstation **R**einforcement **C**ost
TGC	**T**otal **G**rid **C**ost
WT	**W**ind **T**urbine

Symbols

$P^{D}_{i,t,dl,s}$	Active power demand in bus i, in year t, demand level dl and state s
$P^{grid}_{t,dl,s}$	Active power purchased from grid in year t, demand level dl and state s
$P^{dg}_{i,t,dl,s}$	Active power injected by a dg in bus i, in year t, demand level dl and state s
$S^{grid}_{t,dl,s}$	Apparent power imported from grid in year t, demand level dl and state s
$S^{dg}_{i,t,dl,s}$	Apparent power of dg installed in bus i, in year t, demand level dl and state s
$I_{\ell,t,dl,s}$	Current magnitude of ℓ^{th} feeder in year t, demand level dl and state s
v^{cut}_{in}	Cut-in speed of wind turbine
v^{cut}_{out}	Cut-out speed of wind turbine
C_{ℓ}	Cost of reinforcement of feeder ℓ
C_{tr}	Cost of investment in transformer
d	Discount rate
$\mu^{V}_{i,t,dl,s}$	Degree of voltage constraint satisfaction for bus i, in year t, demand level dl and state s
$\mu^{V}_{i,t}$	Degree of voltage constraint satisfaction for bus i, in year t
μ^{V}_{t}	Degree of voltage constraint satisfaction for whole system in year t
$\mu^{I}_{\ell,t,dl,s}$	Degree of thermal constraint satisfaction for feeder ℓ in year t, demand level dl and state s
$\mu^{I}_{\ell,t}$	Degree of thermal constraint satisfaction for feeder ℓ in year t
μ^{I}_{t}	Degree of thermal constraint satisfaction for whole system in year t
$\mu^{S^{grid}}_{t,dl,s}$	Degree of thermal constraint satisfaction for substation in year t and state s
$\mu^{S^{grid}}_{t}$	Degree of overall thermal constraint satisfaction for substation in year t
$\mu^{f_k(X_n)}$	Degree of minimization satisfaction of k^{th} objective function by solution X_n
$S^{D}_{i,t,dl,s}$	Demand in bus i, year t, demand level dl and state s
EP^{λ}_{s}	Electricity price in state s
$E_{grid/dg}$	Emission factor of the grid/dg
FN_n	Front number to which n^{th} solution belongs
GD_n	Global Diversity of n^{th}solution
γ^{ℓ}_{t}	Investment decision in feeder ℓ, in the year t

$\xi_{i,t}^{dg}$	Investment decision for DG technology dg in bus i, in the year t
ψ_t^{tr}	Investment decision in transformer, in the year t
IC_{dg}, OC_{dg}	Investment and operating cost of a dg
d_ℓ	Length of feeder ℓ in km
LD_n^k	Local diversity of n^{th}solution in k^{th} objective function
MD_k	Maximum difference between the values of k^{th} objective function, regarding all solutions
$\overline{S}_{lim}^{dg}$	Maximum operating limit of a dg
$P_{i,t,dl,s}^{net}$	Net active power injected to bus i, in year t, demand level dl and state s
$Q_{i,t,dl,s}^{net}$	Net reactive power injected to bus i, in year t, demand level dl and state s
N_b	Number of buses in the network
N_p	Number of population
N_ℓ	Number of feeders in the network
N_o	Number of objective functions
N_J	Number of combined states
N_s	Number of reduced states
T	Planning/evaluation horizon
ρ	Peak price of energy purchased from the grid
$S_{i,peak}^D$	Peak demand in bus i, in state s
$\lambda_{dl,s}$	Percent of peak electricity price in state s and demand level dl
$D_{dl,s}$	Percent of peak electricity demand in state s and demand level dl
wp_s	Percent of rated capacity of installed wind turbine in state s
$P_{i,r}^w$	Rated power of installed wind turbine
$Q_{i,t,dl,s}^{dg}$	Reactive power injected by a dg in bus i, year t, demand level dl and state s
$Q_{i,t,dl,s}^D$	Reactive power demand in bus i, year t, demand level dl and state s
SF_n	Pseudo fitness of n^{th} particle
$prob_s^l$	Probability of load state s
$prob_s^\lambda$	Probability of electricity price state s
$prob_s^w$	Probability of wind speed state s
$prob_s^c$	Probability of combined state s
ϵ_D	Rate of demand growth

v_{rated}	Rated speed of wind turbine
c	Scale factor of Rayleigh PDF of wind speed
TD_t	Technical dissatisfaction in year t
GC	Total cost paid to grid
DGIC	Total Investment cost of DG units
DGOC	Total operation cost of DG units
FC	Total cost of feeder reinforcement
SC	Total cost of transformer investment
$\overline{S}^{tr}_{safe,t}, \overline{S}^{tr}_{crit,t}$	Upper safe and critical values of operation thermal limits of substation
$\overline{I}^{safe,t}_{\ell}, \overline{I}^{crit,t}_{\ell}$	Upper safe and critical values of operation thermal limits of feeders
$V^{max}_{safe}, V^{min}_{safe}$	Upper and lower safe operation limits of voltage
$V^{max}_{crit}, V^{min}_{crit}$	Upper and lower critical operation limits of voltage
$V_{i,t,dl,s}$	Voltage magnitude in bus i, year t, demand level dl and state s
$\delta_{i,t,dl,s}$	Voltage angle in bus i, year t, demand level dl and state s
v_s	Wind speed in state s

CHAPTER 1

Introduction

1.1 Thesis Motivation

Distributed Generation (DG) is an electric power source connected directly to the distribution network. The capacity of these units are defined differently in the literature. For example in Electric Power Research Institute (EPRI) it is defined below the 50 MW, according to the Gas Research Institute it is defined below the 25 MW and finally the International Conference on Large High Voltage Electric Systems (CIGRE') defines DG as smaller than $50 \mapsto 100$ MW [1]. The DG units have been, in the last decade, in the spotlight of the power industry and scientific community and constitute a new paradigm for on-site electric power generation. There are three key factors driving this change namely, environmental concerns, technological innovation and new government policies [2]. The power injection of DG units into distribution network may change the power flow in distribution feeders, so the size, number of DG modules, location, technology and timing of investment have decisive impacts on the grid and their potential benefits. Due to the important policy implications, determination of optimal DG timing, placement and sizing has been of keen interest to Distribution Network Operators (DNO), DG developers and regulators, to increase their benefits, and regulators, to better understand the distribution network behavior and set up corresponding regulations to provide better services to customers and encourage fair competition. In power systems which are not fully unbundled, the DG investment are done by DNOs so the decisions related to sizing, location, and timing of investment are made by this entity. On the other hand, in an open access environment, the decisions related to DG investment/operation are taken by DG Owners/operators (DGOs) and maintaining the reliability and efficiency of the network is the duty of DNOs. Although many previous works have attacked the DG planning problem

but few of them have focused on the interaction between the conflicting or converging objectives of DGO and DNO. Thus, there is a clear need to enhance the current DG planning methodologies to include an appropriate treatment of various DG technologies, uncertainty handling and different objectives of DGO and DNOs. A win-win strategy is needed which not only promotes DG investment for DGOs but also does not impose additional costs to DNOs (compared to the case when no DG exists in the network). These needs motivate the work proposed in this thesis.

1.2 Thesis Objectives

The work presented in this thesis, analyzes the DG Integration in distribution networks. Two regulatory frameworks have been analyzed namely, regulated DG investment and unbundled DG investment. The multi objective DG integration in the distribution network which is investigated from a planning perspective in centrally controlled DG investment. The objectives of the thesis, in centrally controlled DG investment framework, are outlined as follows: To develop a comprehensive modeling framework for DNO which can optimize different objective functions considering the technical constraints, in order to achieve the full benefits of DG units. The proposed framework should have the following characteristics:

1. Simultaneous modeling of DG and distribution network investment by determining the optimal sizing and location of DG units and also the reinforcement strategies of distribution network (including feeders and substation)

2. Uncertainty modeling of input data

3. Different DG technology modeling (including renewable and conventional technologies)

4. Multi-objective optimization modeling capability for the formulated problem

The main objectives of the thesis, in unbundled DG investment framework, are outlined as follows:

1. To investigate the impact of DG units on distribution network operation when the investments/operation are done by DG developers/operators. The uncertainties associated to DG investment/operation should be taken into account. The proposed model should be able to handle the uncertainties which may have probabilistic, possibilistic or mixed probabilistic-possibilistic nature.

2. To propose a win-win strategy which not only promotes DG investment for DGOs but also does not impose additional costs to DNOs (compared to the case when no DG exists in the network). This strategy should be able to consider various DG technologies, uncertainty handling and different objectives of DGO and DNOs.

1.3 Thesis Organization

This thesis consists of seven chapters. Chapter 2 presents the literature reviews on the main topics of the thesis. Chapter 3 provides a review of multi criteria decision making techniques. Chapter 4 provides a review of uncertainty handling techniques. Chapter 5 presents the model proposed for integration of DG units under centrally controlled investment. Chapter 6 presents the model proposed for DG integration under unbundling rules. Chapter 7 provides a summary of this thesis and recommendations for future work.

1.4 Summary of Contents

Chapter 2 makes a modest attempt to present a review of literature on the published work related to the work of this thesis. This chapter is divided into five sections. Section 2.2 briefly reviews the DG technologies. Section 2.3 deals with the technical, economical and environmental impacts of DG units in distribution networks. The DG integration models are discussed in Section 2.4. Finally Section 2.5 presents the uncertainty modeling methods in DG impact assessments.

Chapter 3 presents the various Multi Criteria Decision Making (MCDM) methods including Multi Objective Decision Making (MODM) and Multi Attribute Decision Making (MADM). In this chapter, the proposed hybrid Immune-GA method for obtaining the

Pareto optimal fronts and also the fuzzy satisfying method used for selection of the final solution is presented.

Chapter 4 presents the used/proposed methods for uncertainty modeling in this thesis. Section 4.2.1 describes the probabilistic methods including Monte Carlo and Two Point Estimate methods. Section 4.3 describes the fuzzy modeling of uncertainties. Section 4.4 proposes a model for mixed probabilistic-possibilistic uncertainties. The Information Gap Decision Theory (IGDT) method is also described in Section 4.5.

Chapter 5 presents a comprehensive dynamic multi-objective model for DG integration in distribution networks. The proposed two-stage algorithm finds the non-dominated solutions by simultaneous minimization of the defined objective functions in the first stage and uses a fuzzy satisfying method to select the best solution from the candidate set in the second stage. The new planning model is applied to a distribution network and its flexibility is demonstrated through different case studies. The solution set provides the planner with an insight into the problem and enables him to choose the best solution according to planning preferences.

In Chapter 6, it is assumed that the DNO is not authorized to invest in DG units and he should just screen and guide, "through incentives", the activities of DG developers. In this chapter, a long-term dynamic multi-objective model is presented for planning of distribution networks regarding the benefits of DNO and DGOs as described in section 6.2. The proposed model simultaneously optimizes two objectives, namely the benefits of DNO and DGO and determines the optimal schemes of sizing, placement and specially the dynamics (i.e., timing) of investments on distributed generation units and network reinforcements over the planning period. The proposed model also considers the uncertainty of electric load, electricity price and wind turbine power generation using the point estimate method. The effect of benefit sharing is investigated for steering the decisions of DGOs. In section 6.3, three different methods of uncertainty handling in DG impact assessment on operating of distribution networks are described.

CHAPTER 2

Literature Review

2.1 Introduction

With the deregulation of power system, the distribution networks are facing various challenges due to several factors. One of the most important factor is the increasing penetration of DG units, both renewable and conventional technologies [3]. The solution to the problem treated in this thesis relies on a number of supporting problems. This chapter offers a review of literature in the following areas:

1. Distributed Generation technologies
2. DG impacts on distribution networks
3. DG integration models in distribution networks
4. Uncertainty modeling in DG impact assessment

2.2 Distributed Generation Technologies

2.2.1 Renewable DG technologies

The Renewable energy technologies will inevitably dominate the fossil based energy supply systems in the near future [4]. There are various renewable technologies available for electricity generation, like: wind turbine, photovoltaic cells, bioenergy, fuel cells, small hydro power, ocean energy and geothermal energy. In this section some of them are described as follows:

2.2.1.1 Wind Turbine

Windmills have been used for at least 3000 years, mainly for grinding grain or pumping water [5]. In contrary to windmills which convert the wind power into the mechanical power, a wind turbine, is a machine which converts the wind energy into electricity. The generation pattern of a wind turbine highly depends on the wind speed in the site. The variation of wind speed, i.e. v, can be modeled using a Weibull [6] PDF and its characteristic function which relates the wind speed and the output of a wind turbine [7].

$$PDF(v) = (\frac{k}{c})(\frac{v}{c})^{k-1} exp(-(\frac{v}{c})^k) \tag{2.1}$$

Where, k is the shape factor and c is the scale factor of the Weibul PDF of wind speed in the studied area.

The generated power of the wind turbine can be determined using its linearized characteristics [7], as follows:

$$P_i^w = \begin{cases} 0, & \text{if } v \leq v_{in}^{cut} \text{ or } v \geq v_{out}^{cut} \\ \frac{v - v_{in}^{cut}}{v_{rated} - v_{in}^{cut}} P_{i,r}^w, & \text{if } v_{in}^{cut} \leq v \leq v_{rated} \\ P_{i,r}^w & \text{else} \end{cases} \tag{2.2}$$

Where, $P_{i,r}^w$ is the rated power of wind turbine installed in bus i, P_i^w is the generated power of wind turbine in bus i, v_{out}^{cut} is the cut out speed, v_{in}^{cut} is the cut in speed and v_{rated} is the rated speed of the wind turbine.

2.2.1.2 Photo Voltaic Cell

The Photo voltaic (PV) units convert the solar radiation into electricity using semiconducting material [4]. The most widely used material for different types of PV technologies is crystalline silicon, representing over 90% of global commercial PV module production in its various forms [8]. The generated power of a photo voltaic module depends on three parameters namely, solar irradiance, ambient temperature of the site, finally the characteristics of the module itself (for example the angle of incidence on the panel that

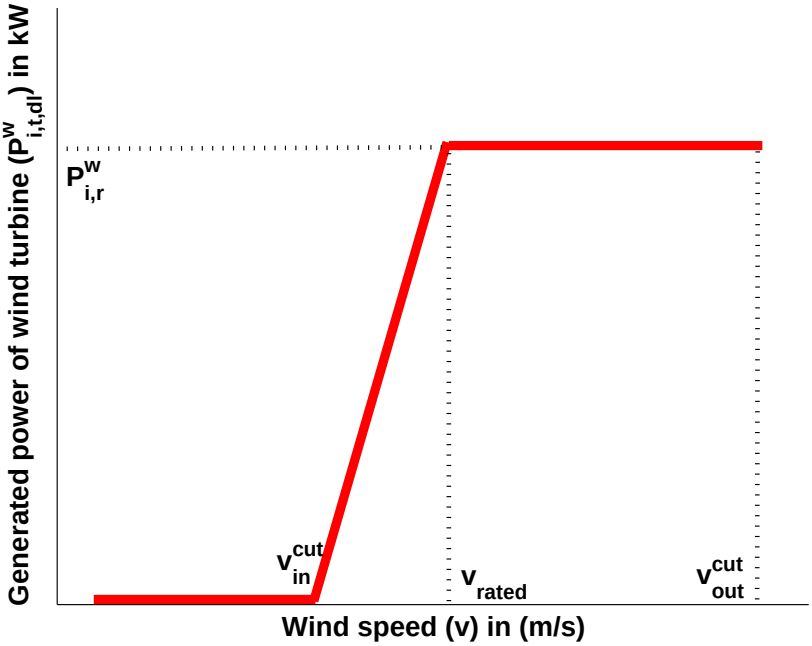

Figure 2.1: The idealized power curve of a wind turbine

has an impact on the overall performance. This angle, in some cases, is optimized and fixed for summer and in some cases tracks the movement of the sun in the sky). The solar irradiance is modeled using a Beta PDF described as follows [9]:

$$PDF(s) = \begin{cases} \frac{\Gamma(\alpha+\beta)}{\Gamma(\alpha)+\Gamma(\beta)} \times s^{\alpha-1} \times (1-s)^{\beta-1} & \text{if } 0 \leq s \leq 1, 0 \leq \alpha, \beta \\ 0 & \text{else} \end{cases} \tag{2.3}$$

where s is solar irradiance kW/m^2; α, β are parameters of the Beta distribution function;

$$\begin{aligned} P^{pv}(s) &= N \times FF \times V(s) \times I(s) \\ FF &= \frac{V_{MPP} \times I_{MPP}}{V_{oc} \times I_{sc}} \\ V(s) &= V_{oc} - K_v \times T_c \\ I(s) &= s_a \times [I_{sc} + K_i(T_c - 25)] \\ T_c &= T_A + s_a \times \frac{N_{OT} - 20}{0.8} \end{aligned} \tag{2.4}$$

where T_c is the cell temperature C°; T_A is the ambient temperature C°; K_v, K_i are voltage and current temperature coefficient $V/C^\circ, A/C^\circ$, respectively; N_{OT} is the nominal operating temperature of cell in C°; FF is the fill factor; I_{sc} is the short circuit current in A; V_{oc} is the open circuit voltage in V; I_{MPP} and V_{MPP} are the current/voltage at maximum power point in A, V; finally, s_a is the average solar irradiance [9]. The solar radiation may change due to clouds in the sky or other climate changes which will cause uncertainty in the produced energy of a photovoltaic cell. For more details please refer to [8].

2.2.1.3 Fuel Cell

It is anticipated that the fuel cell units will play a significant role in future energy conversion, with applications ranging from centralized and distributed power generation to transportation and portable electronics [10]. The mechanism of Fuel Cells is like a battery. It has two poles that generate electricity during a chemical reaction and consumes the containing fuel. The basic principle of a fuel cell was proposed by Friedrich Schonbein in 1838 and it was developed by Sir William Robert Grove in 1843 [11]. In the next five decades, with the quantitative analysis of different types of fuel cell made by scientists the fuel cell units entered in the competitive world of other DG units. Every Fuel cell has four major components as follows: The anode, cathode, electrolyte and the catalyst. The products resulting from the reaction of hydrogen and oxygen in fuel cells would be electricity, heat and water. This kind of power production would cause no noise or environmental emission. For more details please refer to [11] and [10].

2.2.2 Conventional DG technologies

2.2.2.1 Gas Turbine

Gas turbine is a rotary machine which converts the energy of fossil fuel into electricity. In this technology the gas and compressed air are combusted directly into a turbine connected directly to a high speed generator [11]. The characteristic of this kind of DG technology allows it to be used in peak shaving applications. Another advantage of gas turbines is

the fuel flexibility. It can use natural gas, process gas, low-Btu coal gas, and vaporized fuel oil gas [12].

2.2.2.2 Micro Turbine

The MicroTurbines have are recognized as the logical generator to operate for distributed generation due to their modularity, compact design, low emissions, no vibration, low noise levels and very low maintenance [13]. The MicroTurbines can be operated continuously or On-Demand, in stand alone mode or grid connected, individually or multi-pack.The Micro turbine runs on a variety of fuels including low or high pressure natural gas, biogas (landfill, wastewater treatment centers, anaerobic), flare gas, diesel propane, and kerosene [14].

2.2.2.3 Combined heat and power

The Combined heat and power (CHP) DG technology is also named co-generation. In this technology, the electricity and heat are produced simultaneously. It is usually used in large buildings or utility systems. The CHP units offer the following benefits [15]:

1. Higher thermodynamic efficiency.
2. Decreasing the energy consumption costs.
3. Improving the system reliability.

For more details about the design, construction, and operation of these units please refer to [15].

2.2.3 Energy Storage Units

There are serious concerns over reliable and satisfactory operation of the power systems at presence of renewable DG technologies [16]. Large wind penetration can cause various risks in power system reliability and stability [17]. The Energy Storage Units (ESU) are another kind of distributed energy resources which have been used to smooth out the inter-

mittent energy generation of renewable DG technologies (such as solar and wind). If there is an effective method for storing energy, this would greatly reduce the costs and would provide less expensive energy for customers. One promising method is electrochemical method. Other energy storage technologies like Compressed air, metal springs, flywheels, for instance., all have very serious drawbacks [18]. Energy storage units, "coupled with DG units", enhance the DG units in three ways, as follows [19]:

1. It stabilizes and permits DG to run at a constant and stable output, despite load fluctuations and diminishes the maintenance services.

2. It provides energy to ride through instantaneous lacks of primary energy (such as those of sun, wind, and hydro-power sources).

3. It permits DG to operate as a dispatchable unit.

The various application of these units have been reported in the literature. These units can also be used in wind-farms to decrease the bid imbalance and to shift energy from the cheapest to the most expensive, so that the penalty can be reduced and energy can be traded with higher prices [20]. The energy storage can act as an auxiliary source to mitigate the wind power fluctuations and to follow the load demand changes [21]. Energy storage systems offer a means of optimizing energy use and further reducing consumption of diesel fuel (and emission) in hybrid diesel-wind systems, specially in micro grids [22]. In [17], a simulation technique which considers the wind farm and energy storage joint operating strategies was presented. Different operating strategies are compared and the resulting benefits are evaluated. The system impacts of energy storage capacity and operating constraints, wind energy dispatch restrictions, wind penetration level and wind farm location on the reliability benefits from energy storage are illustrated. In [23], a multi-objective methodology (NSGA) was proposed to evaluate the impact of energy storage specific costs on net present value (NPV) of energy storage installations in distribution substations. For each studied technology, sets of optimal economic operation strategies and capacities of the storage device are determined. In [22], a methodology for storage sizing based on stochastic optimization was proposed. The dependence of storage sizing and the cost of delivered energy on wind penetration levels, storage efficiency, and diesel

operating strategies are considered. Results demonstrate that for high wind penetration, the availability of storage, together with an appropriate diesel operating approach, can result in significant cost savings in terms of fuel and operating costs and emissions. In [24], a knowledge-based expert system (KBES) was proposed for the scheduling of an ESU installed in a wind-diesel isolated power system. The proposed program optimizes the cost of operation by determining the diesel generation and the charging/discharging cycles of the storage system from the wind and load profiles one hour in advance. The results obtained show that by minimizing the energy wasted through the dump load with the use of the ESU and KBES controller, the required diesel generation is reduced, and therefore the operating costs and emissions would reduce. In [21], a wind conversion system with integrated energy storage and dispatchable output power is proposed. This system manages the flow of power among the wind-turbine generator, the energy storage and the grid. The results indicates that the wind this system can operate as a dispatchable source with load following capability and can transit smoothly through large dynamics such as those resulted from an islanding event. In [20], a stochastic programming is adopted to determine the optimal operation strategies of ESU. The maximum benefits of wind farm is sought at presence of ESUs. Hybrid genetic algorithm and neural network methods are employed to solve the optimization problem. The obtained results indicate that ESU can improve the profits of wind farm by decreasing the bid imbalance and shifting wind energy from low-price intervals to higher ones. In [25], the uncertainty of the wind power forecast is modeled and quantified. A hydro-pump plant is used to minimize the imbalances due to errors in the wind power forecasting when participating in an electricity market. This would reduce the risk of utilities due to the uncertainty in the wind power prediction and in prices of the reserve market. The utility can control the voltage and frequency and store energy, making the system safer and enhancing the integration of renewable sources. A probabilistic method was proposed in [26] for allocating the energy storage units in distribution networks to avoid energy curtailment of wind turbines. The goal is maximizing the benefits for of DG owners and the utility. A cost/benefit analysis was conducted in order to verify the feasibility of installing an ESU from the perspective of both the utility and the DG owner. In [16], the energy storage units have been used to increase the profit margins of wind farm owners and even provide arbitrage.

The energy storage technologies are as follows: Lead acid-batteries, Ultracapacitors, Super conducting magnetic storage system, Pumped hydroelectric energy storage, Compressed air energy storage, heat storage and flywheel.

2.2.3.1 Batteries

A battery relies on the polarization of positive and negative charges [27]. It is an electrochemical device in which, two electrodes chemically react within a sulfuric acid electrolyte. During discharge process, both of the electrodes are converted to lead sulfate. When the battery is charged, the anode is restored to lead dioxide and the cathode to metallic lead. The number of cycles is limited due to irreversible changes in the electrodes, and highly depends on battery design and depth of discharge [19].

2.2.3.2 Ultra capacitors

The so called supercapacitors, ultracapacitors,or electrochemical capacitors are large capacitors which have been used for energy storage. This technology is an electrical energy storage method which has two electrodes immersed in an electrolyte with a separator between them. The electric charge is stored in the interface between the solid electrode material and the electrolyte [19].

2.2.3.3 Flywheel

The rotating mass or flywheel energy storage is a mechanical technique which have been used to store energy. The applications of this technology span a wide range including intermediate storage for renewable energy generation and direct grid applications from power quality issues to offering an alternative to strengthening transmission [28].

2.2.3.4 Super conducting magnetic storage system

The magnetic field can store energy. This energy is proportional to the value of magnetic field strength. The super conducting magnetic storage system is a superconducting

solenoid coil without an iron core [27].

2.2.3.5 Pumped hydroelectric energy storage

The pumped storage energy storage technique is based on pumping the water into big reservoirs when the demand for electricity is low so that it can be used to run turbine generators when the demand is high [29].

2.2.3.6 Compressed air energy storage

In a compressed-air energy storage system, air is compressed during off-peak hours and stored in large underground reservoirs, which may be naturally occurring caverns, salt domes, abandoned mine shafts, depleted gas and oil fields, or man-made caverns. During peak hours, the air is released to drive a gas turbine generator [30].

2.2.3.7 Heat storage

In storage heat energy storage method, a material is heated and then when this energy is released from the heated material it will be used for electricity generation. Water, soil, solid metals, and salt rock beds are often used for heat storage [19].

2.2.3.8 Hydrogen storage

In recent years, hydrogen gas has been promoted as a potential environmentally friendly fuel. The hydrogen is known as a future energy carrier since it is the only energy carrier that can be produced easily in large amounts and in an appropriate time scale. The energy produced with various methods can be used to produce hydrogen from water by electrolysis. The combustion of hydrogen leads again only to water and the cycle is closed.

2.3 DG Impacts on Distribution Network

The DG integration in distribution networks has great impacts on operation and planning of distribution systems [31]. Different technical, economical and environmental issues have been addressed in the literature such as:

- Active loss reduction [9, 32–40]
- Investment deferral in network capacity [41–43]
- Voltage profile improvement [44, 45]
- Emission reduction [46, 47]
- Voltage stability improvement by increasing the system's loading margin [42, 48]
- Reliability improvement [39, 49, 50], the reliability indices may be improved if DG units are operated and placed in the network properly.
- Increasing the network security (e.g. N-1 criteria) [51]
- Facilitating the system restoration [52]
- Reducing the energy costs in the short term [53]
- Incrementing the load balance factor of radial distribution networks [54] (this may be acheived by freeing up the capacity of highly loaded feeders)
- Risk aversion in load procurement [55, 56], this risk may concern the technical or economical issues.

2.4 DG Integration models in Distribution Networks

2.4.1 Centrally controlled DG integration

Different methods have been proposed to find the optimal size and location of DG units in distribution networks. In [40], a loss sensitivity factor, based on the equivalent current

injection, is formulated for the distribution systems. This factor is employed to find the optimum DG size and location. In [57], a probabilistic methodology was developed to find the optimal location of DG units in distribution networks. These locations are found based on values of loads. In [39], a multi-objective model is proposed to find the optimal location of DG units for minimizing the active losses and also increasing the reliability of the distribution network. A dynamic programming approach is used to solve the multi-objective model. In [58], the optimum allocation of the maximum DG penetration in distribution networks is found considering thermal rating of feeders, transformer capacity, voltage profile and short-circuit level constraints. It is assumed that the type, locations and ratings of DG units are predetermined. In [32], a new methodology based on nodal pricing for optimally allocating distributed generation for profit (reduced loss cost), loss reduction, and voltage improvement including voltage rise phenomenon. Ref. [59] presents a method for optimal sizing and optimal placement of DG units. The objective is defined as a combination of operating cost of DG units and active loss of the network. In [60], an algorithm is presented to identify the optimal location and size of DG in distribution networks. The proposed method has the capability of dealing with randomly distributed load conditions with low power factor for multi-DG systems. It enhances the performance of distribution network in terms of node voltage profile improvement and power loss reduction. A multi-objective approach based on the Bellman-Zadeh algorithm and fuzzy logic is used to determine appropriate DG sites in [61], considering the active losses, voltage profile and feeder loading levels.

The reported models of this category can generally be divided into two major categories: static and dynamic models. In static models, investment decisions are implemented in the first year of the planning horizon [33, 36, 38, 47, 48, 62–69]. In this category, the models are single or multi-objectives. The single-objective models are either originally single-objective [36, 38, 48, 62, 64, 70, 71], or multi-objective which are converted into a single-objective (using a benefit to cost ratio index [63] or an additive utility function [42, 66, 68, 69]); multi-objective models of this category are solved using Pareto optimality concept [33, 47, 65, 67, 72, 73]. In static models, [71] and [67] consider network reinforcement along with DG investment. The second category contains the dynamic single-objective model [74] in which the year of investment (for DG units and network

reinforcements) is also decided by the planner which may not necessarily be the first year of the planning horizon. The dynamic models are those in which the investment year is also determined by the optimization procedure.

2.4.2 DG impact assessment in unbundled environment

In [75], an analytical method is proposed to quantify the value of avoided losses that DG units may cause in distribution networks. Intervals of expected avoided losses are used to account for the variation of avoided losses due to the number, size and location of DG units, as well as for the kind of load distribution on LV networks. In [76], the performance of customer-owned DG units is quantified from different perspectives using a Monte Carlo-based method. The focus of this method is on energy savings and performance indices while considering the cost issues.

2.5 Modeling the uncertainties in DG impact assessment

The methods proposed in the literature for modeling the uncertainties associated to the uncertain variables can be categorized into three categories namely, possibilistic (fuzzy) models, probabilistic methods and Info Gap Decision Theory (IGDT).

- Possibilistic (fuzzy) models: In [77, 78], a fuzzy power flow model is proposed for modeling the uncertainty of loads in a network. They use the extension principle of fuzzy to find the membership function of output when the input values are fuzzy and their membership functions are available. In [33], the load and electricity price values are modeled using fuzzy numbers.

- Probabilistic methods models: In [9], different scenarios are constructed based on the Probability Density Function (PDF) of uncertain values and then a method is proposed to determine the optimal combination of different renewable technologies for minimizing active losses. In [79], a powerful tool was proposed based on Monte Carlo Simulation for modeling the uncertainties of the uncertainties in the locations, exported energy and penetration level, the states (on/off) of the DG units. It is

assumed that the mentioned uncertainties follow a probability distribution function and the mentioned PDF is available for DNO. In [76], the performance of customer-owned DG units is quantified from different perspectives using a Monte Carlo-based method. The focus of this method is on energy savings and performance indices while considering the cost issues. In [57], a probabilistic methodology was developed to determine the region of higher probability for location of DG plants that will feed the loads of the distribution network under study. In this method, the hourly load changes are taken into account.

- IGDT method: In [55, 80], a technique based on IGDT is proposed to derive the bidding strategy in the day-ahead market of a large consumer that procures its electricity demand in both the day-ahead market and a subsequent adjustment market. In [56], a procurement strategy for large consumers is proposed. It is assumed that the supply sources include bilateral contracts, a limited self-generating facility, and the pool. The day ahead price values are considered to be uncertain in both references.

2.6 Conclusions

This chapter makes a modest attempt to present a review of literature on the published work related to the aims of this research. This chapter was divided into five sections. Section 2.2 briefly reviews the DG technologies. Section 2.3 dealt with technical, economical and environmental impacts of DG units in distribution networks. The DG integration models are discussed in Section 2.4. Finally Section 2.5 presented the uncertainty modeling methods in DG impact assessments.

CHAPTER 3

Multi Criteria Decision Making

3.1 Introduction

The Multi Criteria Decision Making models can be divided into two groups namely, Multi Objective Decision Making (MODM) and Multi Attribute Decision Making (MADM) [81]. The main difference between MODM and MADM models lies in the fact that in MADM methods, the planner selects a decision among different choices but in MODM methods the decision makers designs a decision. This chapter offers a review of literature as well as the method proposed in this thesis for obtaining the Pareto optimal fronts in the following areas:

1. Multi Objective Decision Making (MODM) methods
2. Multi Attribute Decision Making (MADM) methods

3.2 Multi Objective Decision Making (MODM)

In Multi Objective Decision Making (MODM) methods, the decision alternatives are constructed considering the constraints of the given problem. In most realistic optimization problems, particularly those applicable in power system, there exists more than one objective function which should be optimized simultaneously. These objectives functions might be in conflict, interdependent or independent of each other so it is impossible to satisfy them all at once. The main difference between the multi objective optimization and traditional single optimization techniques can be categorized in two areas:

1. Several objective functions are to be optimized at the same time.

2. There exists a set of optimal solutions which are mathematically equally good solutions. It means one of them can not be preferred over others and a trade off should be made to select one instead of a unique optimal solution

Generally, every multi-objective optimization problem consists of a number of objectives and several equality and inequality constraints which can be formulated as (3.1).

$$\begin{aligned} &min \quad F(X) = [f_1(X), ..., f_{N_O}(X)] \\ &Subject\ to: \\ &\{G(X) = \bar{0}, H(X) \leq \bar{0}\} \\ &X = [x_1, \cdots, x_m] \end{aligned} \tag{3.1}$$

3.2.1 Pareto optimality

The notion of optimum has been redefined in this context and instead of aiming to find a single solution, it is tried to produce a set of best compromises or trade-offs from which the decision maker will select one. The set of all optimal solutions which are non-dominated by any other solution, is known as Pareto-optimal set. Suppose a minimizing problem with two objectives in conflict, the different solutions for this problem and the Pareto optimal fronts are shown in Fig .3.1. For every two solution in each Pareto front (like A, B) none of them is better than other when all objective functions are considered. Here objective 1 is better minimized in solution A than in B and objective 2 is better minimized in solution B than in A. This also applies for the solutions existing in other fronts. For every solution in the $(i+1)^{th}$ front (for example D in the 2^{nd} front) there exist at least one solution in i^{th} front (here A in the 1^{st} front) that dominates it (is better than it considering all objective functions). Since A and B belong to the first front, there is no solution better than them in respect to all objectives. Each solution in Pareto optimal set has two basic characteristics:

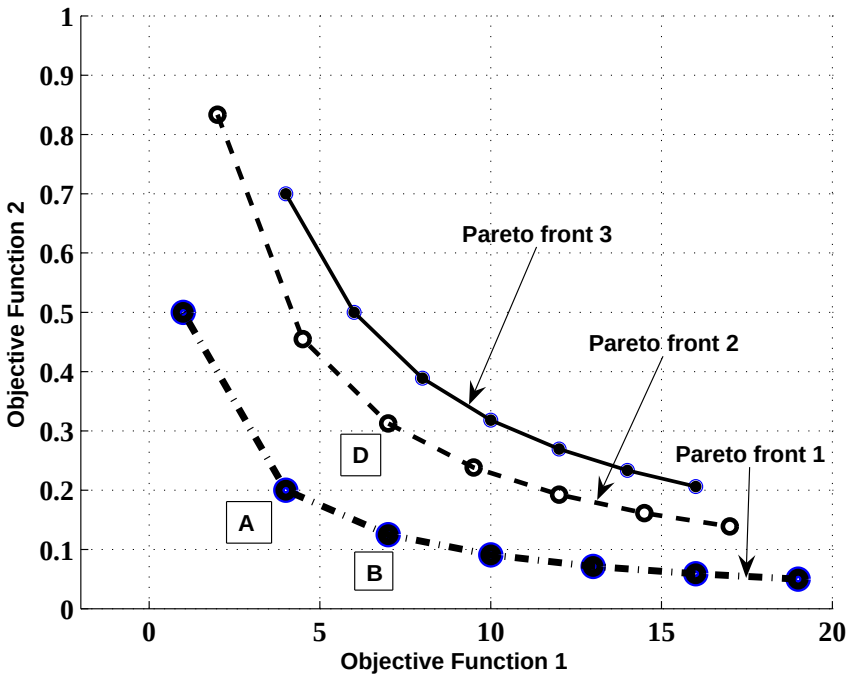

Figure 3.1: Classification of a population to k non-dominated fronts

1. For every two solutions belonging to the same Pareto front (3.2) holds:

$$\forall i \exists j, n | f_n(\bar{x}_i) > f_n(\bar{x}_j) \tag{3.2}$$
$$\bar{x}_j, \bar{x}_i \in S$$

   This means for every solution belonging to Pareto front S, at least one solution exists as which is better than at least in one objective function (named n here). In other words there is no solution in Pareto optimal front which is the best among all members of this set considering all objectives.

2. For every solution belonging to an upper Pareto front and the ones in the lower fronts, (3.3) holds:

$$\forall k \in \{1...N_O\}\, f_k(\bar{x}_1) \leq f_k(\bar{x}_2) \tag{3.3}$$

$$\exists k' \in \{1...N_O\}\, f_{k'}(\bar{x}_1) < f_{k'}(\bar{x}_2) \tag{3.4}$$

$$\bar{x}_1 \in S, \bar{x}_2 \in S^*$$

$$S < S^*$$

One of the classical approach for finding the Pareto optimal set is weighting method in which a relative preference vector is used to weight the objectives and change them into a scalar value [82]. By converting a multi-objective optimization problem into a single objective one, only one optimum solution can be achieved which is very sensitive to the given weights. Evolutionary algorithms seem particularly suitable to solve multi-objective optimization problems, because they deal simultaneously with a set of possible solutions (the so-called population). This allows decision maker to find several optimal solutions (Pareto optimal set) in a single run, instead of having to perform a series of separate runs as in the case of the traditional mathematical methods. Additionally, the classical methods are usually faced with difficulty in non-convex problems. To do this, many heuristic algorithms have been proposed like NSGAII [83], PSO [84] and Tabu search [85]. In all of these algorithms an initial population is created and then it is guided toward the Pareto front. The solutions with smaller distance to Pareto optimal front and more diversity are more preferred. This is repeated through several iterations until the stopping criteria is met. The ultimate goal is to seek the most preferred solution among the Pareto optimal set, in this thesis this is done by using a fuzzy satisfying method which will be discussed in section 3.2.3.

3.2.2 Finding the Pareto optimal front using hybrid Immune-GA method

The Immune Algorithm (IA), first introduced in [86], is inspired by the immune system of human body. When external particles (antigens) enter into the human body, the immune cells (antibodies) have to detect and remove them. The antibodies are randomly generated by immune system and the ones with better match to the antigens are selected

and reproduced (colonized) [87]. This idea is used to deal with optimization problems by considering the objective functions and the constraints as antigens while the solutions construct the antibodies [88]. The Immune Algorithm is an iterative process which creates an initial solution and tries to improve its performance through three operators namely, affinity factor, hyper mutation and clonal selection [89]. The affinity factor is a measure of fitness for each solution which shows how antibodies (solutions) have detected (optimized) the antibodies (objective functions and constraints). The hyper mutation operator is the same as mutation operator in Genetic Algorithm (GA) [87], but in IA, the probability of mutation is proportional to the inverse value of affinity factor of the solution. This means that if the affinity factor of a solution is low, it will be more mutated to explore the solution space and vice versa. The clonal selection is an operator to give a chance of reproduction to each solution. This chance is proportional to the affinity factor of each solution. The concept of fitness in multi-objective optimization is different with single objective optimization because more than one objective should be optimized. The Pareto optimality [82], is used to provide a pseudo fitness value for solution n, i.e. X_n, to be used as its affinity factor, i.e. AF_n. The AF_n should be defined in a way that effectively reflect two important aspects of multi-objective optimization namely, the ability of X_n in minimizing the objective functions and also maintaining the diversity among the solutions and the ability of solution in minimizing the objective functions. This is done by sorting the solutions into different Pareto fronts [82]. The process of fitness assignment is as follows: all of the solutions are sorted to find out the Pareto front they belong. This will determine the front number of each solution, i.e. FN. To evaluate the diversity of the solutions found in each Pareto front, global diversity factor, i.e. GD, is introduced and calculated. This factor shows the average distance of solutions in a given Pareto front. Since there are more than one objective function, a local diversity factor for solution n regarding objective function k, i.e. LD_n^k, is defined here as :

$$LD_n^k = \sum_{X_m \in FN_n} \frac{|f_k(X_n) - f_k(X_m)|}{MD_k} \tag{3.5}$$

Where, in (3.5), the summation is done over all solution existing in the same Pareto front as X_n. The MD_k is the maximum distance between the solutions of the mentioned Pareto

front, regarding just the k^{th} objective function. Then LD_n^k, is normalized by dividing it by the maximum value of LD_n^k over all solutions in the mentioned Pareto front as :

$$LD_n^k = \frac{LD_n^k}{\max(LD_n^k)} \tag{3.6}$$

The global diversity factor for each solution is then calculated as the average of its local diversities as follows:

$$GD_n = \sum_{k=1}^{N_O} \frac{LD_n^k}{N_O} \tag{3.7}$$

Having FN_n and GD_n in hand, the affinity factor of solution n, is defined as follows:

$$AF_n = w_1 \times (FN_n)^{-1} + w_2 \times GD_n \tag{3.8}$$

The first term in (3.8) drives the population toward the lower Pareto optimal fronts and the second term insures the diversity among the solutions. In order to calculate the global diversity of the n^{th} solution, i.e. GD_n, a local diversity factor, i.e. LD_n^k, is defined for each objective function [82]. In initial iterations, a small number of solutions belong to the first Pareto front, so getting closer to Pareto optimal front is more important than maintaining the diversity among them. It is necessary to enable the algorithm in distinguishing between the solutions in different Pareto fronts, w_1 and w_2 in (3.8) are adaptively selected which guarantees that the solution belonging to a lower Pareto front has a bigger affinity factor than a solution belonging to an upper front level (w_1 is bigger than w_2 in the initial iterations) and when most of the solutions are in the Pareto optimal front, w_2 is chosen bigger than w_1 to maintain the diversity among the solutions. In this thesis, the following formulation is proposed to update the weight values, i.e. $w_{1,2}$):

$$\begin{aligned} w_1 &= 100 \times (\max_{n=1}^{N_p}(FN_n) - \min_{n=1}^{N_p}(FN_n)) \\ w_2 &= 50 \end{aligned} \tag{3.9}$$

To do so, each antibody, is a vector containing the investment decision for DG units and network. the steps of the first stage of the solution algorithm are as follows:

Step 1. Generate N_p initial random solutions.

Step 2. Set iteration=1.

Step 3. Calculate OF_1, OF_2 for each solution.

Step 4. Sort the solutions based on the Pareto front they belong to and the global diversity of each solution using (3.7).

Step 5. Calculate the affinity factor using (3.8) for each antibody.

Step 6. Save the best N antibodies in the memory.

Step 7. If the stopping criterion is met, go to step (13), else, continue.

Step 8. Set the cloning counter, i.e. m=1.

Step 9. Select two antibodies of memory, i.e. X_p, X_q based on their affinity factors, using roulette wheel method.

Step 10. Determine the cloning number, i.e. K_m, and the mutation probability, i.e. ς_m, as follows:

$$K_m = round(N_p \times \frac{AF_p + AF_q}{2max(AF_n)}) \tag{3.10}$$
$$\varsigma_m = \varsigma^{min} \times \frac{2max(AF_n)}{AF_p + AF_q}$$

Where, *round* is a function which returns the nearest integer value, ς^{min} is the minimum mutation probability. This would mutate the better solutions with lower mutation probability and also drives the algorithm to clone them more.

Step 11. Clone the selected two antibodies K_m times and generate $2K_m$ new antibodies and save them.

Step 12. Check if $m < N$, then increase cloning counter by one and go to step 9, else construct the new population of antibodies using the union of old and new antibodies, increase iteration by one and go to step 3.

Step 13. End.

The flowchart of the two stages of the proposed method is depicted in Fig.3.2.

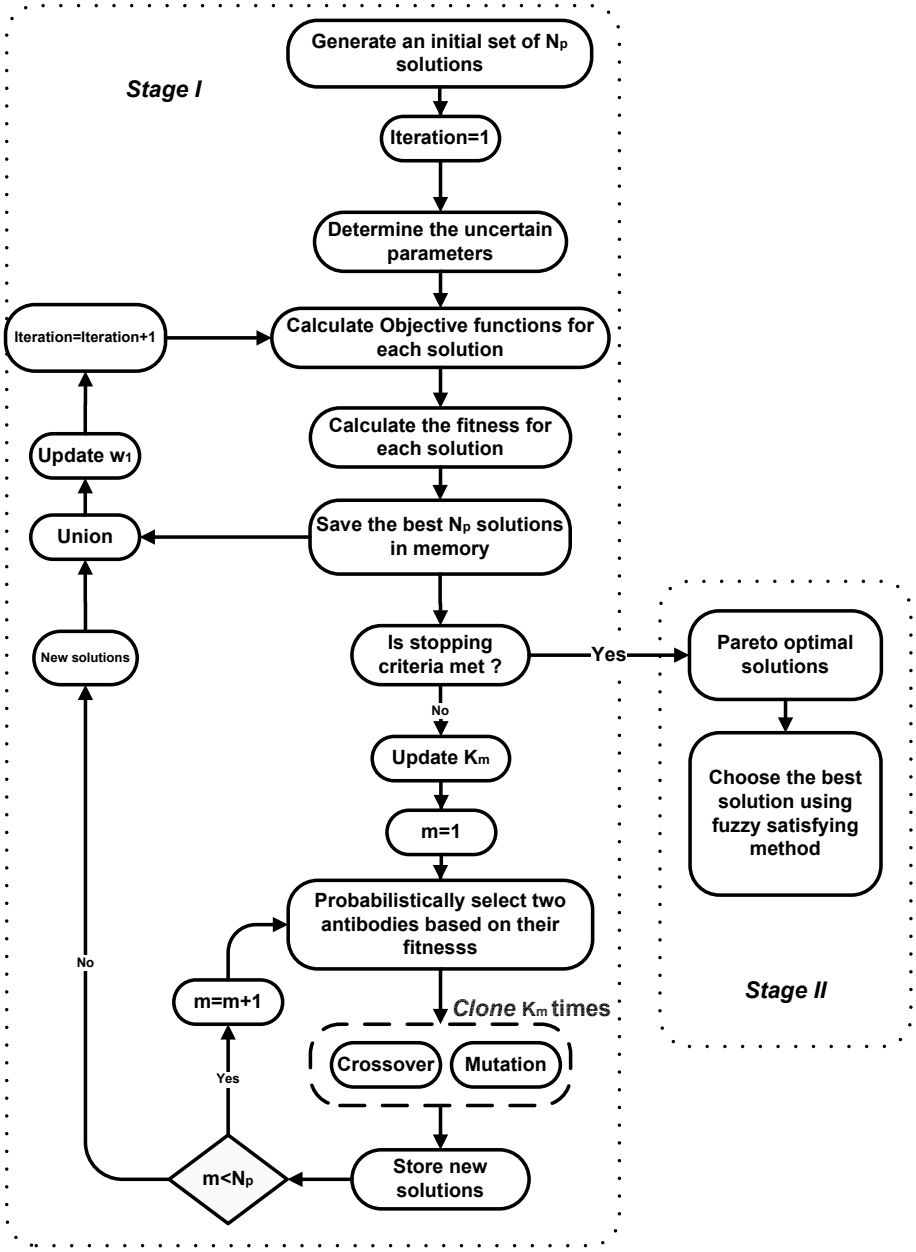

Figure 3.2: The flowchart of the two stages of the proposed model for multi-objective optimization

3.2.3 Choosing final solution using fuzzy satisfying method

The next step after obtaining the Pareto front is to select the solution among the candidates. A fuzzy satisfying method has been used to obtain the satisfactory solution for the decision maker from the Pareto optimal set. For each solution in the Pareto optimal front,

like $\bar{x}_i$, a membership function is defined as $\mu_{f_k}(\bar{x}_i)$. This value shows the level of which $\bar{x}_i$ belongs to the set that minimizes the k^{th} objective function. The value of $\mu_{f_k}(\bar{x}_i)$ varies between 0 to 1. The membership value "0" indicates incompatibility with the set, while "1" means full compatibility. In other words, the membership function gives a numerical description of how the decision maker is satisfied by which level of achievement of solution with respect to a specific objective function. The decision maker is fully satisfied with $\bar{x}_i$ if $\mu_{f_k}(\bar{x}_i) = 1$ and dissatisfied when $\mu_{f_k}(\bar{x}_i) = 0$ [90]. Different types of membership functions have been suggested like linear or exponential ones. The question is how the planner can select the suitable type of membership function. It should be noted that in this work, the decision making is a posteriori not a priory one. This means that no preference should be given to optimizing any objective function before finding the Pareto optimal front. If an exponential membership function is chosen for one of the objectives functions then it is given a priority for minimizing that objective relative to the other objectives because this function will assign a smaller membership function in the vicinity of maximum value of that objective comparing to linear type [91]. Here a linear type of membership function has been used for all objective functions as shown in (3.11).

$$\mu_{f_k}(X) = \begin{cases} 0 & f_k(X) > f_k^{max} \\ \frac{f_k^{max} - f_k(X)}{f_k^{max} - f_k^{min}} & f_k^{min} \leq f_k(X) \leq f_k^{max} \\ 1 & f_k(X) < f_k^{min} \end{cases} \tag{3.11}$$

After defining the membership functions, there are several ways to choose the final solution. Each method considers a different philosophy. Some of these methods are as follows:

1. Conservative approach [33]: a conservative decision can be achieved by trying to find the solution which its Minimum satisfaction is maximum over all objective functions. Using the Max-Min formulation, the final solution can be found by solving (3.12).

$$\max_{i=1}^{N_S}(\min_{k=1}^{N_O} \mu_{f_k}(X_n)) \tag{3.12}$$

This will ensure the decision maker that all objectives are sufficiently optimized.

2. Trade off approach or utility function: a trade-off decision can be achieved by trying to find the solution which its Minimum satisfaction is maximum over all objective functions. Using the Max-Min formulation, the final solution can be found by solving (3.12).

$$\max_{i=1}^{N_S}(\sum_{k=1}^{N_O}\mu_{f_k}(X_n)) \tag{3.13}$$

This method is used when the decision maker is satisfied when the success of the solution in optimizing some objectives can compensate the dissatisfaction in optimizing other objectives. It should be noted that this method is a posteriori approach and is totally different with utility function of weighted sum approach optimization. In this method, first solutions are found and then the best one will be selected. In utility based or weighted sum approach a unique objective function is constructed and then a unique solution will be found. The weighting factors are assumed to be priori known in such methods.

3.3 Multi Attribute Decision Making (MADM)

In Multi Attribute Decision Making (MADM) models (in contrary to MODM models) a set of decision options is available for decision maker [81]. He should choose a plan (the most preferable one) according to the attributes of the available plans. This method has been widely used in electric utility decision problems. In [92] a method based on MADM technique was proposed to support the decision analysis with imprecise information in generation expansion planning. In this method, a set of weights are usually necessary to construct a single utility function for comparing the available planning options. The analytical hierarchy process (AHP) is a powerful method to find such a set of weights [93] which reflects the importance of each attribute over the other ones. This method has been applied in various power systems problems such as: evaluation and selection of an optimum power plant [94], economic and environmental power dispatch [95], modeling and prioritizing demand response programs in power markets [96] and shortlisting the feasible DG plans and identifying the most appropriate plan in developing countries [97].

In [98], an approach based on MADM is used to assess the alternatives for DG technology with respect to their economic, technical and environmental attributes.

3.4 Conclusions

This chapter presents the various MCDM methods including MODM and MADM. In this chapter, the proposed hybrid Immune-GA method for obtaining the Pareto optimal fronts and also the fuzzy satisfying method used for selection of the final solution are described. A brief review on MADM models has been given in section 3.3.

CHAPTER 4

Uncertainty Modeling

4.1 Introduction

This chapter introduces the uncertainty modeling tools for DG and distribution network planing. This chapter offers a review of literature in the following areas:

1. Probabilistic approach
2. Possibilistic approach
3. Proposed mixed Possibilistic-probabilistic approach
4. Information Gap decision theory

4.2 Probabilistic approach

In probabilistic approach, a multi variable function, namely y, $y = f(Z)$ is available. Z is a vector of the form $Z = [z_1, ..., z_m]$, in which z_1 to z_m are random variables with known PDFs. The problem is, knowing the PDFs of all input variables, i.e. z_1 to z_m, what would be the PDF of y? Two methods of stochastic (probabilistic) uncertainty modeling are described as follows:

4.2.1 Monte Carlo simulation

The main concept of MCS method is described as follows [99]: First of all, it will generate a value, i.e. z_i^e, for each input variable z_i, using its own PDF and form the $Z^e = [z_1^e, ..., z_m^e]$ and then calculates the value of y^e using $y^e = f(Z^e)$. This process will be repeated

for a number of iterations, i.e. N_{MC}. The trend of the output, i.e. y, will determine its PDF. This method is often used when the model is complex, nonlinear, or involves many uncertain parameters. A simulation can typically involve over 10000 evaluations of the model, a task which is computationally expensive. Monte Carlo method can be summarized as below:

Step.1 Create a parametric model $Y = f(z_1, z_2, ..., z_n)$.

Step.2 Generate a set of random inputs using their PDF
$Z^e = (z_1^e, z_2^e, ..., z_n^e)$.

Step.3 Evaluate the model and calculate the Y^e.

Step.4 Repeat steps 2 and 3 for $e = 1$ to N_{MC}.

Step.5 Analyze the results using histograms, summary statistics, confidence intervals.

The Monte Carlo method is usually used for validation of the proposed methods in the literature for solving the PPF.

4.2.2 Two point estimate method

The symmetrical two point estimate method (S2PEM) which has the symmetrical location of two sampling points is described in below steps [100]:

Step.1 Determine the number of uncertain variables, n.

Step.2 Set $E(Y) = 0, E(Y^2) = 0$.

Step.3 Set $k = 1$.

Step.4 Determine the locations of concentrations $\epsilon_{k,i}$ and the probabilities of concentrations $P_{k,i}$, as follows:

$$\epsilon_{k,i} = (-1)^{(i+1)}\sqrt{n} \tag{4.1}$$

$$P_{k,i} = \frac{1}{2n} \text{ i=1,2} \tag{4.2}$$

.

Step.5 Determine the concentration points $z_{k,i}$, as follows:

$$z_{k,i} = \mu_{z_k} + \epsilon_{k,i} \times \sigma_{z_i} \tag{4.3}$$
$$i = 1, 2$$

Where, μ_{z_k} and σ_{z_k} are the mean and the standard deviation of z_k, respectively.

Step.6 Run the deterministic power flow for both $z_{k,i}$, as follows:

$$Z = [z_1, z_2, ..., z_{k,i}, ..., z_n] \tag{4.4}$$
$$i = 1, 2$$

Step.7 Calculate $E(Y)$ and $E(Y^2)$ using:

$$E(Y) \cong \sum_{k=1}^{n} \sum_{i=1}^{2} P_{k,i} f(z_1, z_2, ..., z_{k,i}, ..., z_n) \tag{4.5}$$
$$E(Y^2) \cong \sum_{k=1}^{n} \sum_{i=1}^{2} P_{k,i} f^2(z_1, z_2, ..., z_{k,i}, ..., z_n)$$

Step.8 Calculate the mean and the standard deviation as follows:

$$\mu_Y = E(Y) \tag{4.6}$$
$$\sigma_Y = \sqrt{E(Y^2) - E^2(Y)}$$

In unsymmetrical two point estimate method (US2PEM), the location of each sampling point is described as follows:

$$\epsilon_{k,i} = \frac{1}{2}\frac{M_3(z_k)}{\sigma_{z_k}^3} + (-1)^{i+1}\sqrt{n + \frac{1}{2}(\frac{M_3(z_k)}{\sigma_{z_k}^3})^2} \tag{4.7}$$

$$P_{k,i} = (-1)^i \frac{\epsilon_{k,3-i}}{2n\sqrt{n + \frac{1}{2}(\frac{M_3(z_k)}{\sigma_{z_k}^3})^2}} \tag{4.8}$$

$$\tag{4.9}$$

where $M_3(z_k)$ is the third moment of variable z_k.

4.2.3 Scenario based decision making

In this method, various scenarios are generated using the PDF of each uncertain variable, i.e. Z_s, The value of y is calculated as follows:

$$y = \sum_{s\in\Omega_J} \pi_s \times f(Z_s) \tag{4.10}$$

where π_s is the probability of scenario s.
If the number of scenarios are too high then they are reduced using the method described below, to obtain a small set representing the original set. The purpose of scenario reduction is selection of a set, i.e. Ω_S, with the cardinality of N_{Ω_S}, from the original set, i.e. Ω_J [101]. This procedure should be done in a way that makes a trade off between the loss of the information and decreasing the computational burden [102]. The scenario reduction technique used in this work is described as the following steps [103]:

step. 1 Construct the matrix containing the distance between each pair of scenarios $c(s, \acute{s})$

step. 2 Select the fist scenario s_1 as follows:

$$s_1 = arg\left\{\min_{s'\in\Omega_J} \sum_{s\in\Omega_J} \pi_s c(s, s')\right\} \tag{4.11}$$
$$\Omega_S = \{s_1\}, \Omega_J = \Omega_J - \Omega_S$$

step. 3 Select the next scenario to be added to Ω_S as follows:

$$s_n = \tag{4.12}$$
$$arg\left\{\min_{s'\in\Omega_J}\sum_{s\in\Omega_J-\{s'\}}\pi_s\min_{s''\in\Omega_S\cup\{s\}}c(s,s'')\right\}$$
$$\Omega_S=\Omega_S\cup\{s_n\},\Omega_J=\Omega_J-\Omega_S$$

step. 4 If the number of selected set is sufficient then end and go to step 2 ; else continue.

step. 5 The probabilities of each non-selected scenario will be added to its closest scenario in the selected set.

step. 6 End.

For more details please refer to [102] and [104].

4.3 Possibilistic approach

Suppose a multivariate objective function, i.e. $y = f(X)$ is given where X is an uncertain variable described using a membership function. In possibilistic evaluation frameworks, for each uncertain value, i.e. $\tilde{A}$, a membership function, i.e. $\mu_A(x)$, is defined which describes that how much each element, i.e. x, of universe of discourse, i.e. U, belongs to $\tilde{A}$. Different types of membership functions can be used for describing the uncertain values. Here, fuzzy trapezoidal numbers (FTN) with a notation $\tilde{A} = (a_{\min}, a_L, a_U, a_{\max})$ are used as shown in Fig.4.1.

4.3.1 α-cut Method

In engineering problems, the evaluation of a certain quantity is usually in the form of a multivariable function namely, $y = f(x_1, \ldots, x_n)$, if $\tilde{x}_i$ are uncertain then y will be also uncertain, $\tilde{y} = f(\tilde{x}_1, \ldots, \tilde{x}_n)$. The question is that, knowing the membership functions of uncertain input variables $\tilde{x}_i$, what would be the membership function of $\tilde{y}$. The α-cut method [105] answers this question in this way:

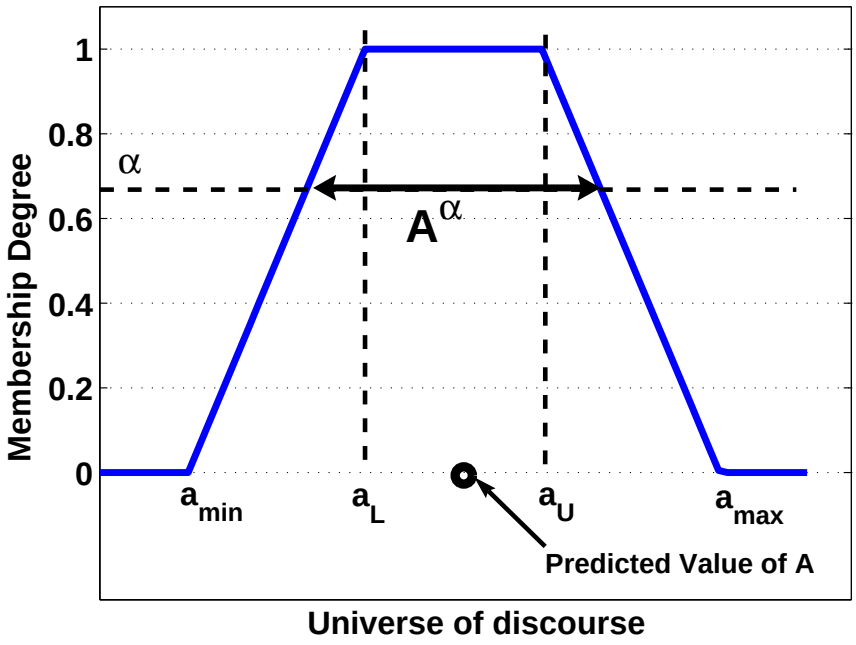

Figure 4.1: Fuzzy Trapezoidal Number

For a given fuzzy set $\tilde{A}$, defined on universe of discourse, i.e. U, the crisp set A^α is defined as all elements of U which have membership degree to $\tilde{A}$, greater than or equal to α, as calculated in (4.13).

$$A^\alpha = \{x \in U \mid \mu_A(x) \geq \alpha\} \tag{4.13}$$
$$A^\alpha = (\underline{A}^\alpha, \bar{A}^\alpha)$$

The α-cut of each input variable, i.e. x_i^α, is calculated using (4.13), then the α-cut of y, i.e. y^α is calculated as follows:

$$y^\alpha = (\underline{y}^\alpha, \bar{y}^\alpha) \tag{4.14}$$
$$\underline{y}^\alpha = \min f(X^\alpha)$$
$$\bar{y}^\alpha = \max f(X^\alpha)$$
$$X^\alpha = [x_1^\alpha, \ldots, x_n^\alpha]$$
$$X^\alpha \in (\underline{X}^\alpha, \bar{X}^\alpha) \tag{4.15}$$

This means for each α-cut, two optimizations are done. One maximization for obtaining the upper bound of y^{α}, i.e. $\bar{y}^{\alpha}$, and one minimization for obtaining the lower bound of y^{α}, i.e. $\underline{y}^{\alpha}$.

4.3.2 Defuzzification

The defuzzification is a mathematical process for converting a fuzzy number into a crisp one [105]. In this work, the centroid method [106] is used for defuzzification of fuzzy numbers. The deffuzzified value of a given fuzzy quantity, i.e. $\tilde{A}$, is calculated as follows:

$$A^{*} = \frac{\int \mu_A(x).x \ \mathrm{dx}}{\int \mu_A(x) \ \mathrm{dx}} \tag{4.16}$$

4.4 Proposed mixed possibilistic-probabilistic approachs

In realistic problems, the planner has a multivariate objective function, i.e. $y = f(X, Z)$, where the possibilistic uncertain parameters are represented by vector X and probabilistic uncertain values are given by vector Z. To deal with such variables they are decomposed into two groups and are dealt with separately.

4.4.1 Mixed possibilistic-Monte Carlo approach

The following steps describe the proposed Mixed possibilistic-Monte Carlo approach [107]:

- Step.1 : For each $z_i \in$ Z, generate a value using its PDF,i.e. z_i^e
- Step.2 : Calculate $(\bar{y}^{\alpha})^e$ and $(\underline{y}^{\alpha})^e$ as follows:

$$\begin{aligned} &(\underline{y}^{\alpha})^e = \min f(Z^e, X^{\alpha}) \\ &(\bar{y}^{\alpha})^e = \max f(Z^e, X^{\alpha}) \\ &St: \\ &X^{\alpha} \in (\underline{X}^{\alpha}, \bar{X}^{\alpha}) \end{aligned} \tag{4.17}$$

These steps are repeated to obtain the PDF of the parameters of the output's membership function. In fact, when both types of the uncertainties exist in the input variables then the parameters of the membership function are stochastic.

4.4.2 Mixed possibilistic-scenario based approach

The following steps describe the proposed Mixed possibilistic-scenario based approach:

- Step.1 : Generate the scenario set describing the behavior of Z, i.e. Ω_J
- Step.2 : Reduce the original scenario set and obtain the reduced set, i.e. Ω_s
- Step.3 : Calculate $(\overline{y}^{\alpha})$ and $(\underline{y}^{\alpha})$ as follows:

$$\begin{aligned} &\underline{y}^{\alpha} = \min \sum_{s \in \Omega_s} \pi_s \times f(Z_s, X^{\alpha}) \\ &\overline{y}^{\alpha} = \max \sum_{s \in \Omega_s} \pi_s \times f(Z_s, X^{\alpha}) \\ &St : \\ &X^{\alpha} \in (\underline{X}^{\alpha}, \overline{X}^{\alpha}) \end{aligned} \tag{4.18}$$

- Step.4 : Calculate the crisp value of y using (4.16)

4.5 Info-Gap decision theory

The Information Gap Decision Theory (IGDT) is a non-probabilistic and non-fuzzy method for quantification of uncertainty. In this context, the uncertainty is defined as the distance between what is known (or predicted) and what may happen in reality [108]. One of the applications of this tool is helping the decision makers to maximize the robustness of their decisions against the failures. The robustness is defined as the immunity of the minimum requirement satisfaction at presence of uncertain parameters [108].

4.5.1 Uncertainty Modeling

There are several models in IGDT method for presenting the uncertainty of parameters. Here, the envelope bound model [108] is used, as follows:

$$\begin{aligned} & x \in U(\alpha, \tilde{x}) \\ & U(\alpha, \tilde{x}) = \left| \frac{x - \tilde{x}}{\tilde{x}} \right| \leq \alpha \end{aligned} \tag{4.19}$$

Where, α is the uncertainty horizon of parameter x, $\tilde{x}$ is the predicted (most expected) value of x and $U(\alpha, \tilde{x})$ is the set of all values of x whose deviation from $\tilde{x}$ is nowhere greater than $\alpha\tilde{x}$. It should be mentioned that both of x and α are uncertain.

4.5.2 System Requirements

The system requirement is highly dependent on the nature of the problem under study. This can be the minimum revenue a company may expect to gain or the maximum money a customer may be willing to pay. Two important subjects should be clarified; first, reaching to the minimum requirements is subject to risk because of uncertain parameters of the problem. Second, the goal is not minimizing the cost that customer should pay or maximizing the revenue that a company may gain. The main purpose of IGDT is to help the decision maker to set the decision variables to the values which hedges him against the risk of not reaching the minimum requirements at presence of the uncertainties of uncontrollable parameters. The minimum requirement can be defined as not surpassing a predefined limit, i.e. r_c, for a given cost function, i.e. $f(x, \bar{q})$, as follows:

$$\begin{aligned} & \text{Goal} : f(x, \bar{q}) \leq r_c \\ & \text{Subject to} \\ & H(x, \bar{q}) = 0 \\ & G(x, \bar{q}) \geq 0 \end{aligned} \tag{4.20}$$

Where, x is the input parameter and $\bar{q}$ is the decision variable. H and G are the equality and inequality constraints, respectively.

4.5.3 Robustness

The robustness of a decision $\bar{q}$ based on the requirement r_c, i.e. $\hat{\alpha}(\bar{q}, r_c)$, is defined as the maximum value of α at which the decision maker is sure that the minimum requirements are always satisfied [108], as follows:

$$\begin{aligned} &\hat{\alpha}(\bar{q}, r_c) = \max \alpha \\ &St: \\ &\text{minimum requirements are always satisfied} \end{aligned} \tag{4.21}$$

The decision making policy is defined as finding the decision variables, i.e. $\bar{q}$, which maximizes the robustness, as formulated below:

$$\begin{aligned} &\max_{\bar{q}} \hat{\alpha}(\bar{q}, r_c) \\ \forall x \in U(\alpha, \tilde{x}) \Longrightarrow &f(x, \bar{q}) \leq r_c \\ &H(x, \bar{q}) = 0 \\ &G(x, \bar{q}) \geq 0 \end{aligned} \tag{4.22}$$

4.6 Conclusions

This chapter presents the proposed methods for uncertainty modeling in this thesis. Section 4.2.1 describes the probabilistic methods including Monte Carlo and Two Point Estimate methods. Section 4.3 described the fuzzy modeling of uncertainties. In Section 4.4 the proposed model for mixed probabilistic-possibilistic uncertainties is explained. Section 4.5 describes the information gap decision theory which will be useful in severe uncertain environment where no PDF nor membership function is available.

CHAPTER 5

Distribution Network Planning Under Centrally Controlled DG Investment

5.1 Introduction

This section presents a long-term dynamic multi-objective model for simultaneous distribution network and distributed generation investment. It is assumed that the DNO can perform investment in both DG and distribution network. The proposed model aims to cover all three aspects of DG planning problem, i.e., siting, sizing and timing of investment simultaneously, when various attributes of the proposed plans, and a variety of DG technologies are considered.

5.2 Problem Formulation

5.2.1 Assumptions

The following assumptions are employed in problem formulation:

- The connection of a DG unit to a bus, is modeled as a negative PQ load as shown in Fig.5.1.
- DNO is authorized to perform investment in DG units

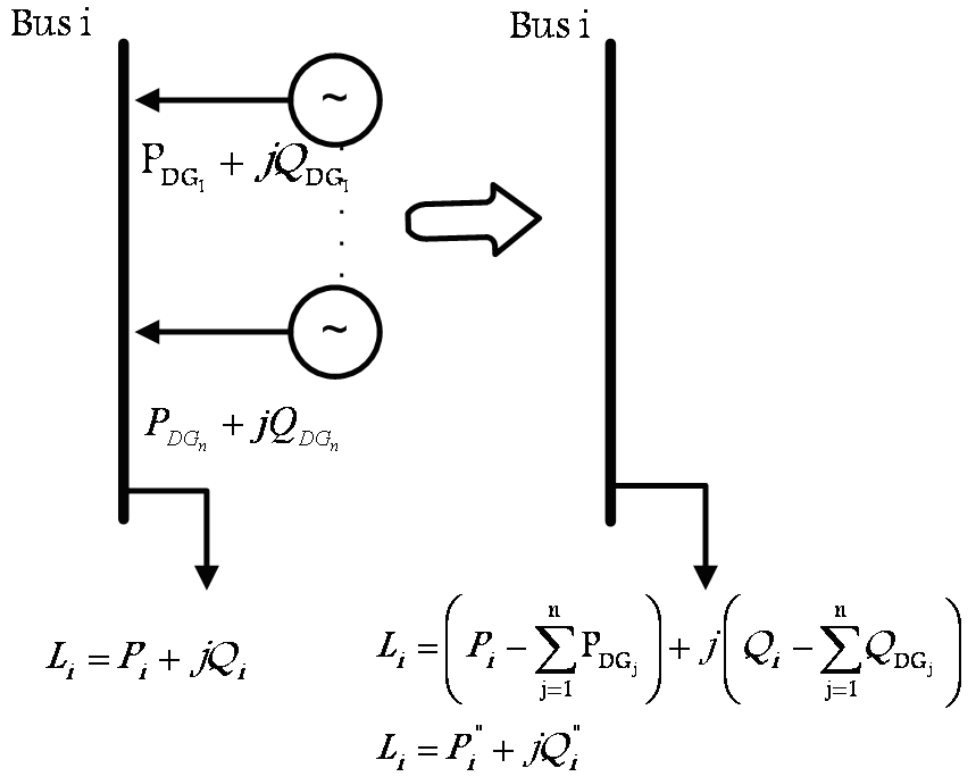

Figure 5.1: The DG connection model to the i^{th} bus

5.2.2 Decision variables

The decision variables are the number of DG units (including non-renewable and wind turbines), to be installed in each bus in each year, i.e., $\xi_{i,t}^{dg}$, respectively; binary investment decision in feeder ℓ in the year t, i.e. γ_t^{ℓ} which can be 0 or 1, and finally the number of new installed transformers in the year t, i.e. ψ_t^{tr}.

5.2.3 Uncertainty modeling

The electricity price and electric load are both uncertain in deregulated environment but these parameters are specifically tied together. An increase/decrease in electric load will tend to increase/decrease in electricity price. Without loss of generality, the correlation between wind speed and load-price pattern can be "approximately" assumed to be independent [109]. If any correlation exists between load-price and wind pattern this can be easily incorporated in scenario generation procedure. The price and load duration curves are divided into N_{dl} levels in each year as shown in Fig. 5.2. The vertical axis in Fig.

5.2, shows the demand/price level factors (the ratio of load/price to the peak value of load/price in this level). The duration of each level is described by τ_{dl}. It is assumed that the demand/price level factors (λ_{dl}, D_{dl}) are normally distributed around their expected values as shown in Fig. 5.2. Each normal distribution is divided into 7 states and the probability of each state is specified in Fig. 5.2. Although the expected price and demand values are dependent but,in each demand level, the variation of price and electric load around its expected value can be assumed to be independent. The electricity price, electrical load and wind generation are modeled as follows:

5.2.3.1 Electricity price

The price of energy purchased from the grid is competitively determined in a liberalized market environment. Assuming a peak electricity price of ρ, the electricity price in demand level dl, and state s can be calculated as:

$$EP^{\lambda}_{dl,s} = \rho \ . \ \lambda_{dl,s} \tag{5.1}$$

5.2.3.2 Electrical load

Assuming a peak load of $S^{D}_{i,peak}$ and a demand growth rate of ϵ_D, the demand in bus i, in year t, demand level dl and state s can be calculated as:

$$S^{D}_{i,t,dl,s} = S^{D}_{i,peak} \ . \ D_{dl,s} \ . \ (1+\epsilon_D)^t \tag{5.2}$$

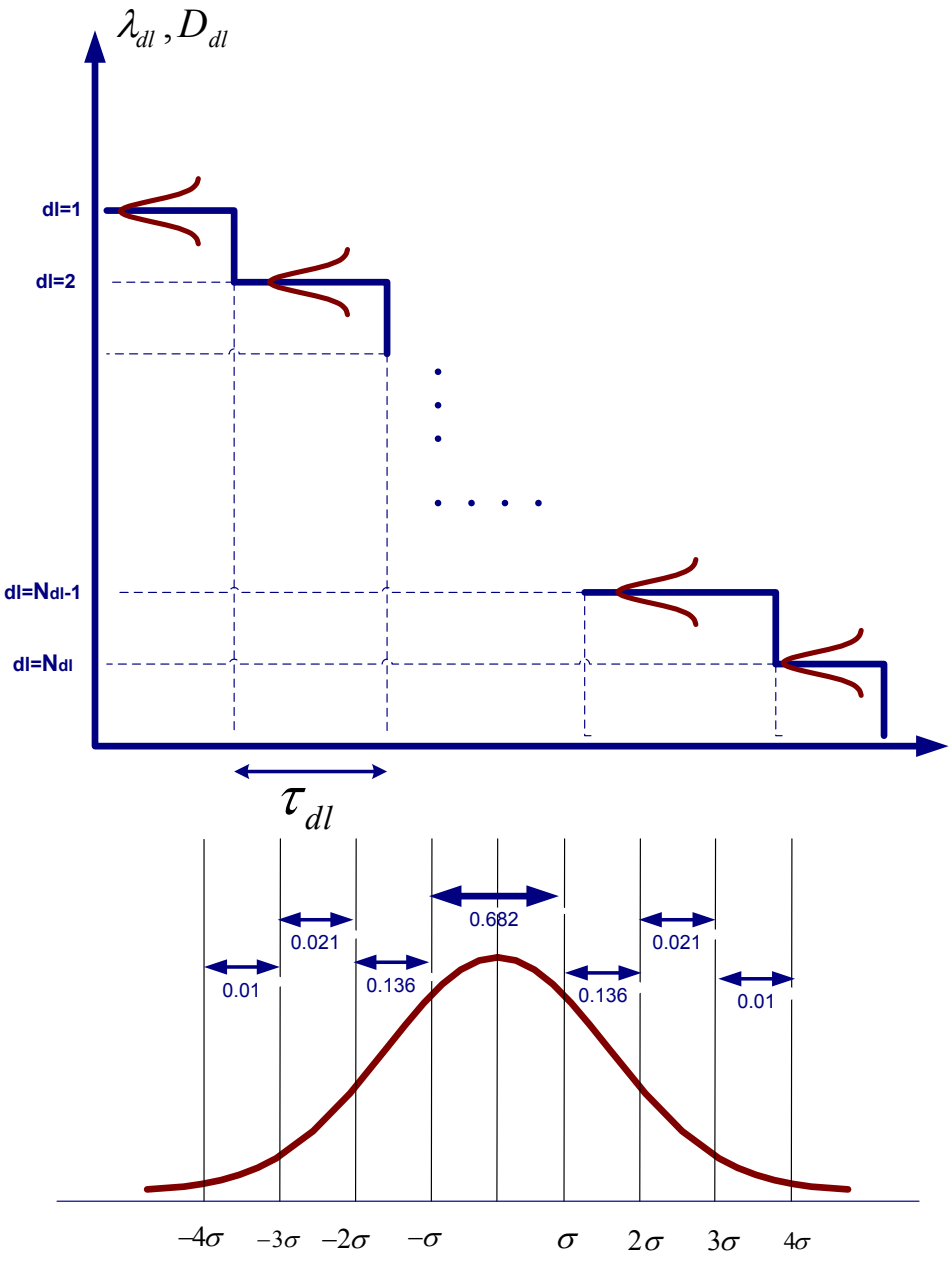

Figure 5.2: The Uncertainty modeling of demand and price level factors

5.2.3.3 Wind speed and wind turbine power generation

The generation schedule of a wind turbine highly depends on the wind speed in the site. There are various methods to model wind behavior. In this work, the variation of wind speed, i.e. v, is modeled using a Rayleigh PDF and its characteristic function which relates the wind speed and the output of a wind turbine.

$$PDF(v) = (\frac{2v}{c^2})\ exp[-(\frac{v}{c})^2] \tag{5.3}$$

where c is the scale factor of the Rayleigh PDF of wind speed in the zone under study. The generated power of the wind turbine is determined using its characteristics as follows:

$$P^w_{i,t}(v) = \sum_{\acute{t}=1}^{t} \xi^{dg}_{i,t}. \begin{cases} 0 & \text{if } v \leq v^{cut}_{in} \text{ or } v \geq v^{cut}_{out} \\ \frac{v - v^{cut}_{in}}{v_{rated} - v^{cut}_{in}} P^w_{i,r} & \text{if } v^{cut}_{in} \leq v \leq v_{rated} \\ P^w_{i,r} & \text{else} \end{cases} \tag{5.4}$$

Where, $P^w_{i,r}$ is the rated power of wind turbine installed in bus i, P^w_i is the generated power of wind turbine in bus i, v^{cut}_{out} is the cut out speed, v^{cut}_{in} is the cut in speed and v_{rated} is the rated speed of the wind turbine. The speed-power curve of a typical wind turbine is depicted in Fig. 2.1. Using the technique described in [109], the PDF of wind speed is divided into several states. In each state, the probability of falling into this state is calculated as follows:

$$prob^w_s = \int_{V_{1,s}}^{V_{2,s}} (\frac{2v}{c^2})\ exp[-(\frac{v}{c})^2]dv \tag{5.5}$$
$$v_s = \frac{V_{2,s} + V_{1,s}}{2}$$

The generated power of wind turbine is calculated using the v_s, as obtained in (5.5), and (5.4).

5.2.3.4 Combined states model

As it is already mentioned, the states of each demand level are independent (the correlation between load and price is already considered in their mean value of D_{dl} and λ_{dl}. In each demand level, the states are combined to construct the whole set of states as follows:

$$C(s) = load(s)\ .\ price(s)\ .\ wind(s) \tag{5.6}$$

$$Prob_s^c = prob_s^l\ .\ prob_s^\lambda\ .\ prob_s^w \tag{5.7}$$

where $Prob_s^c$ is the probability of each combined state.

5.2.4 Constraints

5.2.4.1 Power flow constraints

The load flow equations is slightly different in distribution network with transmission network. The main source of the difference is the unbalance loads and three phase modeling and also neutral current. As indicated in many references, the traditional single line load flow modeling can be used in DG planning applications. In this thesis, the main goal is proposing a new method for DG integration and modeling the different types of uncertainties. Therefore we have not considered the impacts of unbalanced loads or four wires modeling of the load flow calculations which will increase the complexity of the calculations. In this paper, for avoiding the complexity of the calculations, the impact of unbalanced phases/loads in distribution network load flow equations is neglected. However if an unbalanced multiphase load-flow algorithm is needed with the capability to model all components and network features, the algorithms can be extended using the methods proposed in [110, 111]. If the speed of the convergence is of concern (due to radial configuration of the distribution networks and sparse Ybus Matrix), although the traditional load flow techniques still work but distribution load flow techniques can be used to decrease the computational burden [112]. Here for simplicity and without loss of generality we have used the model used in the earlier published works in DG studies [].

The flow equations that should be satisfied for each configuration and state are:

$$
\begin{aligned}
P^{net}_{i,t,dl,s} &= -P^{D}_{i,t,dl,s} + P^{dg}_{i,t,dl,s} \\
Q^{net}_{i,t,dl,s} &= -Q^{D}_{i,t,dl,s} + Q^{dg}_{i,t,dl,s} \\
P^{net}_{i,t,dl,s} &= V_{i,t,dl,s} \sum Y^{t}_{ij} V_{j,t,dl,s} cos(\delta_{i,t,dl,s} - \delta_{j,t,dl,s} - \theta_{ij}) \\
Q^{net}_{i,t,dl,s} &= V_{i,t,dl,s} \sum Y^{t}_{ij} V_{j,t,dl,s} sin(\delta_{i,t,dl,s} - \delta_{j,t,dl,s} - \theta_{ij})
\end{aligned}
\tag{5.8}
$$

5.2.4.2 Operating limits of DG units

Each DG should be operated considering its capacity limits, i.e.:

The DG units should be operated considering the limits of their primary resources, i.e.:

$$
P^{dg}_{i,t,dl} \leq \sum_{\acute{t}=1}^{t} \xi^{dg}_{i,\acute{t}} \times \overline{P}^{dg}_{lim} \tag{5.9}
$$

Where, $\xi^{dg}_{i,t}$ is the number of DG units installed in bus i in year t. $\overline{P}^{dg}_{lim}$ is the operating limit of DG unit.

The power factor of DG unit is kept constant [113] in all demand levels as (5.10).

$$
cos\varphi_{dg} = \frac{P^{dg}_{i,t,dl}}{\sqrt{(P^{dg}_{i,t,dl})^2 + (Q^{dg}_{i,t,dl})^2}} \tag{5.10}
$$

5.2.4.3 Fuzzy technical satisfaction

The satisfaction of soft constraints can be modeled by fuzzy sets. The idea of fuzzifying the technical constraints was used by [114]. In the present work, this idea is extended to model the problem with different states for a dynamic planning problem. Fuzzy modeling is used to quantify the value of satisfaction of technical constraints of voltages and thermal limits of feeders and substation, as follow:

Voltage profile The voltage magnitude of each bus should be kept between the safe operation limits. However, the DNO may ignore violation of these limits to some degree, in hope of achieving a better solution regarding other necessities [114]. The membership

function of the voltage constraint satisfaction is represented by a trapezoidal fuzzy number [33]. Observe that a voltage magnitude between the up and low safe operation limits, i.e., $V_{safe}^{min}, V_{safe}^{max}$ has a satisfactory value of 1. As the voltage exceeds these limits, the value of satisfaction decreases until it becomes zero after the critical voltage values, i.e., $V_{crit}^{min}, V_{crit}^{max}$ (see Table 5.4). This function can be mathematically represented as:

$$\mu_{i,t,dl,s}^{V} = \begin{cases} \frac{V_{i,t,dl,s} - V_{crit}^{min}}{V_{safe}^{min} - V_{crit}^{min}} & V_{crit}^{min} \leq V_{i,t,dl,s} \leq V_{safe}^{min} \\ 1 & V_{safe}^{min} \leq V_{i,t,dl,s} \leq V_{safe}^{max} \\ \frac{V_{i,t,dl,s} - V_{crit}^{max}}{V_{safe}^{max} - V_{crit}^{max}} & V_{safe}^{max} \leq V_{i,t,dl,s} \leq V_{crit}^{max} \\ 0 & else \end{cases} \tag{5.11}$$

The values obtained from (5.11) show the condition of voltage constraint satisfaction for bus i in state s in year t. Since there are more than one state in a real system, the planner will have different satisfaction levels of voltage constraint for a given bus. To obtain an index which shows the condition of a given bus i in year t, it is proposed in this work to calculate the weighted average of satisfaction of voltage over the states, as follows:

$$\mu_{i,t}^{V} = \frac{1}{8760} \sum_{dl=1}^{N_{dl}} \sum_{s=1}^{N_s} prob_s^c \ . \ \tau_{dl} \ . \ \mu_{i,t,dl,s}^{V} \tag{5.12}$$

In (5.12), if the voltage of bus i does not fully satisfy the constraints in state s but the probability of this dissatisfaction is short, the satisfaction of this bus is not very degraded in the whole year t. The average value of $\mu_{i,t}^{V}$ over all buses of the network, can provide information about the overall voltage condition in year t as follows:

$$\mu_{t}^{V} = \frac{\sum_{i=1}^{N_b} \mu_{i,t}^{V}}{N_b} \tag{5.13}$$

Thermal limit of feeders and Substation To maintain the security of the feeders and the substation, the flow of current/energy passing throw them should be kept below the feeders/substation capacity limit. This is incorporated here, in the form of a fuzzy membership function [33]. A strictly monotonically decreasing and continuous function

is considered for this limit, as follows:

$$\mu^{I}_{\ell,t,dl,s} = \begin{cases} 1 & I_{\ell,t,dl,s} \leq \overline{I}^{safe,t}_{\ell} \\ \frac{I_{\ell,t,dl,s} - \overline{I}^{crit,t}_{\ell}}{\overline{I}^{safe,t}_{\ell} - \overline{I}^{crit,t}_{\ell}} & \overline{I}^{safe,t}_{\ell} \leq I_{\ell,t,s} \leq \overline{I}^{crit,t}_{\ell} \\ 0 & I_{\ell,t,s} \geq \overline{I}^{crit,t}_{\ell} \end{cases} \tag{5.14}$$

$$\overline{I}^{safe,t}_{\ell} = \overline{I}_{\ell} + Cap_{\ell} \ . \ \sum_{\acute{t}=1}^{t} \gamma^{\ell}_{\acute{t}}$$

$$\overline{I}^{safe,t}_{\ell} = 0.9 \times \overline{I}^{crit,t}_{\ell}$$

Similar to the voltage limit, an overall satisfaction value is considered for each feeder, as follows:

$$\mu^{I}_{\ell,t} = \frac{1}{8760} \sum_{dl=1}^{N_{dl}} \sum_{s=1}^{N_s} prob^{c}_{s} \ . \ \tau_{dl} \ . \ \mu^{I}_{\ell,t,dl,s} \tag{5.15}$$

An index is needed to provide information about the overall performance of the system regarding the thermal limits. The average value of $\mu^{I}_{\ell,t}$ over all feeders of the network can provide such information as follows:

$$\mu^{I}_{t} = \frac{\sum_{\ell=1}^{N_\ell} \mu^{I}_{\ell,t}}{N_\ell} \tag{5.16}$$

For substation capacity constraint, also, the same philosophy holds, as follows:

$$\mu^{S^{grid}}_{t,dl,s} = \begin{cases} 1 & S^{grid}_{t,dl,s} \leq \overline{S}^{tr}_{safe,t} \\ \frac{S^{grid}_{t,dl,s} - \overline{S}^{tr}_{crit,t}}{\overline{S}^{tr}_{safe,t} - \overline{S}^{tr}_{crit,t}} & \overline{S}^{tr}_{safe,t} \leq S^{grid}_{t,dl,s} \leq \overline{S}^{tr}_{crit,t} \\ 0 & S^{grid}_{t,dl,s} \geq \overline{S}^{tr}_{crit,t} \end{cases} \tag{5.17}$$

$$\mu^{S^{grid}}_{t} = \frac{1}{8760} \sum_{dl=1}^{N_{dl}} \sum_{s=1}^{N_s} prob^{c}_{s} \ . \ \tau_{dl} \ . \ \mu^{S^{grid}}_{t,dl,s}$$

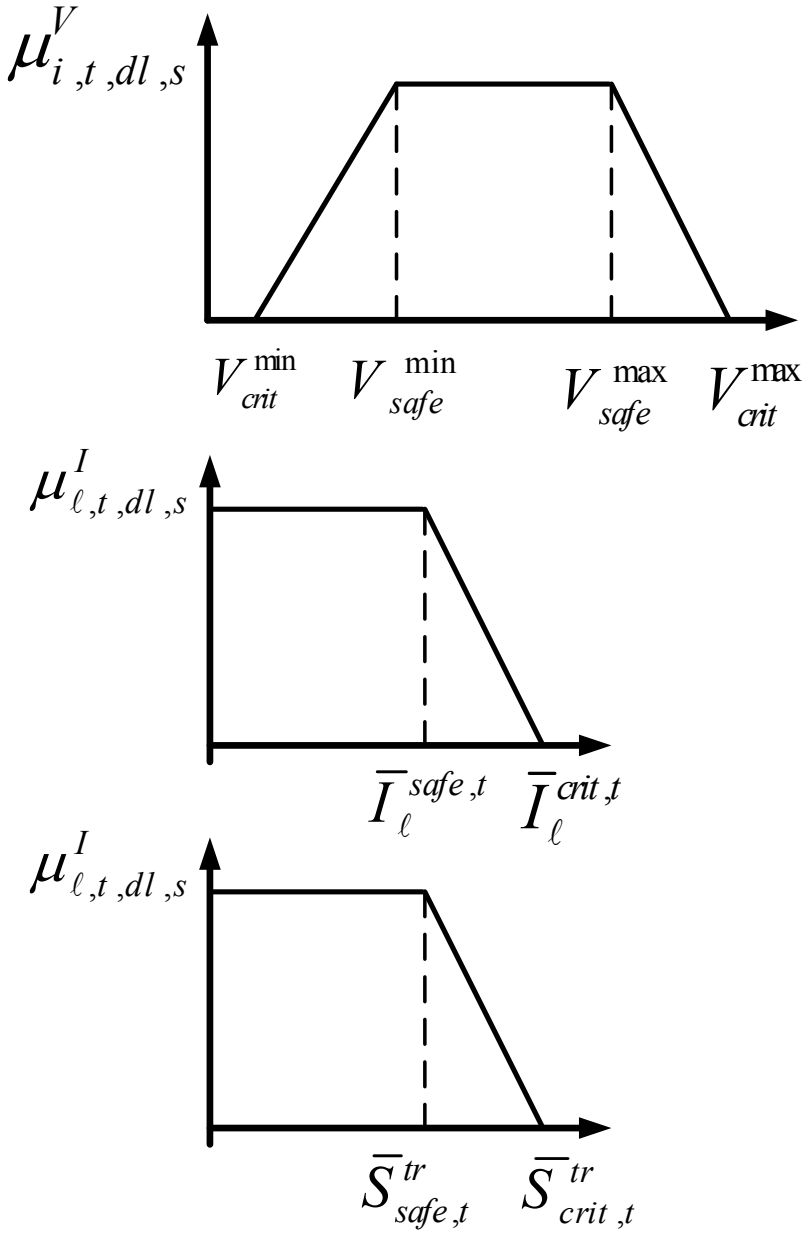

Figure 5.3: Fuzzy technical constraint satisfaction

5.2.5 Objective functions

The proposed model minimizes three objective functions, namely, technical dissatisfaction, total costs and total emissions of the planning problem, as follows:

$$min\,\{OF_1, OF_2, OF_3\}$$
$$subject\ to:$$
$$(5.2) \rightarrow (5.17)$$

The objective functions are formulated next.

5.2.5.1 Technical dissatisfaction

The first objective function to be minimized is dissatisfaction of technical constraints. The technical dissatisfaction, denoted by TD_t, is defined as the maximum dissatisfaction of all technical constraints as follows:

$$TD_t = 1 - min\left\{\mu_t^V, \mu_t^I, \mu_t^{S^{grid}}\right\} \tag{5.18}$$

The objective function to be minimized is proposed here as the multiplication of maximum and average value of yearly technical dissatisfaction over planning horizon as:

$$OF_1 = w_{avg}\ .\ \sum_{t=1}^{T} \frac{TD_t}{T} + w_{sev}.(1 - \min_{t,dl,s,\ell}[\mu_{t,dl,s}^{S^{grid}}, \mu_{i,t,dl,s}^{V}, \mu_{\ell,t,dl,s}^{I}]) \tag{5.19}$$

By minimizing the OF_1, the algorithm tries to simultaneously improve the overall satisfaction of the network, represented by $\sum_{t=1}^{T} \frac{TD_t}{T}$, and the severity of technical dissatisfaction over the planning horizon, represented by the second term. In (5.19) the values of w_{sev} and w_{avg} are the weighting factor representing the importance of severity of technical dissatisfaction and the average dissatisfaction of technical constraints. If w_{sev} is chosen much more bigger than w_{avg}, then the algorithm tries to find solutions which fully satisfy the technical constraints. On the other hand, if w_{avg} is bigger than w_{sev}, then the technical satisfactions of the solutions are more relaxed.

5.2.5.2 Total costs

The second objective function, i.e., OF_2, to be minimized is the total costs which includes the cost of electricity purchased from the grid, the Investment costs and the operating costs of the DG units. The cost of purchasing electricity from the grid can be determined as:

$$TGC = \sum_{t=1}^{T} \sum_{dl=1}^{N_{dl}} \sum_{s=1}^{N_s} prob_s^c \ . \ EP_{t,s}^{\lambda} \ . \ P_{t,s}^{grid} \ . \ \tau_{dl} . \frac{1}{(1+d)^t} \tag{5.20}$$

where T is the planning horizon, N_{dl} is the number of demand levels and N_s is the number of scenarios (states). Investment costs of the DG units can be calculated as:

$$DGIC = \sum_{t=1}^{T} \sum_{i=1}^{N_b} \sum_{dg} \xi_{i,t}^{dg} \ . \ IC_{dg} \ . \ \frac{1}{(1+d)^t} \tag{5.21}$$

where N_b is the number buses in the network.
The operating costs of the DG units can be calculated as:

$$DGOC = \sum_{t=1}^{T} \sum_{i=1}^{N_b} \sum_{dl=1}^{N_{dl}} \sum_{dg} \sum_{s=1}^{N_s} prob_s^c \ . \ \tau_{dl} \ . \ OC_{dg} \ . \ P_{i,t,s}^{dg} \ . \ \frac{1}{(1+d)^t} \tag{5.22}$$

The reinforcement cost of the distribution network is the sum of all costs paid for investment and operation of new feeders and transformers. The total feeder reinforcement cost, i.e. FRC, and substation reinforcement cost, i.e. SC, are calculated as follows:

$$FRC = \sum_{\acute{t}=1}^{T} \sum_{\ell=1}^{N_\ell} C_\ell . d_\ell \ . \ \gamma_{\acute{t}}^{\ell} . \frac{1}{(1+d)^t} \tag{5.23}$$

$$SRC = \sum_{\acute{t}=1}^{T} C_{tr} \ . \ \psi_{\acute{t}}^{tr} \ . \ \frac{1}{(1+d)^t}$$

Where, FRC and SRC are the total feeder and substation reinforcement cost, respectively. C_ℓ, C_{tr} are the cost of each feeder and transformer, respectively.
Thus, OF_2 is defined as:

$$OF_2 = DGIC + DGOC + TGC + FRC + SRC \tag{5.24}$$

5.2.5.3 Total emission

The third objective function, i.e., OF_3, is the total CO_2 produced by the DG units and the main grid. OF_3 can be formulated as:

$$OF_3 = \sum_{t=1}^{T} \sum_{dl=1}^{N_{dl}} \sum_{s=1}^{N_s} prob_s^c \ . \ \tau_{dl} . \Big[E_{grid} \ . \ P_{t,dl,s}^{grid} + \sum_{i=1}^{N_b} \sum_{dg} E_{dg} \ . \ P_{i,t,dl,s}^{dg} \Big] \tag{5.25}$$

5.3 Simulation results

The proposed methodology is applied to a realistic 201-node 10 kV distribution system which is shown in Fig.5.4. The technical data of this network can be found in [115].

Three DG technology options, namely, Micro Turbine (MT), Wind Turbine (WT), Gas Turbine (GT) are considered here. It is also assumed that all buses are candidate for DG investment and more than one DG can be installed in a specific bus. The stopping criterion is reaching to a predefined maximum number of iterations. The Rayleigh parameter of the wind speed in each wind farm has been assumed to be $c = 8.78$ and the other characteristics of wind turbine are given in Table 5.1. Using the technique described in [109], the PDF of wind speed is divided into twelve states as given in Table 5.2.

Table 5.1: The technical characteristics of wind turbines

v_{in}^{cut} (m/s)	v_{rated} (m/s)	v_{out}^{cut} (m/s)	$P_{i,r}^{w}$ (MW)
3	13	25	0.5

The forecasted values of demand and price level factors are given in Table 5.3 [116].

The σ value of each demand level is assumed to be 1% of its forecasted value. Other simulation assumptions and characteristics of the DG units [117, 118] are presented in Table 5.4 and Table 5.5 [117, 118], respectively.

The presented solution algorithm (see Fig. 3.2) was implemented in MATLAB. The number of demand levels,i.e. N_{dl} is assumed to be 24 and the duration of each demand level is 365hr. In (5.19) the values of w_{avg} and w_{sev} are assumed to be 0.8 and 0.2, respectively.

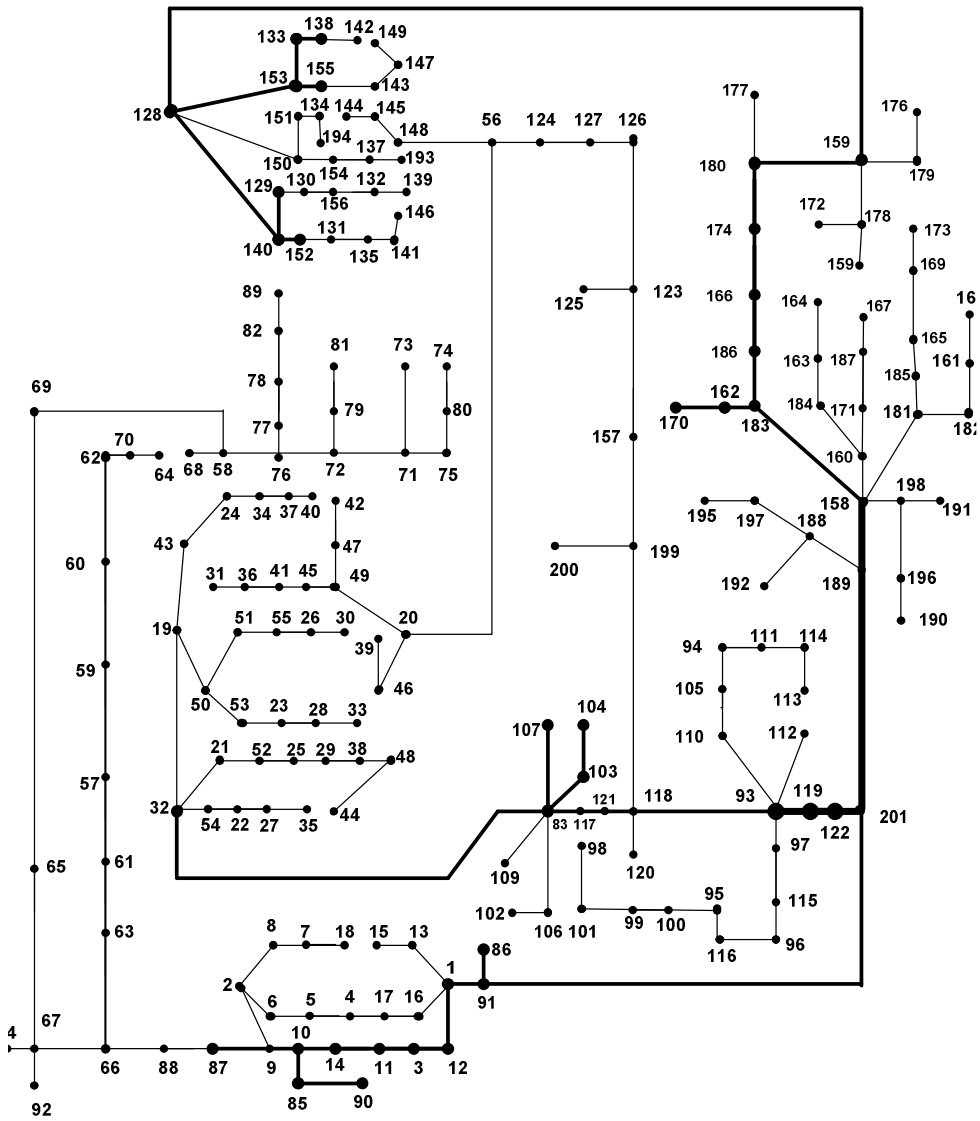

Figure 5.4: Single-line diagram of the real system under study

Table 5.2: Wind turbine generation states

State	wp_s (%)	$Prob_s^w$
1	0	0.1105
2	5	0.0772
3	15	0.0895
4	25	0.0961
5	35	0.0973
6	45	0.0936
7	55	0.0863
8	65	0.0764
9	75	0.0652
10	85	0.0537
11	95	0.0428
12	100	0.1115

Table 5.3: The forecasted values of demand and price level factors in each demand level

dl	D_{dl}	λ_{dl}
1	0.8363	0.9128
2	0.7883	0.6372
3	0.7522	0.4841
4	0.7352	0.4849
5	0.7278	0.4808
6	0.7324	0.4849
7	0.7899	0.6449
8	0.8741	0.9655
9	0.8804	0.9391
10	0.9184	0.9662
11	0.9586	0.9690
12	1.0000	0.9798
13	0.9972	0.9742
14	0.9880	0.9683
15	0.9464	0.9582
16	0.9496	0.9582
17	0.9687	0.9798
18	0.9807	0.9856
19	0.9676	0.9798
20	0.9367	0.9587
21	0.9587	0.9813
22	0.9803	1.0000
23	0.9045	0.9511
24	0.8364	0.9152

Table 5.4: Data used in the study

Parameter	Unit	Value
T	year	8
$\overline{S}^{tr}_{safe,t=0}$	MVA	32
$\overline{S}^{tr}_{crit,t=0}$	MVA	40
E_{grid}	$kgCO_2/MWh$	632
ρ	\$/MWh.	60
ϵ_D	%	1
d	%	12
V^{max}_{safe}	Pu	1.05
V^{max}_{crit}	Pu	(1+5%) . V^{max}_{safe}
V^{min}_{safe}	Pu	0.95
V^{min}_{crit}	Pu	(1-5%) . V^{min}_{safe}
$\overline{I}^{safe,t}_{\ell}$	A	0.9 $\times \overline{I}^{crit,t}_{\ell}$
N_p		80
Maximum iteration		1000

Table 5.5: Characteristics of the DG units

Technology	E_{dg} $(kgCO_2/MWh)$	IC_{dg} $(k\$/MVA)$	OMC_{dg} $\$/MWh)$
MT	503	148	70
GT	773	500	50
CHP	517	1491	45
WT	0	1500	5

5.3.1 Case A: mixed renewable and conventional DG technologies

In this case, both renewable and controllable DG technologies have been considered. The uncertainties of electric load, electricity price and renewable power generation have been considered. Solving the (5.6) gives $7 \times 7 \times 12 = 588$ states for each demand level. All of the states are given in Table 5.6. It is clear that solving the evaluation process for all of these states (for all demand levels) imposes a heavy computational burden. In order to resolve this problem, a scenario reduction technique proposed in [103] has been used to reduce the number of states (see section 4.2.3 for more details). The scenario set is reduced into 110 states (this is chosen based on trial and error) using the described technique. These states are given in Table 5.8. The formulated problem is solved using the proposed two-stage algorithm and 80 non-inferior solutions are found. The planner can choose the best solution based on the planning criteria, as further discussed next. The Pareto optimal front of the search space, found in the first stage, is depicted in Fig.5.5.

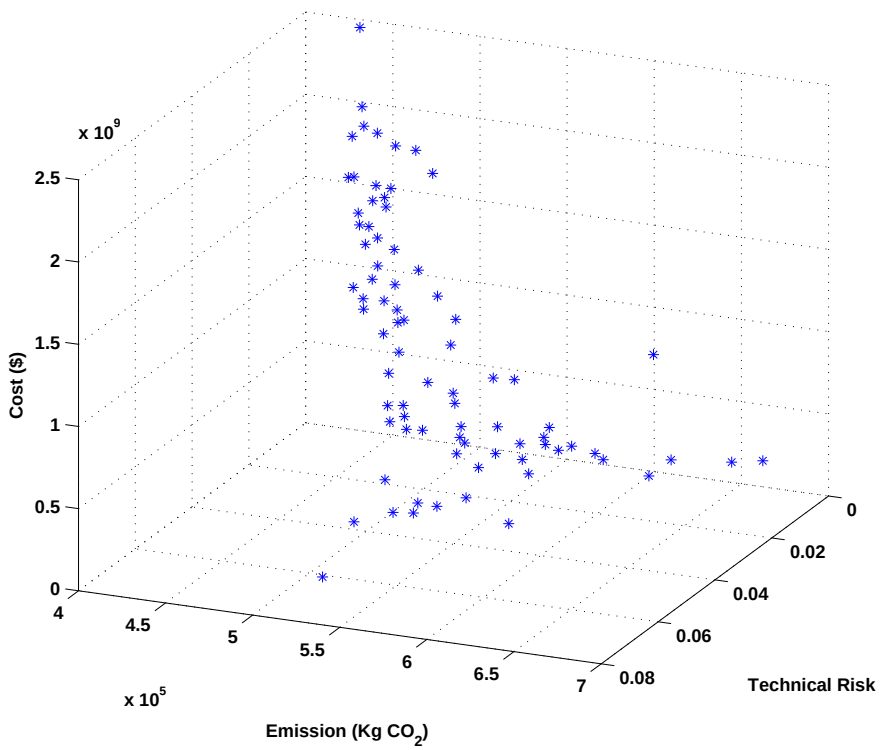

Figure 5.5: Pareto optimal front found by the algorithm in uncertain dynamic DG/network investment model

The variation ranges of all objective functions are given in Table 5.9.

Table 5.6: All combined states

#	D_s	λ_s	w_s	$prob_s^c$	#	D_s	λ_s	w_s	$prob_s^c$	#	D_s	λ_s	w_s	$prob_s^c$	#	D_s	λ_s	w_s	$prob_s^c$	#	D_s	λ_s	w_s	$prob_s^c$	#	D_s	λ_s	w_s	$prob_s^c$
1	0.965	0.965	0	0.0000002	50	0.965	1.015	0.05	0.0000136	99	0.97500000	0.975	0.15	0.0000414	148	0.975	1.025	0.25	4.44E-05	197	0.985	0.985	0.35	0.001797015	246	0.985	1.035	0.45	1.65E-05
2	0.965	0.965	0.05	0.0000001	51	0.965	1.015	0.15	0.0000158	100	0.97500000	0.975	0.25	0.0000444	149	0.975	1.025	0.35	4.50E-05	198	0.985	0.985	0.45	0.001728681	247	0.985	1.035	0.55	1.52E-05
3	0.965	0.965	0.15	0.0000002	52	0.965	1.015	0.25	0.0000170	101	0.97500000	0.975	0.35	0.0000450	150	0.975	1.025	0.45	4.33E-05	199	0.985	0.985	0.55	0.001593858	248	0.985	1.035	0.65	1.35E-05
4	0.965	0.965	0.25	0.0000002	53	0.965	1.015	0.35	0.0000172	102	0.97500000	0.975	0.45	0.0000433	151	0.975	1.025	0.55	3.99E-05	200	0.985	0.985	0.65	0.001411017	249	0.985	1.035	0.75	1.15E-05
5	0.965	0.965	0.35	0.0000002	54	0.965	1.015	0.45	0.0000165	103	0.97500000	0.975	0.55	0.0000399	152	0.975	1.025	0.65	3.53E-05	201	0.985	0.985	0.75	0.001204166	250	0.985	1.035	0.85	9.49E-06
6	0.965	0.965	0.45	0.0000002	55	0.965	1.015	0.55	0.0000152	104	0.97500000	0.975	0.65	0.0000353	153	0.975	1.025	0.75	3.01E-05	202	0.985	0.985	0.85	0.000991775	251	0.985	1.035	0.95	7.56E-06
7	0.965	0.965	0.55	0.0000001	56	0.965	1.015	0.65	0.0000135	105	0.97500000	0.975	0.75	0.0000301	154	0.975	1.025	0.85	2.48E-05	203	0.985	0.985	0.95	0.000790465	252	0.985	1.035	1	1.97E-05
8	0.965	0.965	0.65	0.0000001	57	0.965	1.015	0.75	0.0000115	106	0.97500000	0.975	0.85	0.0000248	155	0.975	1.025	0.95	1.98E-05	204	0.985	0.985	1	0.002057425	253	1	0.965	0	9.81E-05
9	0.965	0.965	0.75	0.0000001	58	0.965	1.015	0.85	0.0000095	107	0.97500000	0.975	0.95	0.0000198	156	0.975	1.025	1	5.15E-05	205	0.985	1	0	0.01025057	254	1	0.965	0.05	6.85E-05
10	0.965	0.965	0.85	0.0000001	59	0.965	1.015	0.95	0.0000076	108	0.97500000	0.975	1	0.0000515	157	0.975	1.035	0	3.09E-06	206	0.985	1	0.05	0.007161484	255	1	0.965	0.15	7.94E-05
11	0.965	0.965	0.95	0.0000001	60	0.965	1.015	1	0.0000197	109	0.97500000	0.985	0	0.0003229	158	0.975	1.035	0.05	2.16E-06	207	0.985	1	0.15	0.008302498	256	1	0.965	0.25	8.53E-05
12	0.965	0.965	1	0.0000002	61	0.965	1.025	0	0.0000031	110	0.97500000	0.985	0.05	0.0002256	159	0.975	1.035	0.15	2.50E-06	208	0.985	1	0.25	0.008914749	257	1	0.965	0.35	8.63E-05
13	0.965	0.975	0	0.0000031	62	0.965	1.025	0.05	0.0000022	111	0.97500000	0.985	0.15	0.0002615	160	0.975	1.035	0.25	2.69E-06	209	0.985	1	0.35	0.009026068	258	1	0.965	0.45	8.31E-05
14	0.965	0.975	0.05	0.0000022	63	0.965	1.025	0.15	0.0000025	112	0.97500000	0.985	0.25	0.0002808	161	0.975	1.035	0.35	2.72E-06	210	0.985	1	0.45	0.008682836	259	1	0.965	0.55	7.66E-05
15	0.965	0.975	0.15	0.0000025	64	0.965	1.025	0.25	0.0000027	113	0.97500000	0.985	0.35	0.0002843	162	0.975	1.035	0.45	2.62E-06	211	0.985	1	0.55	0.008005649	260	1	0.965	0.65	6.78E-05
16	0.965	0.975	0.25	0.0000027	65	0.965	1.025	0.35	0.0000027	114	0.97500000	0.985	0.45	0.0002735	163	0.975	1.035	0.55	2.41E-06	212	0.985	1	0.65	0.007087272	261	1	0.965	0.75	5.79E-05
17	0.965	0.975	0.35	0.0000027	66	0.965	1.025	0.45	0.0000026	115	0.97500000	0.985	0.55	0.0002522	164	0.975	1.035	0.65	2.14E-06	213	0.985	1	0.75	0.0060483	262	1	0.965	0.85	4.77E-05
18	0.965	0.975	0.45	0.0000026	67	0.965	1.025	0.55	0.0000024	116	0.97500000	0.985	0.65	0.0002232	165	0.975	1.035	0.75	1.82E-06	214	0.985	1	0.85	0.004981499	263	1	0.965	0.95	3.80E-05
19	0.965	0.975	0.55	0.0000024	68	0.965	1.025	0.65	0.0000021	117	0.97500000	0.985	0.75	0.0001905	166	0.975	1.035	0.85	1.50E-06	215	0.985	1	0.95	0.003970357	264	1	0.965	1	9.89E-05
20	0.965	0.975	0.65	0.0000021	69	0.965	1.025	0.75	0.0000018	118	0.97500000	0.985	0.85	0.0001569	167	0.975	1.035	0.95	1.20E-06	216	0.985	1	1	0.010334059	265	1	0.975	0	0.001621687
21	0.965	0.975	0.75	0.0000018	70	0.965	1.025	0.85	0.0000015	119	0.97500000	0.985	0.95	0.0001251	168	0.975	1.035	1	3.11E-06	217	0.985	1.015	0	0.002040804	266	1	0.975	0.05	0.001132979
22	0.965	0.975	0.85	0.0000015	71	0.965	1.025	0.95	0.0000012	120	0.97500000	0.985	1	0.0003255	169	0.985	0.965	0	1.95E-05	218	0.985	1.015	0.05	0.001425792	267	1	0.975	0.15	0.001313493
23	0.965	0.975	0.95	0.0000012	72	0.965	1.025	1	0.0000031	121	0.97500000	1	0	0.0016217	170	0.985	0.965	0.05	1.36E-05	219	0.985	1.015	0.15	0.001652958	268	1	0.975	0.25	0.001410354
24	0.965	0.975	1	0.0000031	73	0.965	1.035	0	0.0000002	122	0.97500000	1	0.05	0.0011330	171	0.985	0.965	0.15	1.58E-05	220	0.985	1.015	0.25	0.001774853	269	1	0.975	0.35	0.001427965
25	0.965	0.985	0	0.0000195	74	0.965	1.035	0.05	0.0000001	123	0.97500000	1	0.15	0.0013135	172	0.985	0.965	0.25	1.70E-05	221	0.985	1.015	0.35	0.001797015	270	1	0.975	0.45	0.001373664
26	0.965	0.985	0.05	0.0000136	75	0.965	1.035	0.15	0.0000002	124	0.97500000	1	0.25	0.0014104	173	0.985	0.965	0.35	1.72E-05	222	0.985	1.015	0.45	0.001728681	271	1	0.975	0.55	0.00126653
27	0.965	0.985	0.15	0.0000158	76	0.965	1.035	0.25	0.0000002	125	0.97500000	1	0.35	0.0014280	174	0.985	0.965	0.45	1.65E-05	223	0.985	1.015	0.55	0.001593858	272	1	0.975	0.65	0.001121239
28	0.965	0.985	0.25	0.0000170	77	0.965	1.035	0.35	0.0000002	126	0.97500000	1	0.45	0.0013737	175	0.985	0.965	0.55	1.52E-05	224	0.985	1.015	0.65	0.001411017	273	1	0.975	0.75	0.000956869
29	0.965	0.985	0.35	0.0000172	78	0.965	1.035	0.45	0.0000002	127	0.97500000	1	0.55	0.0012665	176	0.985	0.965	0.65	1.35E-05	225	0.985	1.015	0.75	0.001204166	274	1	0.975	0.85	0.000788096
30	0.965	0.985	0.45	0.0000165	79	0.965	1.035	0.55	0.0000001	128	0.97500000	1	0.65	0.0011212	177	0.985	0.965	0.75	1.15E-05	226	0.985	1.015	0.85	0.000991775	275	1	0.975	0.95	0.000628129
31	0.965	0.985	0.55	0.0000152	80	0.965	1.035	0.65	0.0000001	129	0.97500000	1	0.75	0.0009569	178	0.985	0.965	0.85	9.49E-06	227	0.985	1.015	0.95	0.000790465	276	1	0.975	1	0.001634895
32	0.965	0.985	0.65	0.0000135	81	0.965	1.035	0.75	0.0000001	130	0.97500000	1	0.85	0.0007881	179	0.985	0.965	0.95	7.56E-06	228	0.985	1.015	1	0.002057425	277	1	0.985	0	0.01025057
33	0.965	0.985	0.75	0.0000115	82	0.965	1.035	0.85	0.0000001	131	0.97500000	1	0.95	0.0006281	180	0.985	0.965	1	1.97E-05	229	0.985	1.025	0	0.000322864	278	1	0.985	0.05	0.007161484
34	0.965	0.985	0.85	0.0000095	83	0.965	1.035	0.95	0.0000001	132	0.97500000	1	1	0.0016349	181	0.985	0.975	0	0.000322864	230	0.985	1.025	0.05	0.000225567	279	1	0.985	0.15	0.008302498
35	0.965	0.985	0.95	0.0000076	84	0.965	1.035	1	0.0000002	133	0.97500000	1.015	0	0.0003229	182	0.985	0.975	0.05	0.000225567	231	0.985	1.025	0.15	0.000261506	280	1	0.985	0.25	0.008914749
36	0.965	0.985	1	0.0000197	85	0.975	0.965	0	0.0000031	134	0.97500000	1.015	0.05	0.0002256	183	0.985	0.975	0.15	0.000261506	232	0.985	1.025	0.25	0.00028079	281	1	0.985	0.35	0.009026068
37	0.965	1	0	0.0000981	86	0.975	0.965	0.05	0.0000022	135	0.97500000	1.015	0.15	0.0002615	184	0.985	0.975	0.25	0.00028079	233	0.985	1.025	0.35	0.000284296	282	1	0.985	0.45	0.008682836
38	0.965	1	0.05	0.0000685	87	0.975	0.965	0.15	0.0000025	136	0.97500000	1.015	0.25	0.0002808	185	0.985	0.975	0.35	0.000284296	234	0.985	1.025	0.45	0.000273485	283	1	0.985	0.55	0.008005649
39	0.965	1	0.15	0.0000794	88	0.975	0.965	0.25	0.0000027	137	0.97500000	1.015	0.35	0.0002843	186	0.985	0.975	0.45	0.000273485	235	0.985	1.025	0.55	0.000252156	284	1	0.985	0.65	0.007087272
40	0.965	1	0.25	0.0000853	89	0.975	0.965	0.35	0.0000027	138	0.97500000	1.015	0.45	0.0002735	187	0.985	0.975	0.55	0.000252156	236	0.985	1.025	0.65	0.000223229	285	1	0.985	0.75	0.0060483
41	0.965	1	0.35	0.0000863	90	0.975	0.965	0.45	0.0000026	139	0.97500000	1.015	0.55	0.0002522	188	0.985	0.975	0.65	0.000223229	237	0.985	1.025	0.75	0.000190505	286	1	0.985	0.85	0.004981499
42	0.965	1	0.45	0.0000831	91	0.975	0.965	0.55	0.0000024	140	0.97500000	1.015	0.65	0.0002232	189	0.985	0.975	0.75	0.000190505	238	0.985	1.025	0.85	0.000156903	287	1	0.985	0.95	0.003970357
43	0.965	1	0.55	0.0000766	92	0.975	0.965	0.65	0.0000021	141	0.97500000	1.015	0.75	0.0001905	190	0.985	0.975	0.85	0.000156903	239	0.985	1.025	0.95	0.000125055	288	1	0.985	1	0.010334059
44	0.965	1	0.65	0.0000678	93	0.975	0.965	0.75	0.0000018	142	0.97500000	1.015	0.85	0.0001569	191	0.985	0.975	0.95	0.000125055	240	0.985	1.025	1	0.000325494	289	1	1	0	0.051486675
45	0.965	1	0.75	0.0000579	94	0.975	0.965	0.85	0.0000015	143	0.97500000	1.015	0.95	0.0001251	192	0.985	0.975	1	0.000325494	241	0.985	1.035	0	1.95E-05	290	1	1	0.05	0.035970781
46	0.965	1	0.85	0.0000477	95	0.975	0.965	0.95	0.0000012	144	0.97500000	1.015	1	0.0003255	193	0.985	0.985	0	0.002040804	242	0.985	1.035	0.05	1.36E-05	291	1	1	0.15	0.041701877
47	0.965	1	0.95	0.0000380	96	0.975	0.965	1	0.0000031	145	0.97500000	1.025	0	0.0000511	194	0.985	0.985	0.05	0.001425792	243	0.985	1.035	0.15	1.58E-05	292	1	1	0.25	0.044777099
48	0.965	1	1	0.0000989	97	0.975	0.975	0	0.0000511	146	0.97500000	1.025	0.05	0.0000357	195	0.985	0.985	0.15	0.001652958	244	0.985	1.035	0.25	1.70E-05	293	1	1	0.35	0.045336231
49	0.965	1.015	0	0.0000195	98	0.975	0.975	0.05	0.0000357	147	0.97500000	1.025	0.15	0.0000414	196	0.985	0.985	0.25	0.001774853	245	0.985	1.035	0.35	1.72E-05	294	1	1	0.45	0.043612242

Table 5.7: All combined states: continued

#	D_s	λ_s	w_s	$prob_s^c$	#	D_s	λ_s	w_s	$prob_s^c$	#	D_s	λ_s	w_s	$prob_s^c$	#	D_s	λ_s	w_s	$prob_s^c$	#	D_s	λ_s	w_s	$prob_s^c$	#	D_s	λ_s	w_s	$prob_s^c$
295	1	1	0.55	0.04021086	344	1.015	0.965	0.65	1.34976E-05	393	1.015	1.015	0.75	0.001204166	442	1.025	0.975	0.85	0.0000248	491	1.025	1.025	0.95	0.0000198	540	1.035	0.985	1	0.0000197
296	1	1	0.65	0.035598027	345	1.015	0.965	0.75	1.15189E-05	394	1.015	1.015	0.85	0.000991775	443	1.025	0.975	0.95	0.0000198	492	1.025	1.025	1	0.0000515	541	1.035	1	0	0.0000981
297	1	1	0.75	0.030379468	346	1.015	0.965	0.85	9.48718E-06	395	1.015	1.015	0.95	0.000790465	444	1.025	0.975	1	0.0000515	493	1.025	1.035	0	0.0000031	542	1.035	1	0.05	0.0000685
298	1	1	0.85	0.025021126	347	1.015	0.965	0.95	7.56148E-06	396	1.015	1.015	1	0.002057425	445	1.025	0.985	0	0.0003229	494	1.025	1.035	0.05	0.0000022	543	1.035	1	0.15	0.0000794
299	1	1	0.95	0.01994235	348	1.015	0.965	1	1.9681E-05	397	1.015	1.025	0	0.000322864	446	1.025	0.985	0.05	0.0002256	495	1.025	1.035	0.15	0.0000025	544	1.035	1	0.25	0.0000853
300	1	1	1	0.051906023	349	1.015	0.975	0	0.000322864	398	1.015	1.025	0.05	0.000225567	447	1.025	0.985	0.15	0.0002615	496	1.025	1.035	0.25	0.0000027	545	1.035	1	0.35	0.0000863
301	1	1.015	0	0.01025057	350	1.015	0.975	0.05	0.000225567	399	1.015	1.025	0.15	0.000261506	448	1.025	0.985	0.25	0.0002808	497	1.025	1.035	0.35	0.0000027	546	1.035	1	0.45	0.0000831
302	1	1.015	0.05	0.007161484	351	1.015	0.975	0.15	0.000261506	400	1.015	1.025	0.25	0.00028079	449	1.025	0.985	0.35	0.0002843	498	1.025	1.035	0.45	0.0000026	547	1.035	1	0.55	0.0000766
303	1	1.015	0.15	0.008302498	352	1.015	0.975	0.25	0.00028079	401	1.015	1.025	0.35	0.000284296	450	1.025	0.985	0.45	0.0002735	499	1.025	1.035	0.55	0.0000024	548	1.035	1	0.65	0.0000678
304	1	1.015	0.25	0.008914749	353	1.015	0.975	0.35	0.000284296	402	1.015	1.025	0.45	0.000273485	451	1.025	0.985	0.55	0.0002522	500	1.025	1.035	0.65	0.0000021	549	1.035	1	0.75	0.0000579
305	1	1.015	0.35	0.009026068	354	1.015	0.975	0.45	0.000273485	403	1.015	1.025	0.55	0.000252156	452	1.025	0.985	0.65	0.0002232	501	1.025	1.035	0.75	0.0000018	550	1.035	1	0.85	0.0000477
306	1	1.015	0.45	0.008682836	355	1.015	0.975	0.55	0.000252156	404	1.015	1.025	0.65	0.000223229	453	1.025	0.985	0.75	0.0001905	502	1.025	1.035	0.85	0.0000015	551	1.035	1	0.95	0.0000380
307	1	1.015	0.55	0.008005649	356	1.015	0.975	0.65	0.000223229	405	1.015	1.025	0.75	0.000190505	454	1.025	0.985	0.85	0.0001569	503	1.025	1.035	0.95	0.0000012	552	1.035	1	1	0.0000989
308	1	1.015	0.65	0.007087272	357	1.015	0.975	0.75	0.000190505	406	1.015	1.025	0.85	0.000156903	455	1.025	0.985	0.95	0.0001251	504	1.025	1.035	1	0.0000031	553	1.035	1.015	0	0.0000195
309	1	1.015	0.75	0.0060483	358	1.015	0.975	0.85	0.000156903	407	1.015	1.025	0.95	0.000125055	456	1.025	0.985	1	0.0003255	505	1.035	0.965	0	0.0000002	554	1.035	1.015	0.05	0.0000136
310	1	1.015	0.85	0.004981499	359	1.015	0.975	0.95	0.000125055	408	1.015	1.025	1	0.000325494	457	1.025	1	0	0.0016217	506	1.035	0.965	0.05	0.0000001	555	1.035	1.015	0.15	0.0000158
311	1	1.015	0.95	0.003970357	360	1.015	0.975	1	0.000325494	409	1.015	1.035	0	1.95E-05	458	1.025	1	0.05	0.0011330	507	1.035	0.965	0.15	0.0000002	556	1.035	1.015	0.25	0.0000170
312	1	1.015	1	0.010334059	361	1.015	0.985	0	0.002040804	410	1.015	1.035	0.05	1.36E-05	459	1.025	1	0.15	0.0013135	508	1.035	0.965	0.25	0.0000002	557	1.035	1.015	0.35	0.0000172
313	1	1.025	0	0.001621687	362	1.015	0.985	0.05	0.001425792	411	1.015	1.035	0.15	1.58E-05	460	1.025	1	0.25	0.0014104	509	1.035	0.965	0.35	0.0000002	558	1.035	1.015	0.45	0.0000165
314	1	1.025	0.05	0.001132979	363	1.015	0.985	0.15	0.001652958	412	1.015	1.035	0.25	1.70E-05	461	1.025	1	0.35	0.0014280	510	1.035	0.965	0.45	0.0000002	559	1.035	1.015	0.55	0.0000152
315	1	1.025	0.15	0.001313493	364	1.015	0.985	0.25	0.001774853	413	1.015	1.035	0.35	1.72E-05	462	1.025	1	0.45	0.0013737	511	1.035	0.965	0.55	0.0000001	560	1.035	1.015	0.65	0.0000135
316	1	1.025	0.25	0.001410354	365	1.015	0.985	0.35	0.001797015	414	1.015	1.035	0.45	1.65E-05	463	1.025	1	0.55	0.0012665	512	1.035	0.965	0.65	0.0000001	561	1.035	1.015	0.75	0.0000115
317	1	1.025	0.35	0.001427965	366	1.015	0.985	0.45	0.001728681	415	1.015	1.035	0.55	1.52E-05	464	1.025	1	0.65	0.0011212	513	1.035	0.965	0.75	0.0000001	562	1.035	1.015	0.85	0.0000095
318	1	1.025	0.45	0.001373664	367	1.015	0.985	0.55	0.001593858	416	1.015	1.035	0.65	1.35E-05	465	1.025	1	0.75	0.0009569	514	1.035	0.965	0.85	0.0000001	563	1.035	1.015	0.95	0.0000076
319	1	1.025	0.55	0.00126653	368	1.015	0.985	0.65	0.001411017	417	1.015	1.035	0.75	1.15E-05	466	1.025	1	0.85	0.0007881	515	1.035	0.965	0.95	0.0000001	564	1.035	1.015	1	0.0000197
320	1	1.025	0.65	0.001121239	369	1.015	0.985	0.75	0.001204166	418	1.015	1.035	0.85	9.49E-06	467	1.025	1	0.95	0.0006281	516	1.035	0.965	1	0.0000002	565	1.035	1.025	0	0.0000031
321	1	1.025	0.75	0.000956869	370	1.015	0.985	0.85	0.000991775	419	1.015	1.035	0.95	7.56E-06	468	1.025	1	1	0.0016349	517	1.035	0.975	0	0.0000031	566	1.035	1.025	0.05	0.0000022
322	1	1.025	0.85	0.000788096	371	1.015	0.985	0.95	0.000790465	420	1.015	1.035	1	1.97E-05	469	1.025	1.015	0	0.0003229	518	1.035	0.975	0.05	0.0000022	567	1.035	1.025	0.15	0.0000025
323	1	1.025	0.95	0.000628129	372	1.015	0.985	1	0.002057425	421	1.025	0.965	0	3.09E-06	470	1.025	1.015	0.05	0.0002256	519	1.035	0.975	0.15	0.0000025	568	1.035	1.025	0.25	0.0000027
324	1	1.025	1	0.001634895	373	1.015	1	0	0.01025057	422	1.025	0.965	0.05	2.16E-06	471	1.025	1.015	0.15	0.0002615	520	1.035	0.975	0.25	0.0000027	569	1.035	1.025	0.35	0.0000027
325	1	1.035	0	9.81E-05	374	1.015	1	0.05	7.16E-03	423	1.025	0.965	0.15	2.50E-06	472	1.025	1.015	0.25	0.0002808	521	1.035	0.975	0.35	0.0000027	570	1.035	1.025	0.45	0.0000026
326	1	1.035	0.05	6.85E-05	375	1.015	1	0.15	8.30E-03	424	1.025	0.965	0.25	2.69E-06	473	1.025	1.015	0.35	0.0002843	522	1.035	0.975	0.45	0.0000026	571	1.035	1.025	0.55	0.0000024
327	1	1.035	0.15	7.94E-05	376	1.015	1	0.25	8.91E-03	425	1.025	0.965	0.35	2.72E-06	474	1.025	1.015	0.45	0.0002735	523	1.035	0.975	0.55	0.0000024	572	1.035	1.025	0.65	0.0000021
328	1	1.035	0.25	8.53E-05	377	1.015	1	0.35	9.03E-03	426	1.025	0.965	0.45	2.62E-06	475	1.025	1.015	0.55	0.0002522	524	1.035	0.975	0.65	0.0000021	573	1.035	1.025	0.75	0.0000018
329	1	1.035	0.35	8.63E-05	378	1.015	1	0.45	8.68E-03	427	1.025	0.965	0.55	2.41E-06	476	1.025	1.015	0.65	0.0002232	525	1.035	0.975	0.75	0.0000018	574	1.035	1.025	0.85	0.0000015
330	1	1.035	0.45	8.31E-05	379	1.015	1	0.55	8.01E-03	428	1.025	0.965	0.65	2.14E-06	477	1.025	1.015	0.75	0.0001905	526	1.035	0.975	0.85	0.0000015	575	1.035	1.025	0.95	0.0000012
331	1	1.035	0.55	7.66E-05	380	1.015	1	0.65	7.09E-03	429	1.025	0.965	0.75	1.82E-06	478	1.025	1.015	0.85	0.0001569	527	1.035	0.975	0.95	0.0000012	576	1.035	1.025	1	0.0000031
332	1	1.035	0.65	6.78E-05	381	1.015	1	0.75	6.05E-03	430	1.025	0.965	0.85	1.50E-06	479	1.025	1.015	0.95	0.0001251	528	1.035	0.975	1	0.0000031	577	1.035	1.035	0	0.0000002
333	1	1.035	0.75	5.79E-05	382	1.015	1	0.85	4.98E-03	431	1.025	0.965	0.95	1.20E-06	480	1.025	1.015	1	0.0003255	529	1.035	0.985	0	0.0000195	578	1.035	1.035	0.05	0.0000001
334	1	1.035	0.85	4.77E-05	383	1.015	1	0.95	3.97E-03	432	1.025	0.965	1	3.11E-06	481	1.025	1.025	0	0.0000511	530	1.035	0.985	0.05	0.0000136	579	1.035	1.035	0.15	0.0000002
335	1	1.035	0.95	3.80E-05	384	1.015	1	1	1.03E-02	433	1.025	0.975	0	5.11E-05	482	1.025	1.025	0.05	0.0000357	531	1.035	0.985	0.15	0.0000158	580	1.035	1.035	0.25	0.0000002
336	1	1.035	1	9.89E-05	385	1.015	1.015	0	2.04E-03	434	1.025	0.975	0.05	3.57E-05	483	1.025	1.025	0.15	0.0000414	532	1.035	0.985	0.25	0.0000170	581	1.035	1.035	0.35	0.0000002
337	1.015	0.965	0	1.95E-05	386	1.015	1.015	0.05	1.43E-03	435	1.025	0.975	0.15	4.14E-05	484	1.025	1.025	0.25	0.0000444	533	1.035	0.985	0.35	0.0000172	582	1.035	1.035	0.45	0.0000002
338	1.015	0.965	0.05	1.36E-05	387	1.015	1.015	0.15	1.65E-03	436	1.025	0.975	0.25	4.44E-05	485	1.025	1.025	0.35	0.0000450	534	1.035	0.985	0.45	0.0000165	583	1.035	1.035	0.55	0.0000001
339	1.015	0.965	0.15	1.58E-05	388	1.015	1.015	0.25	1.77E-03	437	1.025	0.975	0.35	4.50E-05	486	1.025	1.025	0.45	0.0000433	535	1.035	0.985	0.55	0.0000152	584	1.035	1.035	0.65	0.0000001
340	1.015	0.965	0.25	1.70E-05	389	1.015	1.015	0.35	1.80E-03	438	1.025	0.975	0.45	4.33E-05	487	1.025	1.025	0.55	0.0000399	536	1.035	0.985	0.65	0.0000135	585	1.035	1.035	0.75	0.0000001
341	1.015	0.965	0.35	1.72E-05	390	1.015	1.015	0.45	1.73E-03	439	1.025	0.975	0.55	3.99E-05	488	1.025	1.025	0.65	0.0000353	537	1.035	0.985	0.75	0.0000115	586	1.035	1.035	0.85	0.0000001
342	1.015	0.965	0.45	1.65E-05	391	1.015	1.015	0.55	1.59E-03	440	1.025	0.975	0.65	3.53E-05	489	1.025	1.025	0.75	0.0000301	538	1.035	0.985	0.85	0.0000095	587	1.035	1.035	0.95	0.0000001
343	1.015	0.965	0.55	1.52E-05	392	1.015	1.015	0.65	1.41E-03	441	1.025	0.975	0.75	3.01E-05	490	1.025	1.025	0.85	0.0000248	539	1.035	0.985	0.95	0.0000076	588	1.035	1.035	1	0.0000002

Table 5.8: The reduced selected states

New	Old	D_s	λ_s	w_s	$prob_s^c$	New	Old	D_s	λ_s	w_s	$prob_s^c$
1	132	0.815345895	0.9127907	1	0.00177	56	296	0.8362522	0.9127907	0.65	0.0356
2	193	0.823708417	0.89909884	0	0.00278	57	297	0.8362522	0.9127907	0.75	0.03038
3	194	0.823708417	0.89909884	0.05	0.00194	58	298	0.8362522	0.9127907	0.85	0.02502
4	195	0.823708417	0.89909884	0.15	0.00225	59	299	0.8362522	0.9127907	0.95	0.01994
5	196	0.823708417	0.89909884	0.25	0.00242	60	300	0.8362522	0.9127907	1	0.05191
6	197	0.823708417	0.89909884	0.35	0.00245	61	301	0.8362522	0.926482561	0	0.01025
7	198	0.823708417	0.89909884	0.45	0.00236	62	302	0.8362522	0.926482561	0.05	0.00836
8	199	0.823708417	0.89909884	0.55	0.00217	63	303	0.8362522	0.926482561	0.15	0.0097
9	200	0.823708417	0.89909884	0.65	0.00192	64	304	0.8362522	0.926482561	0.25	0.01041
10	201	0.823708417	0.89909884	0.75	0.00164	65	305	0.8362522	0.926482561	0.35	0.01054
11	202	0.823708417	0.89909884	0.85	0.00135	66	306	0.8362522	0.926482561	0.45	0.01014
12	204	0.823708417	0.89909884	1	0.00277	67	307	0.8362522	0.926482561	0.55	0.00935
13	205	0.823708417	0.9127907	0	0.01197	68	308	0.8362522	0.926482561	0.65	0.00828
14	206	0.823708417	0.9127907	0.05	0.00836	69	309	0.8362522	0.926482561	0.75	0.00706
15	207	0.823708417	0.9127907	0.15	0.0097	70	310	0.8362522	0.926482561	0.85	0.00582
16	208	0.823708417	0.9127907	0.25	0.01041	71	311	0.8362522	0.926482561	0.95	0.00571
17	209	0.823708417	0.9127907	0.35	0.01054	72	312	0.8362522	0.926482561	1	0.01033
18	210	0.823708417	0.9127907	0.45	0.01014	73	313	0.8362522	0.935610468	0	0.00176
19	211	0.823708417	0.9127907	0.55	0.00935	74	324	0.8362522	0.935610468	1	0.00177
20	212	0.823708417	0.9127907	0.65	0.00828	75	361	0.848795983	0.89909884	0	0.00276
21	213	0.823708417	0.9127907	0.75	0.00706	76	362	0.848795983	0.89909884	0.05	0.00194
22	214	0.823708417	0.9127907	0.85	0.00582	77	363	0.848795983	0.89909884	0.15	0.00225
23	215	0.823708417	0.9127907	0.95	0.00571	78	364	0.848795983	0.89909884	0.25	0.00242
24	216	0.823708417	0.9127907	1	0.01033	79	365	0.848795983	0.89909884	0.35	0.00245
25	217	0.823708417	0.926482561	0	0.00276	80	366	0.848795983	0.89909884	0.45	0.00236
26	218	0.823708417	0.926482561	0.05	0.00194	81	367	0.848795983	0.89909884	0.55	0.00217
27	219	0.823708417	0.926482561	0.15	0.00225	82	368	0.848795983	0.89909884	0.65	0.00192
28	220	0.823708417	0.926482561	0.25	0.00242	83	369	0.848795983	0.89909884	0.75	0.00164
29	221	0.823708417	0.926482561	0.35	0.00245	84	370	0.848795983	0.89909884	0.85	0.00135
30	222	0.823708417	0.926482561	0.45	0.00236	85	372	0.848795983	0.89909884	1	0.00277
31	223	0.823708417	0.926482561	0.55	0.00217	86	373	0.848795983	0.9127907	0	0.01025
32	224	0.823708417	0.926482561	0.65	0.00192	87	374	0.848795983	0.9127907	0.05	0.00836
33	225	0.823708417	0.926482561	0.75	0.00164	88	375	0.848795983	0.9127907	0.15	0.0097
34	226	0.823708417	0.926482561	0.85	0.00135	89	376	0.848795983	0.9127907	0.25	0.01041
35	228	0.823708417	0.926482561	1	0.00277	90	377	0.848795983	0.9127907	0.35	0.01054
36	276	0.8362522	0.889970933	1	0.00177	91	378	0.848795983	0.9127907	0.45	0.01014
37	277	0.8362522	0.89909884	0	0.01197	92	379	0.848795983	0.9127907	0.55	0.00935
38	278	0.8362522	0.89909884	0.05	0.00836	93	380	0.848795983	0.9127907	0.65	0.00828
39	279	0.8362522	0.89909884	0.15	0.0097	94	381	0.848795983	0.9127907	0.75	0.00706
40	280	0.8362522	0.89909884	0.25	0.01041	95	382	0.848795983	0.9127907	0.85	0.00582
41	281	0.8362522	0.89909884	0.35	0.01054	96	383	0.848795983	0.9127907	0.95	0.0049
42	282	0.8362522	0.89909884	0.45	0.01014	97	384	0.848795983	0.9127907	1	0.01033
43	283	0.8362522	0.89909884	0.55	0.00935	98	385	0.848795983	0.926482561	0	0.00274
44	284	0.8362522	0.89909884	0.65	0.00828	99	386	0.848795983	0.926482561	0.05	0.00194
45	285	0.8362522	0.89909884	0.75	0.00706	100	387	0.848795983	0.926482561	0.15	0.00225
46	286	0.8362522	0.89909884	0.85	0.00582	101	388	0.848795983	0.926482561	0.25	0.00242
47	287	0.8362522	0.89909884	0.95	0.00652	102	389	0.848795983	0.926482561	0.35	0.00245
48	288	0.8362522	0.89909884	1	0.01033	103	390	0.848795983	0.926482561	0.45	0.00236
49	289	0.8362522	0.9127907	0	0.05149	104	391	0.848795983	0.926482561	0.55	0.00217
50	290	0.8362522	0.9127907	0.05	0.03597	105	392	0.848795983	0.926482561	0.65	0.00192
51	291	0.8362522	0.9127907	0.15	0.0417	106	393	0.848795983	0.926482561	0.75	0.00164
52	292	0.8362522	0.9127907	0.25	0.04478	107	394	0.848795983	0.926482561	0.85	0.00135
53	293	0.8362522	0.9127907	0.35	0.04534	108	396	0.848795983	0.926482561	1	0.00277
54	294	0.8362522	0.9127907	0.45	0.04361	109	457	0.857158505	0.9127907	0	0.00176
55	295	0.8362522	0.9127907	0.55	0.04021	110	468	0.857158505	0.9127907	1	0.00177

Table 5.9: Variation range of objective function for all solution in Pareto optimal front

	OF_1	OF_2 (\$)	OF_3 (Ton CO_2)
f_k^{min}	0.0026	9.7208×10^7	4.323×10^5
f_k^{max}	0.0689	2.4936×10^9	6.6973×10^5

In the second stage, the planner can choose the most preferred solution using the fuzzy satisfaction method introduced in section 3.2.3. The final solution is solution #68. The investment plan of this solution is described in Table 5.10.

Table 5.10: The investment plan obtained for the final solution

DGtech	$\xi_{i,t}^{dg}$	Year	Bus
Micro Turbine	4	1	201
	1	1	39,114,26
	1	2	164,201
	1	3	39
Gas Turbine	1	1	152,102
	1	2	14,177
	1	3	177,102
	1	4	76
	1	5	201
	1	7	14
	1	8	201
Wind Turbine	1	1	26,39,64,89,114,139
	3	1	201

The various costs related to the selected solution are given in Table 5.11.

It would be interesting to know how much accuracy is lost if the scenarios are reduced. The final solution (which was already found using the $N_s = 110$) is reevaluated using various values of N_s. The exact values of this solution is obtained if all scenarios are considered. This value is taken as a reference for comparing the results obtained by various number of reduced scenarios. The computation error due to scenario reduction is depicted versus the number of reduced scenarios,i.e N_s, Fig.5.6.

This figure shows that, in our specific example, if the number of scenarios is chosen to be greater than 93, then the accuracy is acceptable and the fluctuation is highly reduced and the error will be less than 0.005%.

Table 5.11: Investment/operating cost in final solution (M$) (Dynamic DG and network investment))

Year	GC	IC (for DG units)	Substation	Feeder
1	9.624959	18.4675	0	0
2	9.670223	2.485	0	34.5
3	9.662216	1.7425	0	89.25
4	9.680735	0.5	0	0
5	9.705028	0.5	0	73.5
6	9.813719	0	0	25.2
7	9.835628	0.5	0	90
8	9.861077	0.5	0.2	78

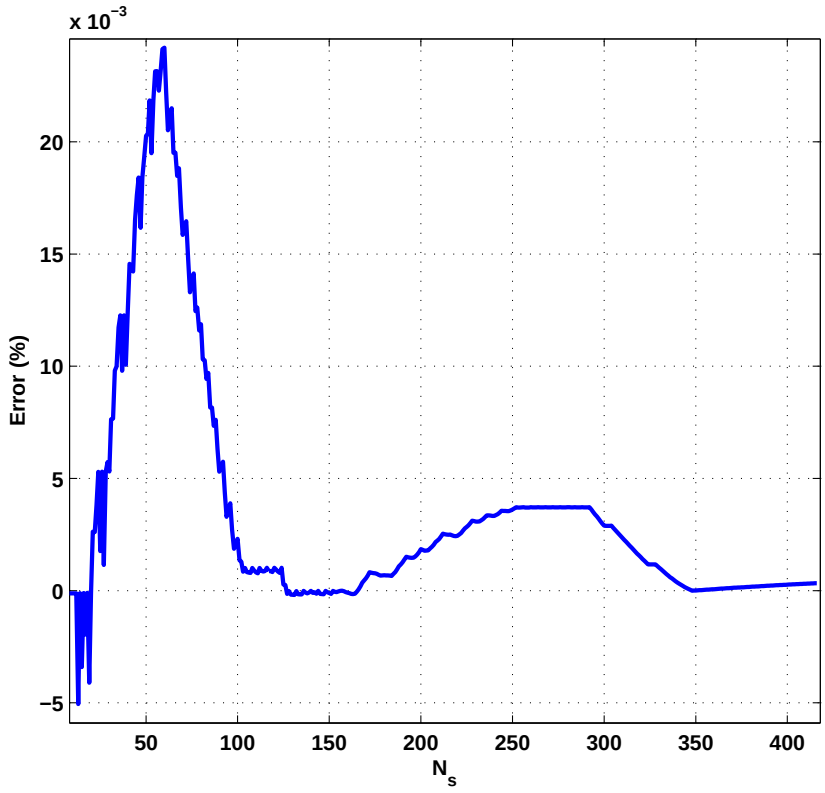

Figure 5.6: Sensitivity analysis of the computation accuracy versus the number of scenarios

5.3.2 Case B: conventional DG technologies without considering uncertainty

In this case, just controllable DG technologies have been considered. The uncertainties of electric load, electricity price and renewable power generation have been neglected. It is assumed that the values of demand and price level factors are as described in Table 5.3. For making he comparison easier, only two objective function, namely total costs and the technical dissatisfaction are considered. Six planning models have been simulated which their characteristics have been described in Table 5.12. Each of these models are simulated for 100 iterations and the results (the obtained Pareto optimal fronts are depicted in Fig. 5.7 to 5.12).

The Pareto optimal front found in "Model A" is depicted in Fig. 5.7 which is dynamic and simultaneously performs the DG and network investment.

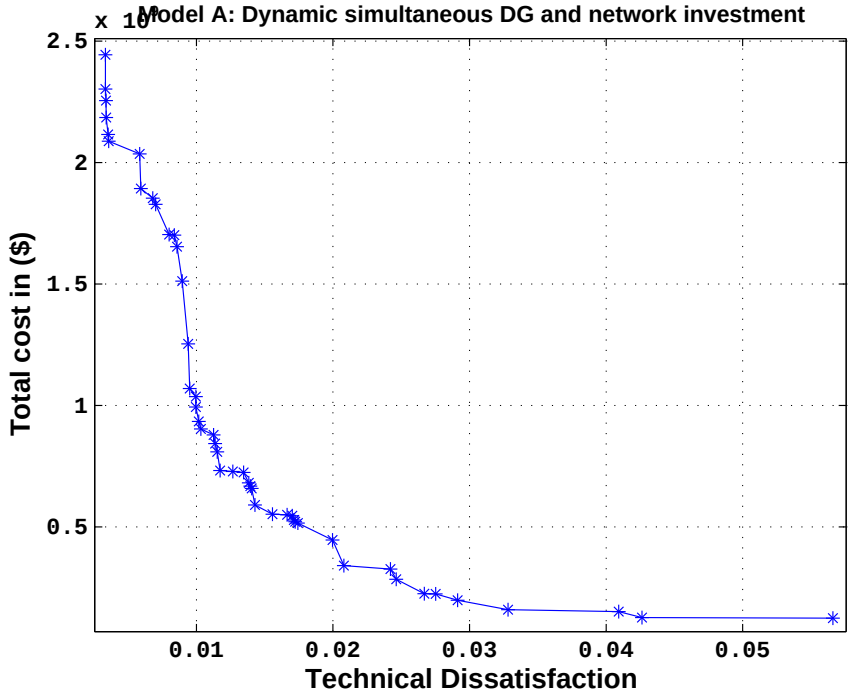

Figure 5.7: Pareto optimal front found of Model A: Dynamic simultaneous DG and network investment

The Pareto optimal front found in "Model B" is depicted in Fig. 5.8 which is static and simultaneously performs the DG and network investment.

The Pareto optimal front found in "Model C" is depicted in Fig. 5.9 which is dynamic and just performs the network investment.

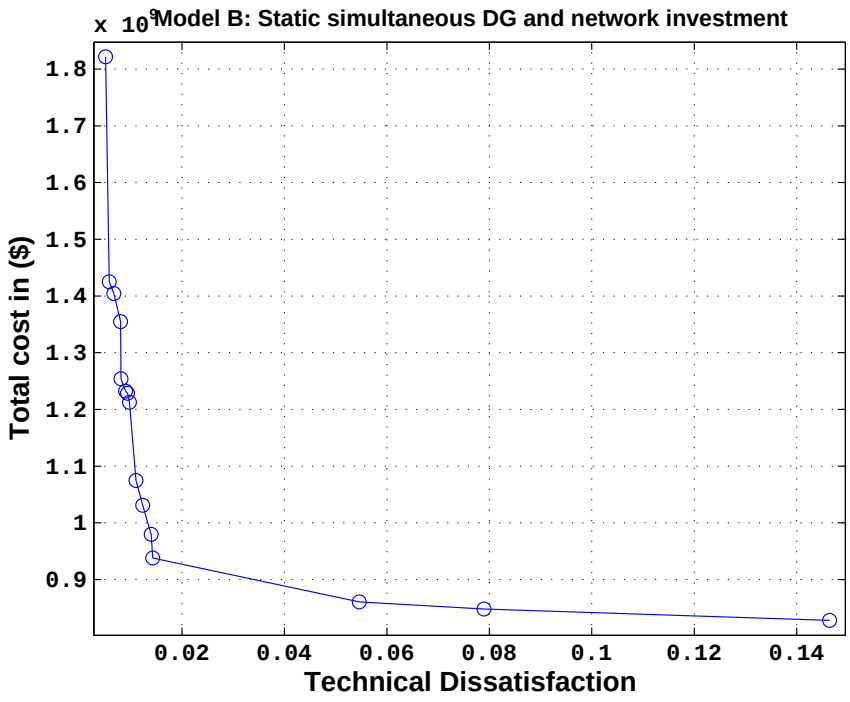

Figure 5.8: Pareto optimal front found of Model B: Static simultaneous DG and network investment

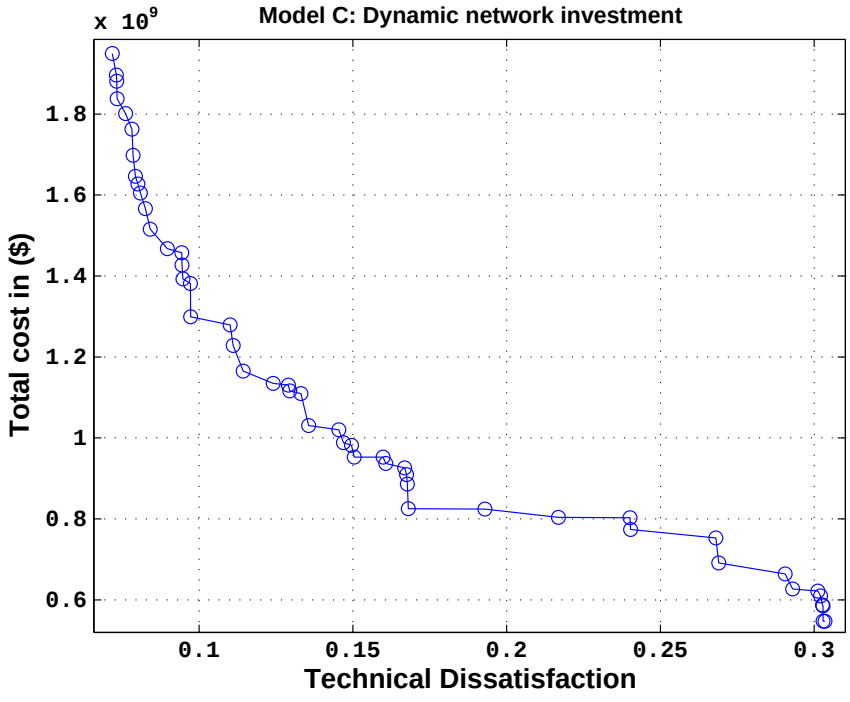

Figure 5.9: Pareto optimal front found of Model C: Dynamic network investment

The Pareto optimal front found in "Model D" is depicted in Fig. 5.10 which is static and just performs the network investment.

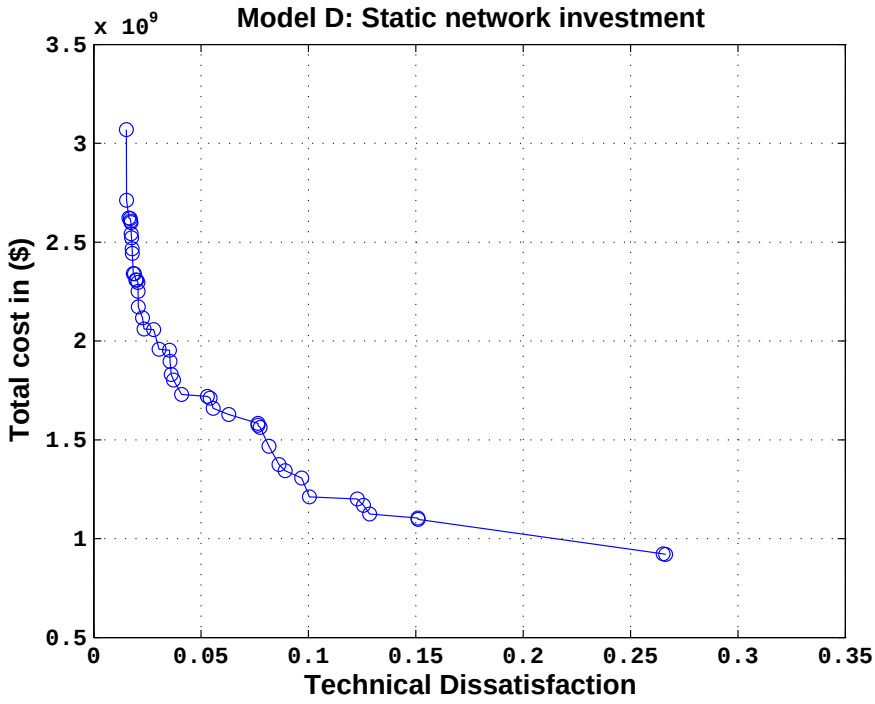

Figure 5.10: Pareto optimal front found of Model D: Static network investment

The Pareto optimal front found in "Model E" is depicted in Fig. 5.11 which is static and just performs the DG investment.

The Pareto optimal front found in "Model F" is depicted in Fig. 5.12 which is dynamic and just performs the DG investment.

The variation rage of objective functions in each model and also the number of solutions in the Pareto optimal front have been given in Table 5.13.

Table 5.12: The technical description of various DG/distribution network planning models

Model	DG	Network	Static	Dynamic
A [113, 119]	√	√		√
B [120]	√	√	√	
C		√		√
D		√	√	
E	√		√	
F [121]	√			√

The model can be directly used in power market model in which the DNO is authorized

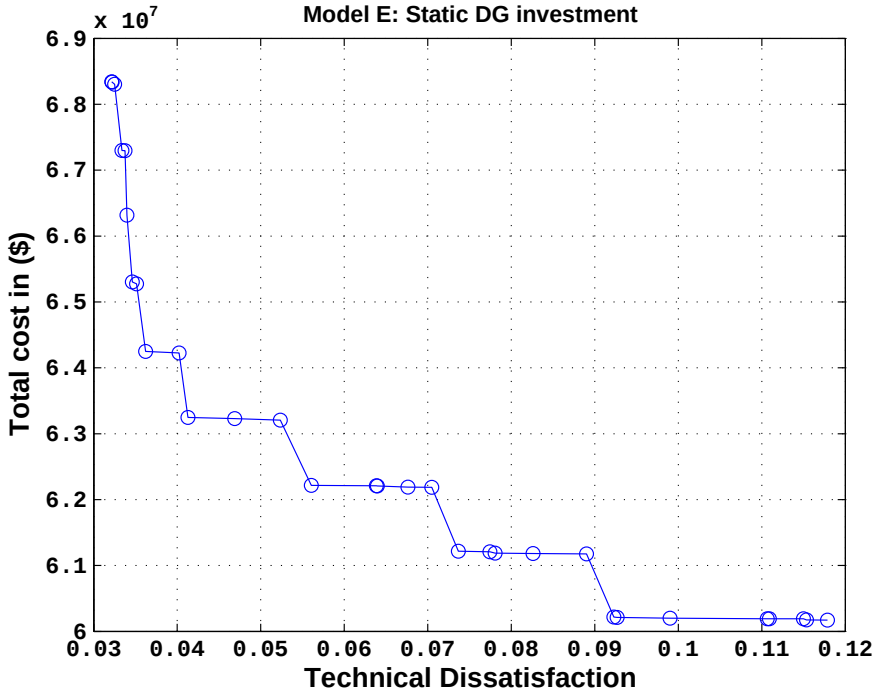

Figure 5.11: Pareto optimal front found of Model E: Static DG investment

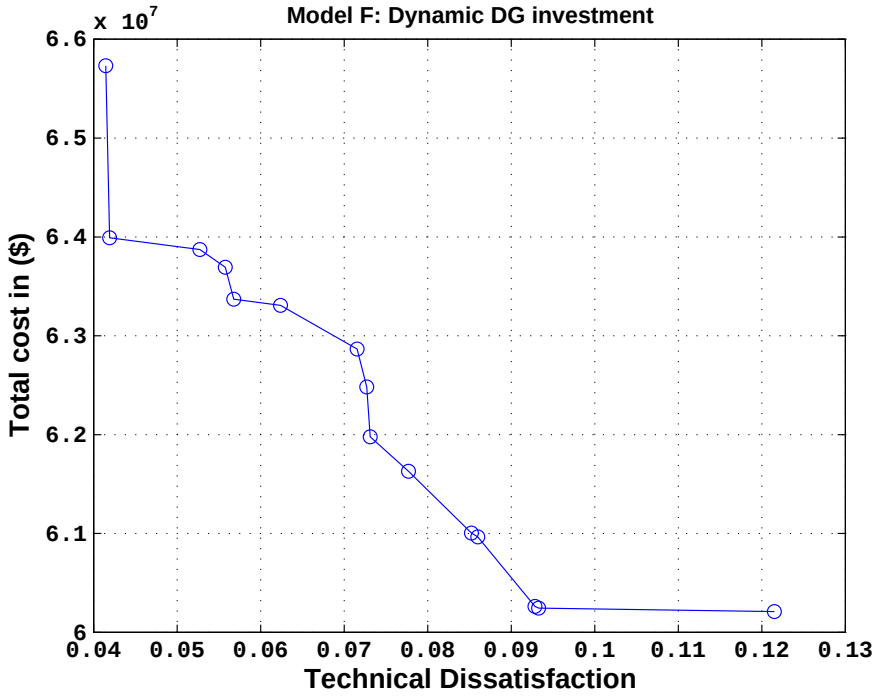

Figure 5.12: Pareto optimal front found of Model F: Dynamic DG investment

Table 5.13: The variation range of objective functions in various DG/distribution network planning models

Model	Number of solutions in Pareto optimal front	*Cost*		Technical dissatisfaction	
		min	max	min	max
A	47	124518917.8	2444211810	0.003342014	0.056602793
B	15	827889605.9	1821779276	0.005092014	0.146418843
C	50	547109813.7	1949588572	0.071751831	0.303485731
D	45	920342146	3068764410	0.015190972	0.266324765
E	42	60171160.47	68341367.83	0.032157433	0.117865948
F	15	60209856.76	65733007.98	0.041442527	0.121504941

for DG investment. However, in power market models where the DG investment is done by independent investors instead of DNO, It can be easily modified to be used in such regulatory frameworks. The decisions related to investment and operating of DG units are made by private entities. In this case, the values of $\xi_{i,t}^{dg}$ are determined by DG owners. The decision variables of DNO are γ_t^{ℓ} and ψ_t^{tr} (network investment options).

The provided information would also be useful as a technical, economical and environmental signal for regulators. It can be used for regulating the incentives to encourage the private section to invest in what DG technology and where to be more beneficial.

For example, knowing the the number of solutions on the Pareto optimal front which use a specific bus as a location for DG installation may help the planner in identifying the key buses in system planning. The percentages of appearance of each bus in the solution set are shown in Fig. 5.13. This will show which bus is present in most optimal solutions of the Pareto front. Even if the DNO is not the DG investor, he can identify the appropriate locations for encouraging the private sector investment. In this case, there are two buses that appear in all solutions namely, 152 and 201. The percent of appearance in Pareto optimal solutions of model A are described in Table 5.14.

5.4 Conclusions

This chapter presents a comprehensive dynamic multi-objective model for DG integration in distribution networks. The proposed two-step algorithm finds the non-dominated solutions by simultaneous minimization of active losses, costs and emissions in the first stage (using the algorithm presented in Section 3.2.2) and uses a fuzzy satisfying method to select the best solution from the candidate set in the second stage. The new planning

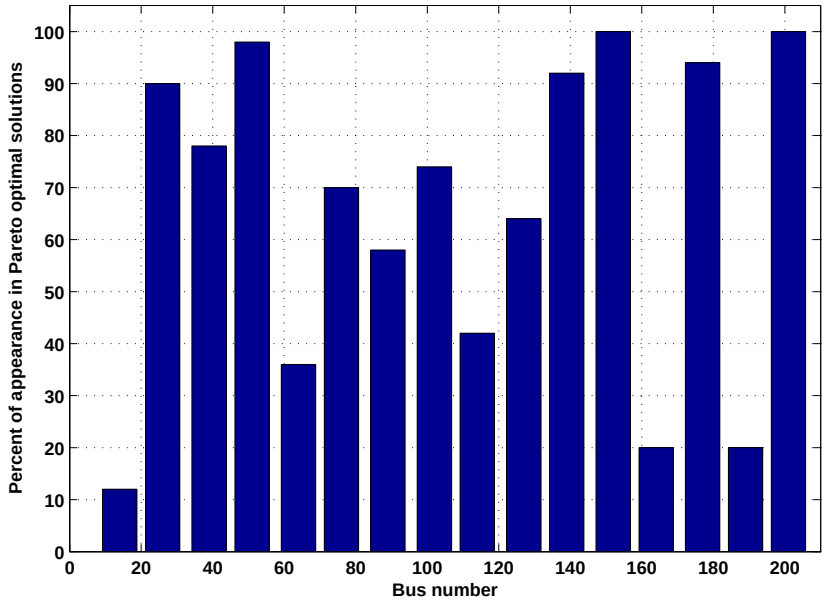

Figure 5.13: Percent of appearance of each bus in the solutions of Pareto optimal front found by Model A

Table 5.14: The Percent of appearance of each bus in Pareto optimal front

Bus	Percent of appearance in Pareto optimal front (%)
152	100
201	100
51	98
177	94
139	92
26	90
39	78
102	74
76	70
127	64
89	58
114	42
64	36
164	20
189	20
14	12

model is applied to a distribution network and its flexibility is demonstrated through different case studies. The solution set provides the planner with an insight into the problem and enables him to choose the best solution according to planning preferences.

CHAPTER 6

Distribution Network Planning and Operation under Unbundled DG Investment

6.1 Introduction

In deregulated power systems, the distribution network operator (DNO) is not responsible for investment in Distributed Generation (DG) units. The investment and operating decisions related to DG units are then taken by entities other than DNO. The DNO should be able to evaluate the technical effects of these decisions while they are associated with uncertainties. This work proposes a fuzzy evaluation tool for analyzing the effect of investment and operation of DG units on active losses and the ability of distribution network in load supply at presence of uncertainties. The considered uncertainties are related to load values, installed capacity and operating schedule of DG units. The proposed model is applied on a distribution network to demonstrate its functionality.

6.2 DG impact on Distribution network planning

6.2.1 Problem Formulation

The assumptions used in problem formulation, decision variables, constraints and the objective functions are explained in this section.

6.2.1.1 Assumptions

The following assumptions are employed in problem formulation:

- Connection of a DG unit to a bus i is modeled as a negative PQ load as Fig. 5.2.

- The daily load variations over the long-term is modeled as a load duration curve with N_{dl} demand levels [119] (see Fig.5.2). Assuming a base load, $P^D_{i,base} + i \times Q^D_{i,base}$, a Demand Level Factor, D_{dl}, and a demand growth rate, ϵ_D, the demand in bus i, in year t and in demand level dl is computed as follows:

$$P^D_{i,t,dl} = P^D_{i,base} \times D_{dl} \times (1+\epsilon_D)^t \qquad (6.1)$$
$$Q^D_{i,t,dl} = Q^D_{i,base} \times D_{dl} \times (1+\epsilon_D)^t$$

  Where, $P^D_{i,t,dl}, Q^D_{i,t,dl}$ are the actual active and reactive demand in bus i, year t and demand level dl, respectively.

- The price of energy, i.e. EP_{dl}, purchased from the grid is competitively determined in a liberalized market environment and thus, it is not constant during different demand levels. Without loosing generality, it is assumed that the electricity price at each demand level can be determined as follows:

$$EP_{dl} = \rho \times \lambda_{dl} \qquad (6.2)$$

  where the peak price (i.e. ρ), and the forecasted values of Price Level Factors (i.e. λ_{dl}), are assumed to be known.

6.2.1.2 Decision variables

The decision variables are the number of renewable and non-renewable DG units, to be installed in each bus in each year, i.e., $\xi^{dg}_{i,t}$; binary investment decision in feeder ℓ in the year t, i.e. γ^ℓ_t which can be 0 or 1, and finally the number of new installed transformers in the year t, i.e. ψ^{tr}_t.

6.2.1.3 Operating limits of DG units

The DG units should be operated considering the limits of their primary resources, i.e.:

$$P_{i,t,dl}^{dg} \leq \sum_{\acute{t}=1}^{t} \xi_{i,\acute{t}}^{dg} \times \overline{P}_{lim}^{dg} \tag{6.3}$$

Where, $\xi_{i,t}^{dg}$ is the number of DG units installed in bus i in year t. $\overline{P}_{lim}^{dg}$ is the operating limit of DG unit.

The power factor of DG unit is kept constant [113] in all demand levels as follows:

$$cos\varphi_{dg} = \frac{P_{i,t,dl}^{dg}}{\sqrt{(P_{i,t,dl}^{dg})^2 + (Q_{i,t,dl}^{dg})^2}} \tag{6.4}$$

6.2.1.4 Voltage profile

The voltage magnitude of each bus should be kept between the operations limits, as follows:

$$V_{min} \leq V_{j,t,dl} \leq V_{max} \tag{6.5}$$

6.2.1.5 Capacity limit of feeders and substation

The flow of current/energy passing through the feeders and the substation should be kept below the feeders/substation capacity limit as follows:

$$I_{\ell,t,dl} \leq \overline{I}_{\ell} + Cap_{\ell} \times \sum_{\acute{t}=1}^{t} \gamma_{\acute{t}}^{\ell} \tag{6.6}$$

$$I_{\ell,t,dl} = \frac{V_{i,t,dl} - V_{j,t,dl}}{Z_{\ell}^{t}}$$

i, j are the sending and receiving ends of feeder ℓ

where, $Cap_{\ell} \times \sum_{\acute{t}=1}^{t} \gamma_{\acute{t}}^{\ell}$ represents the added capacity of feeder due to the investments made until year t. The $I_{\ell,t,dl}$ is the current magnitude of feeder ℓ in year t and demand level dl. $\overline{I}_{\ell}$ is the capacity of feeder ℓ at the beginning of the planning horizon.

For substation capacity constraint, also, the same philosophy holds, as follows:

$$S_{t,dl}^{grid} \leq \overline{S}_{tr} + Cap_{tr} \times \sum_{\acute{t}=1}^{t} \psi_{\acute{t}}^{tr} \tag{6.7}$$

Where, $Cap_{tr} \times \sum_{\acute{t}=1}^{t} \psi_{\acute{t}}^{tr}$ represents the added capacity of substation resulting from adding new transformers (or replacing them) until year t. $S_{t,dl}^{grid}$ is the apparent power passing through substation in year t and demand level dl. Cap_{tr} is the capacity of transformer to be added in substation. $\overline{S}_{tr}$ is the capacity of substation at the beginning of the planning horizon.

6.2.1.6 Emission Limit

The total emission produced in each year should not exceed a certain limit, i.e. E_{lim}. The emission produced by the main grid in year t and demand level dl, is computed by is computed by multiplying the purchased power from grid in each demand level, i.e. $P_{t,dl}^{grid}$, by the emission factor of the grid, i.e. E_{grid}. The total emission generated by the DG units is computed by multiplying the power generated by each DG by its emission factor, i.e. E_{dg}. This value is summed over all buses in the network to consider all installed DG units. The two introduced terms are multiplied by the duration of each load level, i.e. τ_{dl}, and summed together as follows:

$$\begin{aligned} TE_t &= \sum_{dl=1}^{N_{dl}} \tau_{dl} [E_{grid} P_{t,dl}^{grid} + \sum_{i=1}^{N_b} E_{dg} P_{i,t,dl}^{dg}] \\ TE_t &\leq Elim \end{aligned} \tag{6.8}$$

Where, TE_t is the total emission in year t, E_{grid}, E_{dg} are the emission factor of main grid and DG unit, respectively.

6.2.2 Uncertainty handling

In this work, the uncertainty of three parameters are taken into account namely, wind power generation, electric load and electricity price. In this section, the uncertainty modeling of uncertain parameters of this study is described first and then the method used for handling them is given.

6.2.2.1 Wind Turbine generation uncertainty modeling

The generation schedule of a wind turbine highly depends on the wind speed in the site. There are various methods to model wind behavior like time-series model [122], relative frequency histogram [123] or considering all possible operating conditions of the wind turbines and accommodating the model in a deterministic planning problem [109]. The variation of wind speed, i.e. v, is modeled using a Rayleigh Probability Density Function (PDF) [109] and its characteristic function which relates the wind speed and the output of a wind turbine.

$$f_w(v) = (\frac{2v}{c^2})\ exp[-(\frac{v}{c})^2] \tag{6.9}$$

where c is the scale factor of the Rayleigh PDF of wind speed in the zone under study. The generated power of the wind turbine in each demand level is approximated using its characteristics as follows:

$$P^w_{i,t}(v) = \sum_{\acute{t}=1}^{t} \xi^{dg}_{i,t}. \begin{cases} 0 & \text{if } v \leq v^{cut}_{in} \text{ or } v \geq v^{cut}_{out} \\ \frac{v - v^{cut}_{in}}{v_{rated} - v^{cut}_{in}} P^w_{i,r} & \text{if } v^{cut}_{in} \leq v \leq v_{rated} \\ P^w_{i,r} & \text{else} \end{cases} \tag{6.10}$$

Where, $P^w_{i,r}$ is the rated power of wind turbine installed in bus i, P^w_i is the generated power of wind turbine in bus i, v^{cut}_{out} is the cut out speed, v^{cut}_{in} is the cut in speed and v_{rated} is the rated speed of the wind turbine. The speed-power curve of a typical wind turbine is depicted in Fig. 2.1.

6.2.2.2 Electric demand and market price uncertainty modeling

The variation of electric demand and market price is modeled using (5.2) and (5.1), respectively. However, the values of D_{dl} and λ_{dl} are uncertain values. In this work, it is assumed that an appropriate forecasting tool is available to forecast the price and demand uncertainty (like [124]) to estimate their associated probability density functions. The uncertainty of these values are assumed to follow a Lognormal PDF as used in [125]. This means for each demand level, (i.e. dl), a mean and standard deviation is specified for λ_{dl} and D_{dl}.

$$f_{\lambda}(\lambda_{dl}) = \frac{1}{\sqrt{2\pi(\sigma_{dl}^{\lambda})^2}}\ exp[-\frac{(\lambda_{dl}-\mu_{dl}^{\lambda})^2}{2(\sigma_{dl}^{\lambda})^2}] \tag{6.11}$$
$$f_{D}(D_{dl}) = \frac{1}{\sqrt{2\pi(\sigma_{dl}^{D})^2}}\ exp[-\frac{(D_{dl}-\mu_{dl}^{D})^2}{2(\sigma_{dl}^{D})^2}]$$

The method used for handling these uncertainties is the two point estimate method (2PEM) [126] which is described in Section 4.2.2.

6.2.3 Objective functions

The proposed model maximizes two objective functions, namely, total benefits of DNO and DGO benefits, as follows:

$$\max\{OF_1, OF_2\}$$
$$\textit{subject to: } (6.1) \rightarrow (6.11)$$

The objective functions are formulated next.

6.2.3.1 DNO: Costs and Benefits

The first objective function, i.e., OF_1, to be maximized is the total saving accrued to DNO due to the presence of DG units in distribution network. For calculating these benefits, the cost and benefits of the DNO are introduced and computed. The cost payable by

DNO includes the cost of electricity purchased from the grid for compensating the active losses, i.e. LC, reinforcement costs of feeders, i.e. FRC and substation, i.e. SRC and finally the emission costs due to energy purchased from main grid and DG units, i.e. TEC. Each term is explained as follows: The cost of purchasing electricity from the grid can be determined as:

$$LC = \sum_{t=1}^{T} \sum_{dl=1}^{N_{dl}} \left(EP_{dl} \times P_{t,dl}^{loss} \right) \times \tau_{dl} \times \frac{1}{(1+d)^t} \tag{6.12}$$

Where, LC is the cost of active losses, ρ is the base electricity price and $P_{t,dl}^{loss}$ is the active power loss in year t and demand level dl. d is the discount rate.
The last term of DNO cost is total emission cost, i.e., TEC, which is comprised of the emission produced by the electricity purchased from main grid and the DG units over planning horizon from $t = 1$ to $t = T$. TEC, is formulated as follows:

$$TEC = \sum_{t=1}^{T} TE_t \times E_c \times \frac{1}{(1+d)^t} \tag{6.13}$$

where E_c is the cost of each Ton of generated CO_2. The total cost that DNO should pay, DNO_c is computed as follows:

$$DNO_c = LC + FRC + SRC + TEC \tag{6.14}$$

To compute the benefits of DNO due to presence of DG units, the value of DNO_c is computed two times, one when no DG unit is present, i.e. DNO_c^{nodg} and one when DG units are participated in the planning problem, i.e. DNO_c^{dg}. The differences of these two values show the benefits of DNO, i.e. DNO_b, thanks to DG units, as follows:

$$DNO_b = DNO_c^{nodg} - DNO_c^{dg} \tag{6.15}$$

6.2.3.2 DGO: Costs and Benefits

The cost that DGO should pay is the sum of operating and investment cost of DG units. The installation cost of the DG units is computed as:

$$IC = \sum_{t=1}^{T} \sum_{i=1}^{N_b} \sum_{dg} (\xi_{i,t}^{dg} \times IC_{dg}) \times \frac{1}{(1+d)^t} \tag{6.16}$$

where IC_{dg} is the investment cost of DG units.
The operating cost of the DG units is computed as:

The benefits of DGO are coming from selling energy to the distribution network consumers. The price of energy that DG units can sell their energy depends on the way they play in the market. They can have bilateral contracts with consumers at fixed price or they can sell their output power at market price. In this section, it is assumed that DGO sell their produced power at market price, as follows:

$$DGO_b = \sum_{t=1}^{T} \sum_{dl=1}^{N_{dl}} \tau_{dl} \times \sum_{i=1}^{N_b} EP_{dl} \times P_{i,t,dl}^{dg} \tag{6.17}$$

6.2.3.3 Objective functions

As it is observed till now, the DNO and DGO follow different goals of their investment. The question is how to guide the decisions of DGO toward the benefits of DNO while he can just be encouraged to that. In this section, the effect of DG units in investment deferral of distribution network is precisely modeled and computed by comparing two cases when DG is present or not, as follows:

$$\begin{aligned} OF_1 &= (1-\beta) \times DNO_b \\ OF_2 &= (DGO_b - DGO_c) + \beta \times DNO_b \end{aligned} \tag{6.18}$$

6.2.4 Simulation results

The proposed methodology is applied to an actual distribution network which is shown in Fig.6.1.

This system has 574 nodes, 573 sections and 180 load points. The average load and power factor at each load point are 55.5 kW and 0.9285, respectively [127]. This network is fed through a 20kV substation with total power rated at $\bar{S}_{tr,s}^{t=0} = 20$ MVA. The options for reinforcing the network are as follows: transformers with a capacity of Cap_{tr}=10 MVA and a cost of C_{tr}=0.2 Million \$ for each; replacing the feeders at a cost of C_{ℓ}=0.15 Million \$/km [71]. In this section, the non-renewable and renewable DG technologies are taken into account. The characteristics of Gas turbine, Micro turbine and CHP units are given in Table 5.5 and wind turbine power curve and it's rating is described in Table 5.1. Four demand levels, i.e., minimum, medium, base and high are considered in this simulation. The predicted values of demand and price level factors and their duration are given in Table 6.1. The other needed data are given in Table 6.2. The standard deviations of demand level factors, i.e.σ_{dl}^{D}, and price level factors, i.e.σ_{dl}^{λ} are assumed to be 2% of their corresponding mean values.

Table 6.1: The predicted values of demand and price level factors and their duration

Parameter	High	Base	Medium	Minimum
μ_{dl}^{D}	1.25	1	0.87	0.75
μ_{dl}^{λ}	1.65	1	0.82	0.65
τ_{dl} (hr)	73	2847	2920	2920

The proposed model enables the planner to consider different wind speed parameter during different demand levels but here, for simplicity it is assumed that the changes of wind pattern during the different demand levels can be neglected; the stopping criterion for the search algorithm is reached with a maximum number of iterations. Other simulation assumptions and characteristics of the DG units are presented in Table 6.19. The total cost of DNO for investing in distribution network is computed to be 1.15542×10^7\$ when no DG investment is done. The formulated problem was implemented in MATLAB [128] and solved using the proposed two-stage algorithm. In order to clarify the purpose of this section, two scenarios are considered namely no benefit sharing and benefit sharing; additionally, the proposed heuristic method is compared to other heuristic methods too,

Table 6.2: Data used in the study

Parameter	Unit	Value
T	year	5
N_p		50
N_o		2
c		8.78
E_{lim}	$kgCO_2$	30000 [9]
E_{grid}	$kgCO_2/MWh$	910 [9]
E_c	$\$/TonCO_2$	10 [35]
ρ	\$/MWh.	70 [66]
ϵ_D	%	3.5
d	%	12
$V_{\max}$	Pu	1.05
$V_{\min}$	Pu	0.95
Maximum iteration		1000

as follows:

6.2.4.1 Scenario I: No benefit sharing $\beta = 0$

First of all, no benefit sharing scenario is analyzed. In this scenario, it is assumed that all benefits of DG existence in the network are received by DNO. The formulated problem in Section 6.2.1 was solved assuming $\beta = 0\%$. The Pareto optimal front has 20 non-inferrior solutions which are depicted in Fig.6.2. The Pareto optimal front shown in Fig.6.2 demonstrates that if there is no benefit sharing then the DG investment in 13 solutions can not be beneficial to DGOs. Analysing the Fig.6.2, shows that only 7 solutions have positive net profit for DGO. The values of objective functions of Pareto optimal solutions are tabulated in Table 6.3. The planning scheme for solution #1 is described in Table 6.4. In this case, both DGO and DNO have positive benefit values. Three DG technologies are used namely, Wind turbine, Gas turbine and CHP. The installation bus and also the timing of investment are given in Table 6.4. In this solution, the network reinforcement is done by feeder reinforcement and no investment is needed in substation.

Table 6.3: The Pareto Optimal Front of Scenario I with $\beta = 0$

Profits in 10^6\$			
Solution #	OF_1	OF_2	β
1	0.0399	1.1399	0
2	6.2215	-0.9267	0
3	0.0974	0.4392	0
4	0.0782	1.0632	0
5	6.0782	-0.5667	0
6	0.7847	0.3596	0
7	2.8510	-0.2142	0
8	1.9387	0.1024	0
9	5.7155	-0.4920	0
10	1.2401	0.2277	0
11	3.5812	-0.2257	0
12	2.0134	-0.0954	0
13	1.3965	0.1541	0
14	4.0098	-0.3078	0
15	4.5975	-0.3233	0
16	2.4960	-0.1722	0
17	5.2794	-0.4500	0
18	2.3015	-0.1471	0
19	5.1275	-0.4007	0
20	4.7250	-0.3967	0

6.2.4.2 Scenario II: Benefit sharing with non-zero β

In this scenario, the share of DGO of DNO's benefit , i.e. β, is determined by the optimization procedure. This means that the share of DGO is not assumed to be zero. The obtained Pareto optimal front contains 20 non-inferior solutions as it is given in Fig.6.3. All of the solutions have non-negative values for both objective functions. This means that all of the solutions propose positive profit for both DNO and DGO. The difference between different solutions refers to the amount of benefit that each of them may be willing to make. The share of DNO of DG benefits, β varies from 29% to 98.5%. The simulation results of the proposed algorithm are given in Table 6.5. In Table 6.5, the values of OF_1, OF_2 and the satisfaction of each solution in maximizing each objective function $\mu^{OF_k(X_n)}$ are given for each value of β. Now the non-inferior solutions are obtained by the IGA method. It just remains to select the final solution. Referring to (3.12), the solution which has the maximum of minimum satisfaction (for both objective functions) is solution #11. The planning scheme for solution #11 is described in Table 6.6. In this

Table 6.4: The Planning scheme of solution #1 in scenario I

Year	Bus			FRC	SRC
t	CHP	WT	GT	(10^5\$)	(10^5\$)
1	574,226,167,200,366	0		4.7333	0
2		456		10.7390	0
3	574	261		8.9660	0
4				10.2120	0
5			332,19	14.1790	0

case, both DGO and DNO have positive benefit values. Four DG technologies are used namely, Wind turbine, Gas turbine, CHP and Diesel generator. The installation bus and also the timing of investment are also provided in Table 6.6. In this solution, the network reinforcement is done by feeder and substation reinforcement.

Table 6.5: The Pareto Optimal Front of Scenario II with variable β

Solution#	Profits in 10^6\$			Satisfaction	
n	OF_1	OF_2	β	$\mu_{OF_1}(X_n)$	$\mu_{OF_2}(X_n)$
1	3.5152	0.0391	0.290	1.000	0.000
2	0.0747	3.9232	0.985	0.000	1.000
3	0.7747	3.8067	0.853	0.203	0.970
4	2.9154	0.9363	0.356	0.826	0.231
5	0.9625	3.4101	0.821	0.258	0.868
6	1.4843	2.4801	0.719	0.410	0.628
7	0.1065	3.8606	0.977	0.009	0.984
8	2.5762	1.5350	0.540	0.727	0.385
9	1.1856	2.9067	0.782	0.323	0.738
10	3.2821	0.8998	0.326	0.932	0.222
11	2.0178	2.3618	0.602	0.565	0.598
12	3.4326	0.4737	0.290	0.976	0.112
13	2.0229	2.1970	0.595	0.566	0.556
14	3.4080	0.5543	0.322	0.969	0.133
15	2.3171	1.6675	0.540	0.652	0.419
16	1.3709	2.7152	0.727	0.377	0.689
17	2.0406	1.8383	0.602	0.571	0.463
18	2.5302	1.5488	0.508	0.714	0.389
19	2.1716	1.6697	0.540	0.609	0.420
20	1.2722	2.8178	0.751	0.348	0.715

Table 6.6: The Planning scheme of solution #11 in scenario II

Year	Bus				FRC	SRC
t	CHP	Diesel	WT	GT	(10^5\$)	(10^5\$)
1	574			352	5.7639	0
2	504-35		574		7.2362	0
3					8.6461	0
4	420-574				18.8580	2
5	574	574	59	574	25.7470	0

6.2.4.3 Comparing with other methods

The proposed algorithm is compared with four other methods namely, Particle Swarm Optimization combined with Simulated Annealing method (PSO-SA) [129], Non-dominated sorting Genetic Algorithm (NSGA-II) [91], Immune Algorithm [113] and Tabu Search (TS) [85]. The Pareto optimal front found by each method is depicted in Fig.6.4.

In Table 6.7, the number of Pareto optimal solutions found by each method, the maximum and minimum values of OF_1, OF_2 and the computing time of each algorithm are compared. The comparison shows that the solutions found by the proposed IGA can not be dominated by the solutions found by other methods. This means there is no solution in the Pareto optimal fronts found by other methods that can propose higher values in both OF_1, OF_2 compared to ones found by IGA. They may even provide more non-inferior solutions but since they can not dominate the solutions of IGA it does not give a priority to them. Another aspect is the computational time; it is always appealing to reduce the computational burden of the algorithms but there is always a trade off between the performance and computational burden. The computing time for the proposed IGA is higher when compared with some algorithms like (PSO-SA, IA,TS). This is mainly because of high number of power flow computation in this method. The computation time can be effectively reduced using fast radial power flow solution techniques like those proposed in [130,131]. It should be noted that the proposed planning method is not going to be used on-line, so the computational burden would not cause serious problem.

Table 6.7: Performance comparison between the proposed method and other methods

Method	no of Pareto optimal solutions	min(OF_1) (10^6\$)	max(OF_1) (10^6\$)	min(OF_2) (10^6\$)	max(OF_2) (10^6\$)	Running time (s)
IGA	20	0.0747	3.5152	0.0391	3.9232	29746
NSGA-II	24	0.1529	2.4121	0.0147	2.7261	36057
PSO-SA	19	0.1612	2.1611	0.1516	2.4331	26789
IA	22	0.0462	1.9633	0.0113	2.3262	19344
TS	16	0.1688	1.7407	0.1945	1.7275	23482

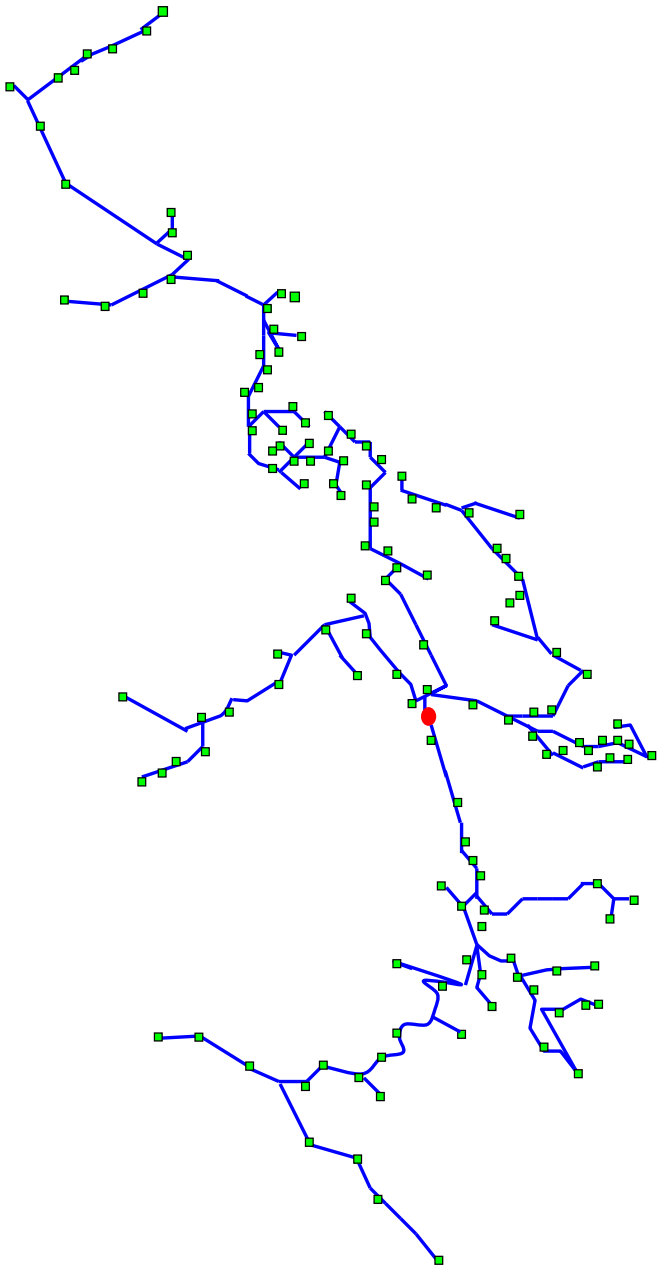

Figure 6.1: A 574-node distribution network

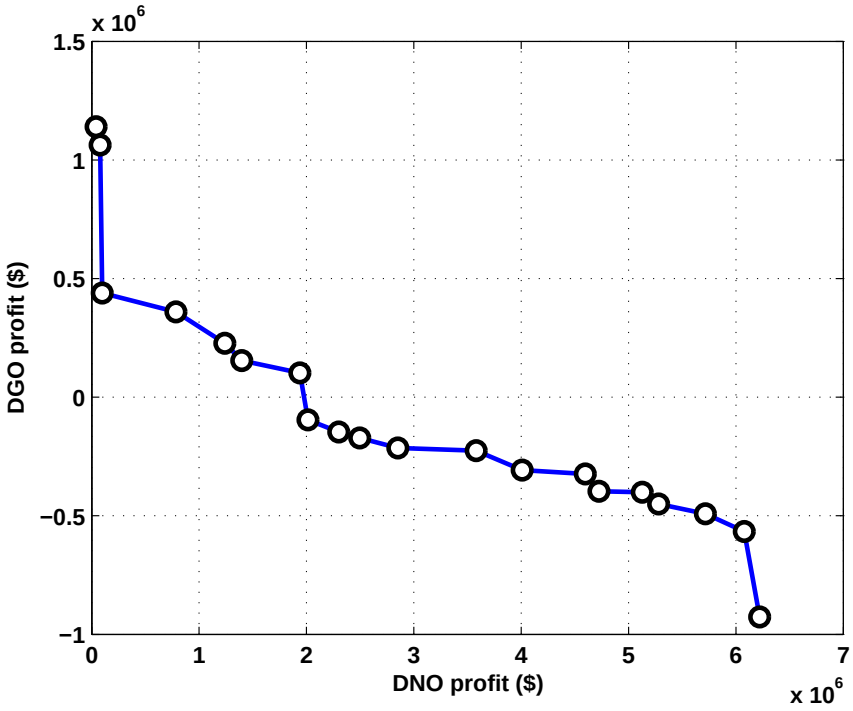

Figure 6.2: Pareto optimal front with $\beta = 0\%$

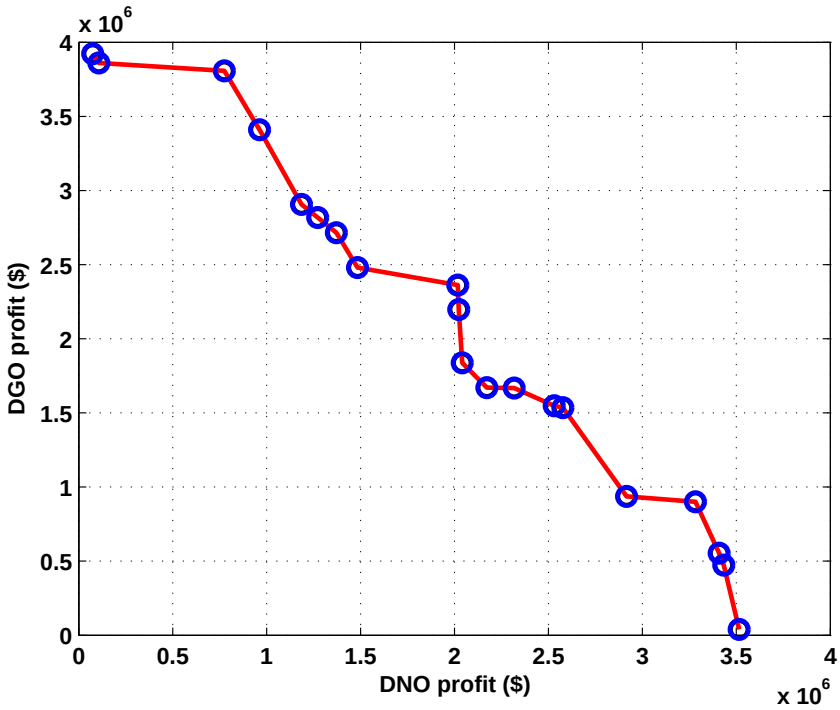

Figure 6.3: Pareto optimal front with variable β

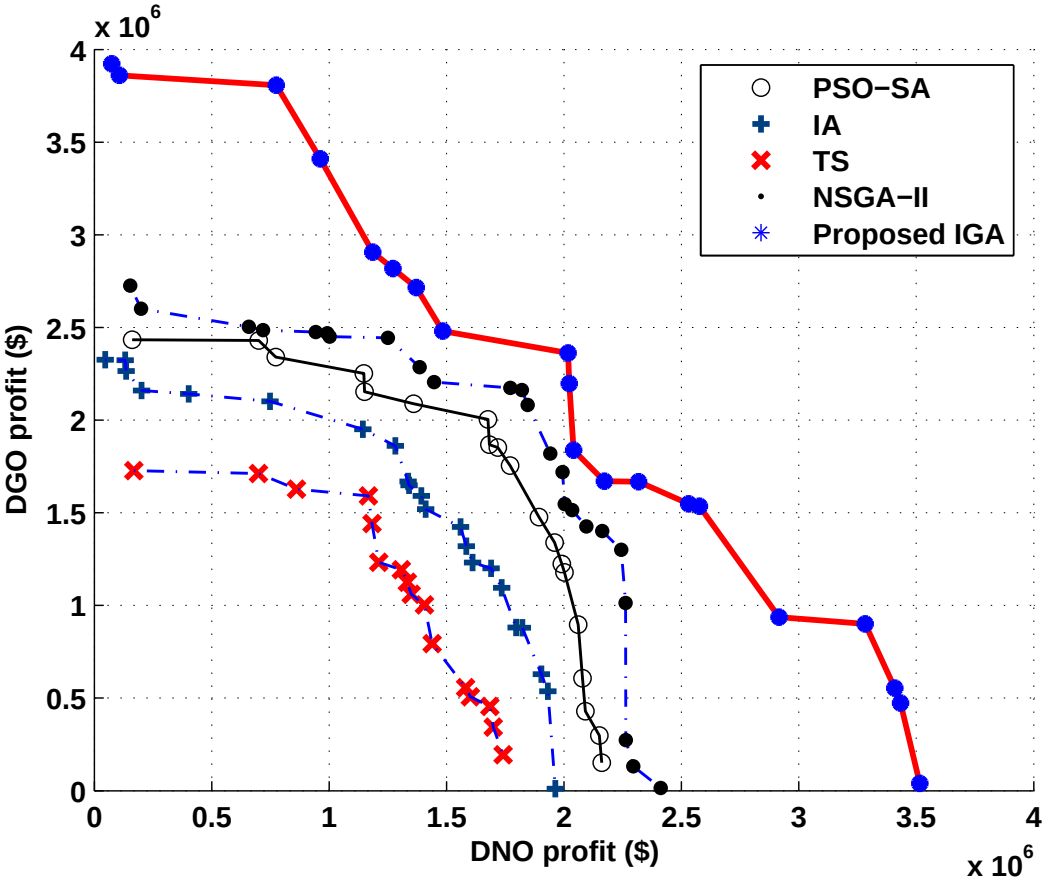

Figure 6.4: Comparing the proposed IGA methodology with other methods

6.3 DG impact on Distribution network operation

6.3.1 Probabilistic problem formulation

The idea of using stochastic techniques for uncertainty modeling is useful when statistical information is available about the uncertain parameters. This means that the behavior of uncertain parameters is described using a PDF. The probabilistic methods are widely used in power system operations and planning to deal with a variety of uncertainties [50]. The probabilistic power flow (PPF) is a tool which handles the uncertainties associated with input data of traditional power flow problem. A great deal of attention has been paid to the PPF problem in the literature. The PPF was first introduced in 1976 [132]. In [133], a convolution based technique was applied to consider the interdependent demands. In [134], a linearized set of load-flow equations were introduced to reduce the complexity of the problem. In [135], a combined Monte Carlo simulation technique and linearized power flow equations was employed. A Cumulant based method was proposed in [136] to deal with PPF problem. An enhancement to the traditional Cumulant method was implemented in [137], named Limit corrected Cumulant method (LCCM) which specifically addressed errors in the existing Cumulant method. This method produces multiple probability density functions (PDFs) and finds the final PDF combining the obtained PDFs. A hybrid Cumulant and Gram-Charlier expansion theory was introduced in [138] to reduce the computational time while maintaining a high degree of accuracy. In [139], an efficient Point Estimate Method (PEM) was proposed to handle the uncertainties of bus injections and line parameters. Four different versions of PEM were tried and tested in [140]. In [141], a Monte-Carlo simulation based method was applied to the nonlinear three-phase load flow equations of distribution networks including wind farms. A Latin Hypercube Sampling (LHS) combined with Cholesky decomposition method (LHS-CD) was proposed in [142]. In [143], Cornish-Fisher expansion series were used to obtain the cumulative distribution function (CDF) of the output variables. In [144], a model based on 2PEM was used to take into account the correlated wind power resources and load values.

6.3.1.1 Power flow equations

The power flow equations to be satisfied are:

$$
\begin{aligned}
P_i^{net} &= -P_i^D + P_i^{w/pv} \\
Q_i^{net} &= -Q_i^D + Q_i^{w/pv} \\
P_i^{net} &= V_i \sum_{j=1}^{N_b} Y_{ij} V_j cos(\delta_i - \delta_j - \theta_{ij}) \\
Q_i^{net} &= V_i \sum_{j=1}^{N_b} Y_{ij} V_j sin(\delta_i - \delta_j - \theta_{ij})
\end{aligned}
\tag{6.19}
$$

where P_i^{net}, Q_i^{net} are the net injected active and reactive power to bus i, respectively. The $P_i^{w/pv}, Q_i^{w/pv}$ are the active and reactive power of wind turbine/PV cells in bus i. Y_{ij} and θ_{ij} are the admittance's magnitude and angle, respectively.

6.3.1.2 Voltage limits

The voltage magnitude of each bus, i.e. V_i should be kept between the operating limits, as (6.5).

6.3.1.3 Feeders and substation capacity limit

To maintain the security of the feeders and substation, the flow of current/energy passing through them should be kept below the feeders/substation capacity limit as (6.6). For substation capacity constraint, the same philosophy holds, as (6.7).

6.3.1.4 Uncertainty modeling

In this study, the uncertain parameters are electric load in each bus and also the generated power of wind turbines and PV cell modules. The uncertainty modeling of each parameter is described as follows:

- Electric load modeling The electric load of each bus is modeled as a normal PDF:

$$PDF(S_i^D) = \frac{1}{\sqrt{(2\pi\sigma_i^D)}}\ exp[-\frac{(S_i^D - \mu_i^D)^2}{2\sigma^2}] \tag{6.20}$$

  where S_i^D is the apparent power demand in bus i and μ_i^D, $(\sigma_i^D)^2$ are the mean and variance of demand in bus i, respectively.

- Wind Turbine generation pattern modeling The generated power of a wind turbine is modeled as described in section 2.2.1.1.

- Photo voltaic cell generation pattern modeling The generated power of a photo voltaic modules is modeled as described in section 2.2.1.1.

6.3.1.5 Output variables

In this section, two variables are of interest namely, Purchased active power from main grid, i.e. P^{grid} and active power losses, i.e. P^{loss}. The total active loss is calculated as follows:

$$P^{loss} = \sum_{i=1}^{N_b} P_i^{net} \tag{6.21}$$

where N_b is the number of all buses in the network.

6.3.1.6 Two point estimate uncertainty handling method

Two point estimate uncertainty handling method is used here. This method is described in section 4.2.2.

6.3.1.7 Simulation results

Two case studies have been analyzed in this section: the first one is a radial 9-bus distribution network and the second one is a realistic 574-node distribution network. The results obtained by the S2PEM and US2PEM are compared with different methods namely,

Monte Carlo, Latin Hypercube sampling (LHS) [142] and Gram Charlier method [138]. The technical characteristics of wind turbines and PV modules are described in Table.5.1 and 6.8, respectively [9]. The Weibull parameters of the wind speed in each wind farm for case-I are assumed to be $c = 8.78$, $k = 1.75$. The Beta parameters of solar radiation are assumed to be $\alpha = 6.38, \beta = 3.43$. In this study, for modeling the uncertainty of wind turbine, 10000 wind samples are generated using (5.3) then they are passed through speed-power curve of the wind turbine as depicted in Fig.2.1. The output of the wind turbine is shown in Fig.6.5 and used for representing the generated wind power.

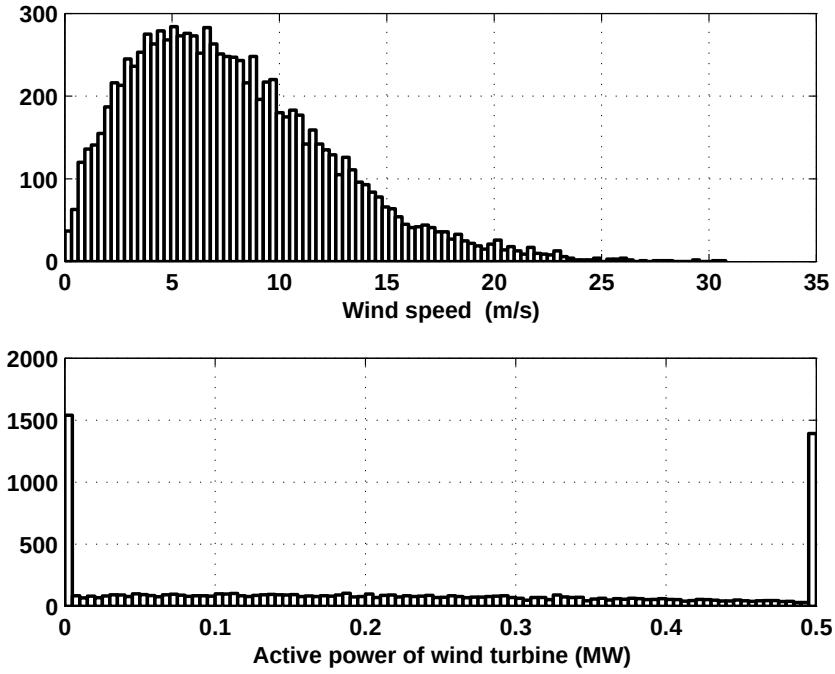

Figure 6.5: The histogram of wind speed and power out put of a 0.5 MW wind turbine

Table 6.8: The technical characteristics of PV modules

I_{sc} (A)	V_{oc} (V)	I_{MPP} (A)	V_{MPP} V	K_v (mV/C°)	K_i (mA/C°)	N_{OT} (C°)
5.32	21.98	4.76	17.32	14.40	1.22	43

6.3.1.8 Case-I: A 9-bus test network

This case is a radial 9-bus distribution network and its single line diagram is presented in Fig.6.6 [119].

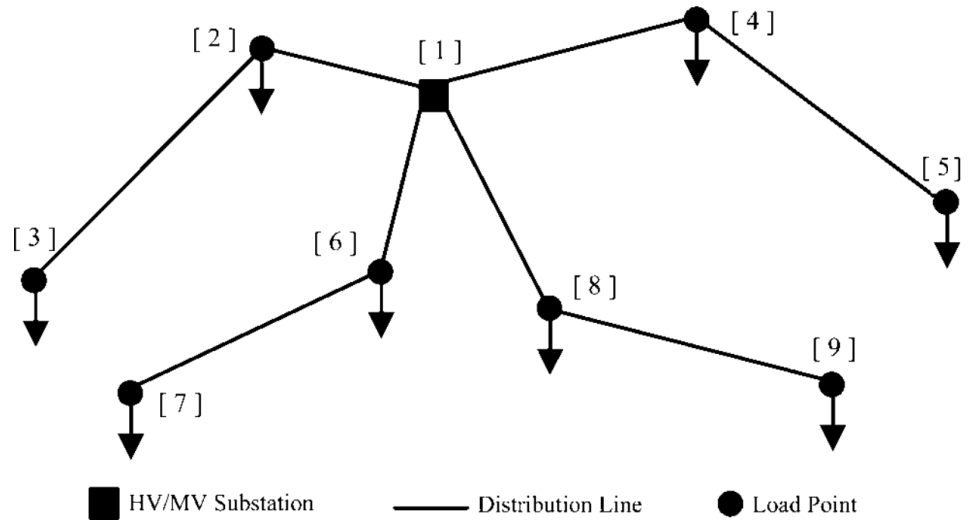

Figure 6.6: The single line diagram of the 9-node distribution network

This network is assumed to have two wind turbines which their data have been given in Table 6.9.

Table 6.9: The installed DGs in Case-I

Bus	No of PV modules	No of WT
3	0	1
9	500	1

In Table 6.9, the number of DG resources and their installation buses are specified. The results obtained for this case, include the mean and standard deviation values of active losses and imported power grid, absolute values of errors and also the running time. The same problem has been simulated with other probabilistic approches such as Monte Carlo Simulation (MCS), Symmetrical two Point Estimate Method (S2PEM), Latine Heybercube Sampling (LHS) and Gram Charlier (all coded in MATLAB environemnt). The comparisons between the obtainded results are presented in Table 6.10.

Table 6.10: Comparison of results in Case-I (the values are in MW)

Method		μ_{loss}	$err(\%)$	σ_{loss}	$err(\%)$	μ_{Pgrid}	$err(\%)$	σ_{Pgrid}	$err(\%)$	Time (s)
MCS		0.8764	0.0000	0.0205	0.0000	33.5080	0.0000	0.3705	0.0000	946.25
S2PEM		0.8415	3.9788	0.0211	3.1247	34.4988	2.9570	0.3841	3.6787	0.1400
LHS		0.8450	3.5809	0.0211	2.8122	34.3997	2.6613	0.3828	3.3108	143.3817
Gram Charlier	4th order	0.8482	3.2228	0.0210	2.5310	34.3106	2.3952	0.3815	2.9797	7.3361
	5th order	0.8510	2.9005	0.0200	2.2779	34.2303	2.1557	0.3606	2.6818	8.3152
	6th order	0.8993	2.6105	0.0209	2.0501	32.8579	1.9401	0.3616	2.4136	9.1634
	7th order	0.8558	2.3494	0.0209	1.8451	34.0931	1.7461	0.3625	2.1722	9.8642
US2PEM		0.8579	2.1145	0.0208	1.6606	32.9814	1.5715	0.3777	1.9550	0.1720

The PDF of active power losses and imported power from the main grid are depicted in Fig.6.8 and Fig.6.7, respectively.

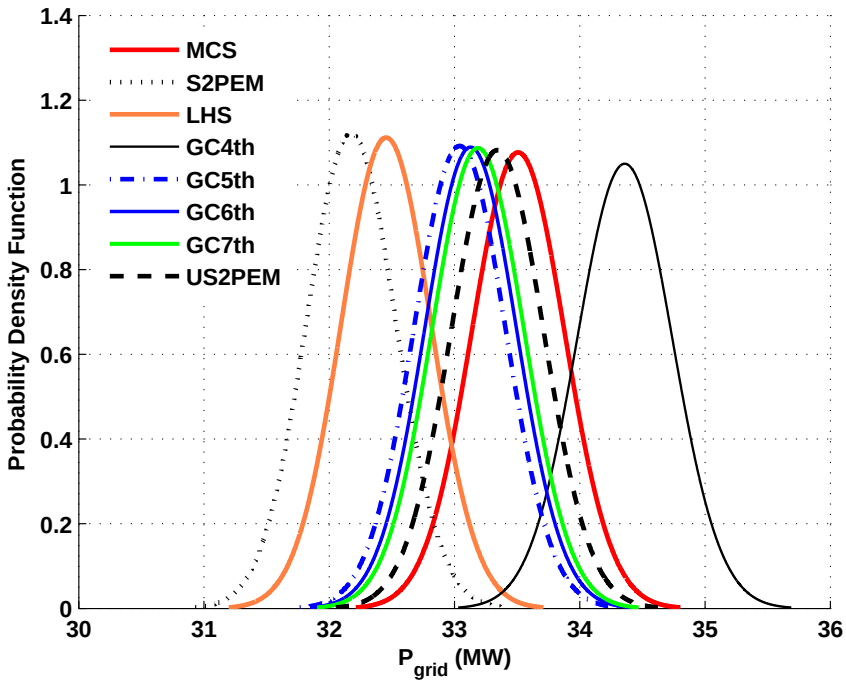

Figure 6.7: Probability density function of imported power from main grid in Case-I

6.3.1.9 Case II: A realistic 574-bus urban French network

The second case is a 20-kV, 574-node distribution system, depicted in Fig.6.1, which is extracted from a real French urban network. This system has 573 sections with total length of 52.188 km, and 180 load points. This network is fed through one substation. These data have been extracted from reports of Electricitè de France (EDF) [145] where more details can be found in [127].

The speed-power characteristics of the wind turbines in case II are the same as case I and In Table 6.13, the number of DG resources and their installation bus are provided.

The results obtained for this case includes the mean and standard deviation values of active losses and imported power grid, absolute values of errors and also the running times have been all presented in Table 6.12. The PDF of imported power from main grid is depicted in Fig.6.9.

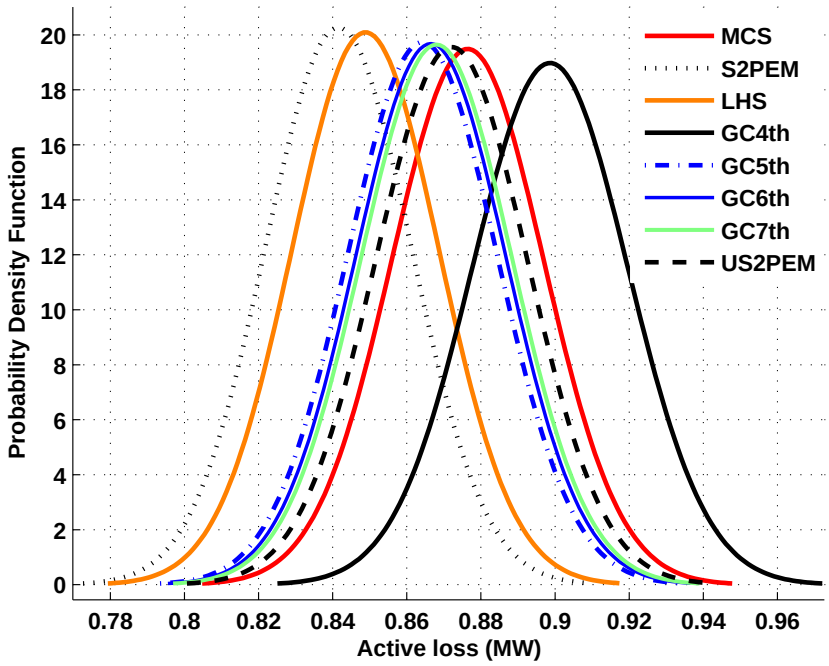

Figure 6.8: Probability density function of active losses in Case-I

Table 6.11: The installed DGs in Case-II

Bus	No of PV modules	No of WT
15	300	0
283	100	2
344	0	1
495	200	7
426	0	2
163	0	1

Table 6.12: Comparison of results in Case-II (the values are in MW)

Method		μ_{loss}	$err(\%)$	σ_{loss}	$err(\%)$	μ_{Pgrid}	$err(\%)$	σ_{Pgrid}	$err(\%)$	Time (s)
MCS		0.2565	0.0000	0.0811	0.0000	8.0918	0.0000	0.2483	0.0000	1264.3480
S2PEM		0.2691	4.9082	0.0840	3.5671	7.8688	-2.7559	0.2400	3.3413	16.4800
LHS		0.2470	3.7226	0.0791	2.4129	8.3047	2.6315	0.2561	3.1350	650.2130
Gram Charlier	4th order	0.2646	3.1578	0.0828	2.0959	7.8988	2.3852	0.2415	2.7285	79.6498
	5th order	0.2618	2.0469	0.0795	1.9356	8.2640	2.1279	0.2541	2.3284	81.3450
	6th order	0.2607	1.6454	0.0823	1.4744	8.2479	1.9292	0.2431	2.1105	83.8510
	7th order	0.2527	1.4714	0.0798	1.6296	7.9554	1.6852	0.2531	1.9205	90.1354
US2PEM		0.2591	1.0298	0.0822	1.2948	8.2106	1.4679	0.2525	1.6951	21.3450

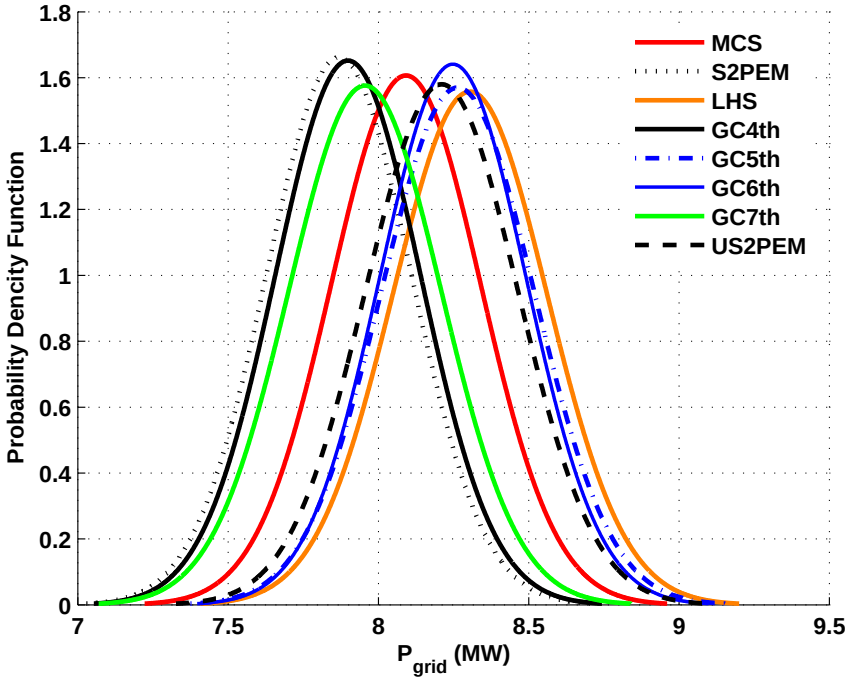

Figure 6.9: Probability density function of imported power from main grid in Case-II

6.3.2 Fuzzy problem formulation

The idea of using fuzzy arithmetic for uncertainty modeling is useful when no statistical information is available about the uncertain parameters [77].

6.3.2.1 DG Modeling

DG units are modeled as negative PQ loads with constant power factor [36], as (5.10).

6.3.2.2 Uncertainty Modeling

The three main sources of uncertainties considered in this section are electric loads, installed capacity of DG units and their operating schedule. The explanation of each parameter is described as follows:

- *Fuzzy load* : The load variation curve over each year is modeled using multiplication of three parameters. The first one is the base load, $S^D_{i,base}$, in the first year of the evaluation period and each year is divided into N_{dl} demand levels. A Demand Level Factor, D^f_{dl}, is assigned to each demand level which is the forecasted value of "load to peak ratio" varying between 0 and 1. The duration of demand level dl is denoted by τ_{dl}. The uncertainty of D^f_{dl} is modeled using Fuzzy Trapezoidal Number (FTN), described as follows:

$$\tilde{D}_{dl} = (dlf_{min}, dlf_L, dlf_U, dlf_{max}) \times D^f_{dl} \tag{6.22}$$

  Assuming a demand growth rate, ϵ_D, the demand in bus i, in demand level dl and year t is calculated as follows:

$$\begin{aligned}
\tilde{P}^D_{i,t,dl} &= P^D_{i,base} \times \tilde{D}_{dl} \times (1+\epsilon_D)^t \\
\tilde{Q}^D_{i,t,dl} &= Q^D_{i,base} \times \tilde{D}_{dl} \times (1+\epsilon_D)^t \\
\tilde{S}^D_{i,t,dl} &= \tilde{P}^D_{i,t,dl} + j\tilde{Q}^D_{i,t,dl} \\
S^D_{i,base} &= P^D_{i,base} + jQ^D_{i,base}
\end{aligned} \tag{6.23}$$

where $\tilde{S}^{D}_{i,t,dl}$, $\tilde{P}^{D}_{i,t,dl}$ and $\tilde{Q}^{D}_{i,t,dl}$ are the apparent, active and reactive fuzzy power demand in bus i, demand level dl and year t; $S^{D}_{i,t,dl}$, $P^{D}_{i,t,dl}$ and $Q^{D}_{i,t,dl}$ are the predicted values of apparent, active and reactive power demand in bus i, demand level dl and year t.

- *Fuzzy installed capacity :* In deregulated environment, the DNO is not responsible for investment in DG units and private sector will invest in the network based on its own interests. The DNO can only analyze the network and identify the interests of DG investors and predict their actions. These facts imply that the capacity of DG units in each bus is not a certain value. In this section, the installed capacity of DG units are modeled as a Fuzzy Trapezoidal Number (FTN), namely $\tilde{\varsigma}^{dg}_{i}$, as follows:

$$\tilde{\varsigma}^{dg}_{i} = (\varsigma^{dg}_{\min}, \varsigma^{dg}_{L}, \varsigma^{dg}_{U}, \varsigma^{dg}_{\max}) \times Cap^{dg,f}_{i}$$

where $Cap^{dg,f}_{i}$ denotes the forecasted value of DG capacity to be installed in bus i.

- *Fuzzy DG generation:* The generation schedules of DG units are determined by DG owners and are not centrally controlled by DNO. In this section, the apparent power of DG units are modeled as a FTN, namely $\tilde{S}^{dg}_{i}$, as follows:

$$\tilde{S}^{dg}_{i,t,dl} = (\epsilon_{min} \times \tilde{\varsigma}^{dg}_{i}, \epsilon_{L} \times \tilde{\varsigma}^{dg}_{i}, \tilde{\varsigma}^{dg}_{i}, \tilde{\varsigma}^{dg}_{i})$$

Although the capacity of installed DG in a given bus, $\tilde{\varsigma}^{dg}_{i}$, is uncertain but the DG generation, $\tilde{S}^{dg}_{i,t,dl}$, can not exceed the installed capacity of DG unit in any α-cut. The minimum generated power of DG unit is highly dependent on the decision of its owner and technical characteristics of DG. In $\alpha = 1$, the percentage of $\tilde{\varsigma}^{dg}_{i}$ which may DG decrease its generated power is specified by ϵ_L and in $\alpha = 0$, this is done using ϵ_{min}.

6.3.2.3 Fuzzy Power flow equations

The power flow equations which must be satisfied for each α-cut, in demand level dl and year t, are as follows:

$$\begin{aligned}
\tilde{P}^{net}_{i,t,dl} &= -\tilde{P}^{D}_{i,t,dl} + \tilde{P}^{dg}_{i,t,dl} \\
\tilde{Q}^{net}_{i,t,dl} &= -\tilde{Q}^{D}_{i,t,dl} + \tilde{Q}^{dg}_{i,t,dl} \\
\tilde{P}^{net}_{i,t,dl} &= \tilde{V}_{i,t,dl} \sum Y_{ij} \tilde{V}_{j,t,dl} \times cos(\tilde{\delta}_{i,t,dl} - \tilde{\delta}_{j,t,dl} - \theta_{ij}) \\
\tilde{Q}^{net}_{i,t,dl} &= \tilde{V}_{i,t,dl} \sum Y_{ij} \tilde{V}_{j,t,dl} \times sin(\tilde{\delta}_{i,t,dl} - \tilde{\delta}_{j,t,dl} - \theta_{ij})
\end{aligned} \tag{6.24}$$

where $\tilde{P}^{net}_{i,t,dl}$ and $\tilde{Q}^{net}_{i,t,dl}$ are the net active and reactive power injected to the network in bus i, in demand level dl and year t, respectively.

6.3.2.4 Voltage limits

The magnitude of voltage in each bus i in demand level dl and year t should be kept between the safe operating limits as (6.5).

6.3.2.5 Thermal limits of feeders and substation

To maintain the security of the feeders and substations, the flow of current/energy passing through them should be kept below their thermal limit as (6.6).

6.3.2.6 Evaluation indices

Two evaluation indices are introduced and computed in this section namely load repression and active loss. The fisrt one (load repression) shows the robustness of the networks's abbility in supplying the loads at presence of different uncertainties and technical constraints. The second index is well known acitive loss in the network which somehow represents the efficiency of the network.

Load repression The distribution networks are designed for forecasted values of loads. The DNOs need some evaluation tools to determine the robustness of distribution network against different uncertainties. These uncertainties include investment/operating of DG units and also forecasted values of loads in the network. The load repression index introduced in [146], is used to identify the difference between the possible (predicted) values of load and what can be supplied in each bus. If these two values are different in a bus, its load is repressed. First of all, the differences between two important concepts are explained and then their application will be demonstrated. The predicted value of load in bus i is obtained by multiplication of three parameters namely, base value of load in bus i , $S^D_{i,base}$, forecasted value of demand level factor in demand level dl, D^f_{dl}, and load growth factor until year t, $(1+\epsilon_D)^t$. The forecasted value of load is shown in Fig.6.10 and calculated as follows:

$$S^f_{i,t,dl} = S^D_{i,base} \times D^f_{dl} \times (1+\epsilon_D)^t \tag{6.25}$$

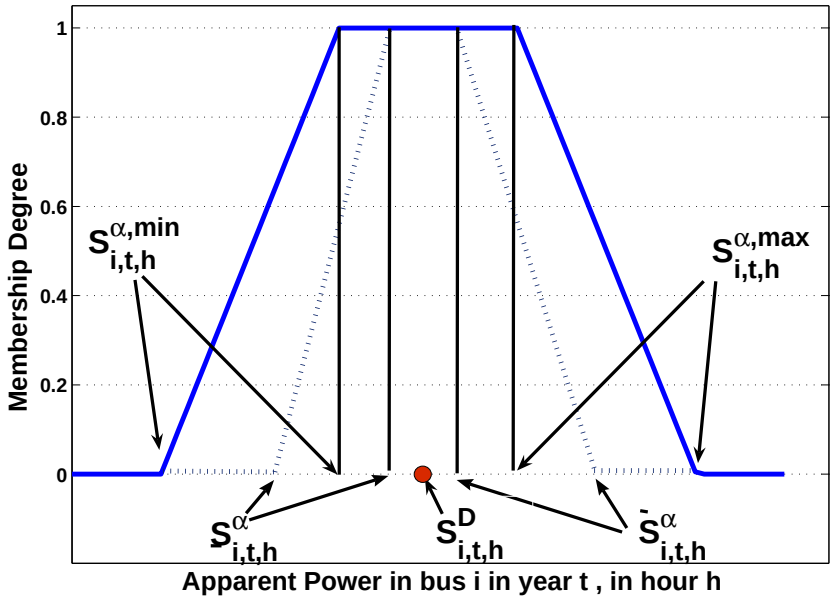

Figure 6.10: Fuzzy load repression

The distribution network is designed to meet the forecasted values of load, $S^f_{i,t,dl}$, during the planning horizon. As it is already explained, the DNO needs some diagnostic

tools to investigate if the ability of network in load supply is robust against different uncertainties. In order to explain the load repression index, two concepts are introduced, as follows:

The first concept is the maximum/minimum possible load due to prediction in each α-cut, $S_{i,t,dl}^{\alpha,\max/\min}$, which are defined as follows:

$$\begin{aligned} S_{i,t,dl}^{\alpha,\min} &= S_{i,base}^{D} \times \underline{D}_{dl}^{\alpha} \times (1+\epsilon_D)^t \\ S_{i,t,dl}^{\alpha,\max} &= S_{i,base}^{D} \times \overline{D}_{dl}^{\alpha} \times (1+\epsilon_D)^t \\ S_{i,t,dl}^{\alpha,\min} &\leq S_{i,t,dl}^{\alpha} \leq S_{i,t,dl}^{\alpha,\max} \end{aligned} \tag{6.26}$$

It should be noted that the limits introduced in (6.26) are not calculated values. They are predicted by DNO for describing the behaviors of load in each bus.

The second concept is that, hypothetically, the magnitude of each load can take any value between the limits posed by (6.26), in each α-cut, $S_{i,t,dl}^{\alpha,\min} \leq S_{i,t,dl}^{\alpha} \leq S_{i,t,dl}^{\alpha,\max}$, but because of some technical considerations like voltage limits or thermal capacity of feeders/transformers as mentioned in (6.40) and (6.41), the predicted limits may not be reachable. Whenever a load in a bus can not reach its predicted limits, it is called repressed. The maximum/minimum load that can be supplied due to technical constraints, are indicated as $\overline{S}_{i,t,dl}^{\alpha}$ and $\underline{S}_{i,t,dl}^{\alpha}$, respectively and depicted in Fig.6.10. A method was proposed in [146] for calculating the upper and lower bounds of active/reactive values of loads in each bus. In this section, it is modified as follows: first, for calculating the upper bound of load in a given α-cut, in addition to the constraints considered in [146], voltage limits are also considered in calculations. The second issue is that when the uncertainty of a load is concerned, it is mainly toward its magnitude not its power factor. This implies that if the calculation of the active and reactive values of load is done independently then the loads can have any power factor which are not realistic. In this section, it is assumed that the only uncertain value of the load in each bus is the magnitude of it. The DNO checks the maximum and minimum load in bus i, $\overline{S}_{i,t,dl}^{\alpha}, \underline{S}_{i,t,dl}^{\alpha}$, which distribution network is able to

supply in each demand level, as follows:

$$\begin{aligned} &\underline{S}^{\alpha}_{i,t,dl} = \min S^{\alpha}_{i,t,dl} \\ &\overline{S}^{\alpha}_{i,t,dl} = \max S^{\alpha}_{i,t,dl} \\ &\textit{Subject to:} \\ &\textit{Constraints} \end{aligned} \tag{6.27}$$

The load repression index in demand level dl and year t, $rep_{i,t,dl}$, is defined as the sum of the area in membership function of each load that can not be supplied in a given network (distinguished in Fig. 6.10) and calculated as follows:

$$rep_{i,t,dl} = \Delta(S^{\alpha,\min}_{i,t,dl}, S^{\alpha,\max}_{i,t,dl}) - \Delta(\underline{S}^{\alpha}_{i,t,dl}, \overline{S}^{\alpha}_{i,t,dl}) \tag{6.28}$$

where Δ is the operator for calculating the surface under the membership function of fuzzy parameter. The total load repression in each year, $Yrep_t$, is defined as the sum of the multiplication of load repression in each load level dl by its duration τ_{dl} over all load buses of the system, as follows:

$$Yrep_t = \sum_{dl=1}^{N_{dl}} \sum_{i=1}^{N_b} rep_{i,t,dl} \times \tau_{dl} \tag{6.29}$$

The total load repression in bus i over the evaluation period, $Brep_i$, is calculated as follows:

$$Brep_i = \sum_{t=1}^{T} \sum_{dl=1}^{N_{dl}} rep_{i,t,dl} \times \tau_{dl} \tag{6.30}$$

The total load repression of the distribution network over the evaluation period, $Trep$, is calculated as follows:

$$Trep = \sum_{t=1}^{T} Yrep_t \tag{6.31}$$

Active losses The total active losses in each α-cut is calculated as the sum of all active losses in demand levels of each year, over the evaluation period.

$$\tilde{P}_{loss} = \sum_{t=1}^{T} \sum_{dl=1}^{N_{dl}} \sum_{i=1}^{N_b} \tilde{P}_{i,t,dl}^{net} \times \tau_{dl} \tag{6.32}$$

For calculating $\tilde{P}_{loss}$, the α-cut concept introduced in section 4.3.1 is used as follows:

$$\begin{aligned} & P_{loss}^{\alpha} = (\underline{P}_{loss}^{\alpha}, \overline{P}_{loss}^{\alpha}) \\ & \overline{P}_{loss}^{\alpha} = \max \sum_{t=1}^{T} \sum_{dl=1}^{N_{dl}} \sum_{i=1}^{N_b} P_{i,t,dl}^{net,\alpha} \times \tau_{dl} \\ & \underline{P}_{loss}^{\alpha} = \min \sum_{t=1}^{T} \sum_{dl=1}^{N_{dl}} \sum_{i=1}^{N_b} P_{i,t,dl}^{net,\alpha} \times \tau_{dl} \\ & \textit{Subject to:} \\ & \textit{Constraints} \end{aligned} \tag{6.33}$$

6.3.2.7 Simulation results

The proposed methodology is applied to two distribution systems to demonstrate its abilities. The first case is a 9-node distribution test system and the second one is a realistic 574-node distribution network.

6.3.2.8 Case-I

The proposed method is applied on a 11-kV, 9-bus distribution network which is shown in Fig.6.6 [33]. This network is fed through a transformer with $S_{max}^{grid} = 40MVA$ and has 8 aggregated load points. The rate of load growth, ϵ_D, is considered to be 2%. The technical characteristics of the network can be found in [33]. The evaluation period, T, is 5 years and the minimum and maximum value of operating limits of voltage, V_{min}, V_{max}, are 0.95 and 1.05 pu, respectively. The load duration curve is divided into four demand levels namely, high, normal, medium and minimum, where the forecasted values of them, D_{dl}^{f}, are 1, 0.941, 0.866 and 0.686, respectively. The duration of each load level, τ_{dl}, is assumed to be 73, 2847, 2920, 2920 hours, respectively. The demand level factors are described as

Table 6.13: Predicted values of DG capacities and their uncertainties

Cases	DG #	DG Technology	Bus	$Cap_i^{dg,f}$	$\zeta_{\min}^{dg}$	ζ_L^{dg}	ζ_U^{dg}	$\zeta_{\max}^{dg}$
I	1	Gas Turbine	2	400 kVA	0	0.9	1.05	1.1
	3	Gas Turbine	9	200 kVA	0.1	0.6	1.1	1.2
	2	CHP	3	500 kVA	0	0	1.00	1.15
II	1	Gas Turbine	15	500 kVA	0	0.9	1.05	1.1
	2	Gas Turbine	283	1 MVA	0.1	0.6	1.1	1.3
	3	Gas Turbine	344	500 kVA	0	0.9	1.05	1.1
	4	Gas Turbine	495	3.5 MVA	0.1	0.4	1.12	1.25
	5	CHP	426	500 kVA	0	0.2	1.07	1.15
	6	CHP	163	500 kVA	0	0.1	1.03	1.2

fuzzy trapezoidal numbers as explained in section 6.3.2.2. The specification of membership functions of demand level factors is done by DNO based on his prior experiences. It is not necessary that all of the demand level factors have the same membership functions but here, for simplicity, a non-symmetrical membership function is used for all buses of the network, as follows: In $\alpha = 0$,

$$dlf_{max} = (1 + U_{dlf}), dlf_{min} = (1 - 0.7 \times U_{dlf})$$

In $\alpha = 1$,

$$dlf_U = (1 + 0.5 \times U_{dlf}), dlf_L = (1 - 0.6 \times U_{dlf})$$

where U_{dlf} is a factor for demonstrating the severity of uncertainty, varying between zero and one.

The capacity of DG which might be installed in a given bus is not determined by DNO and he should have an estimation about this value. In this section, it is assumed that the buses which have the possibility of DG investment are identified and the potential DG capacity which may be installed there is predicted. This process is not necessarily precise and is subject to uncertainties associated to the decisions of the DG investors. In the given network, there are three buses which are candidate for DG installation, namely bus 2, 3 and 9. The forecasted values of the DG capacities and their associated uncertainties are given in Table. 6.13.

For example for DG #1, in $\alpha = 1$, the lower bound of the DG capacity is $0.9 \times 400 = 360kVA$ and the upper bound is $1.05 \times 400 = 420kVA$. This means that the maximum degree of belief of the planner is that the capacity of DG will have a value between 360 and 420 kVA. In $\alpha = 0$, the lower bound of DG capacity is still zero, this means that the planner can not specify a minimum limit for the capacity of DG that may be installed in the given bus and its upper bound is $1.1 \times 400 = 440kVA$. This means the DG owner/investor may decide not to invest in DG and the maximum value of capacity which an investor may be interested (or able to) to install in bus i=2 is 440 kVA. The same concept holds for the data specified for other DG units. The values of ϵ_{min} and ϵ_L in (6.24) are used to model the operational uncertainties of investor-owned DG units. These values are highly dependent on DG technology and decisions of DG owner for making more profits. For Gas turbine DG units, DG owner tries to produce electricity as much as possible. This means that DNO expects these units to produce power near their capacity limit. In this section, ϵ_L is considered to be 0.9 for Gas Turbine technology. On the other hand for CHP units, the DG operation is more uncertain because DG owner has two options for making benefits namely, selling power and heat. If DG owner decides to produce heat then he will have to reduce its output power and vice-versa. For CHP units, ϵ_L is considered to be 0.4. For both DG technologies, ϵ_{min} is 0. In other words, the maximum belief of DNO ($\alpha = 1$) indicates that the DG owner will produce more than ϵ_L % of its rated capacity but it is not guaranteed and he might produce less or even stop generating power which is less expected but possible ($\alpha = 0$).

The introduced indices are calculated and the effect of load uncertainties on them are investigated.

6.3.2.9 Calculating the technical indices

In order to clarify the application of load repression index, it is calculated when no uncertainty exists in demand level factors, $U_{dlf} = 0\%$. It is expected to obtain $Trep = 0$ because the distribution network is designed for this purpose. The DNO may be interested to know the answers of the following questions: how much the current network is robust against load uncertainty?; when will be the reinforcement actions required? The load

repression indices are recalculated for $U_{dlf} = 5\%$. As it can be observed in Table.6.14, there is no load repression in the system in the evaluation period. This means the system will face no problem even there is 5% uncertainty in demand. The second index to be calculated is the actives losses. This index is calculated using (6.33) and the crisp value of total active losses is obtained as 17764 MWh. Now the effect of demand uncertainty on the proposed indices is assessed. The uncertainty of demand level factors, U_{dlf}, is varied and its effect on the total yearly load repression, $Yrep_t$, total load repression in the evaluation period, Trep, and finally the total active loss is investigated. The yearly load repression, $Yrep_t$, is calculated for different U_{dlf} and the variation of this parameter is given in Table.6.14. The values of $Yrep_t$ in Table.6.14 show that the network supplies its loads when there is no uncertainty in the predicted values of load ($U_{dlf} = 0\%$). When the uncertainty increases the load repression occurs in the system. The first load repression occures in year t=5, and ($U_{dlf} = 25\%$). With the increase of demand uncertainty, the load repression index shows an ascending pattern. The limits of fuzzy loss variation, the crisp values of active losses and total load repression for the given configuration of the network are calculated for different demand level uncertainties are given in Table. 6.15.

Table 6.14: The yearly load repression under different uncertainties of demand level factors in Case-I

U_{dlf}	$Yrep_t(MWh)$				
%	$t=1$	$t=2$	$t=3$	$t=4$	$t=5$
$0 \rightarrow 20$	0	0	0	0	0
25	0	0	0	0	4.23
30	0	0	0	0	10.68
35	0	0	0	6.88	21.82
40	0	1.14	7.25	17.90	60.63

6.3.2.10 DG penetration level impact investigation

In this section, the impact of DG penetration level on crisp active losses and total load repression is analyzed. In this case, it is assumed that the demand uncertainty is $U_{dlf} = 30\%$. Two different DG scenarios were created and assessed, as follows:

- "Multi DGs" scenario: In this scenario, more than one DG exist in the distribution network. The capacity of each DG unit is assumed to be equal to 1 MW. Different

Table 6.15: The Trep and active losses under different uncertainties of demand level factors in Case-I

U_{dlf}	$\tilde{P}_{loss}(MWh)$				$(\tilde{P}_{loss})^*$	Trep
%	$\underline{P}_{loss}^{\alpha=0}$	$\underline{P}_{loss}^{\alpha=1}$	$\overline{P}_{loss}^{\alpha=1}$	$\overline{P}_{loss}^{\alpha=0}$	(MWh)	(MWh)
0	11842.7	12421.4	18817.1	25048.7	17196	0
5	10814.2	11639.7	20145.7	27713.2	17764	0
10	9846.9	10889.9	21523.7	30518.1	18407	0
15	8939.1	10172.0	22951.1	33379.7	19101	0
20	8088.6	9485.7	24406.1	36269.0	19831	0
25	7292.7	8830.7	25864.9	37762.9	20182	4.23
30	6548.9	8206.4	27336.3	41939.0	21329	10.68
35	5856.0	7612.0	28804.1	44585.7	22057	28.71
40	5213.3	7046.8	30269.1	46968.9	22728	86.91

amount of DG units are connected to the network and the crisp values of active losses and total load repression are given in Table. 6.16.When DG units are in bus 5 and 7, the load repression is the same as the case when they are installed in bus 4,6 equal to 1412.1 MWh. The values of active losses are different in these two cases. The load repression can be reduced more if the DG units are installed in bus 3,8. With three DG units in 4,8,3 buses the load repression can be eliminated completely.

Table 6.16: The Trep and active losses in multi DG scenario in Case-I

Bus	Total DG capacity	Trep (MWh)	Crisp Loss (MWh)
5,9	2	1407.80	28999
5,7	2	1412.10	29044
4,6	2	1412.10	29987
7,9	2	1407.80	29086
2,6	2	41.38	30265
2,9	2	37.11	29748
3,6	2	7.27	29606
2,3	2	4.27	29803
3,8	2	3.00	29539
2,9,8	3	30.3	29049
4,8,3	3	0	28675
3,9,5	3	0	27755
3,4,9,8	4	0	27556

- "Single DG" scenario: In this scenario, just one DG is installed in different nodes of the distribution network. The capacity of each unit is gradually increased from 0 to 8 MW. The variation of active losses and load repression are depicted in Fig.6.11.

Initially, the active losses gradually decreases with the increase of DG capacity and after a certain value of DG capacity it starts to increase. The impact of DG capacity

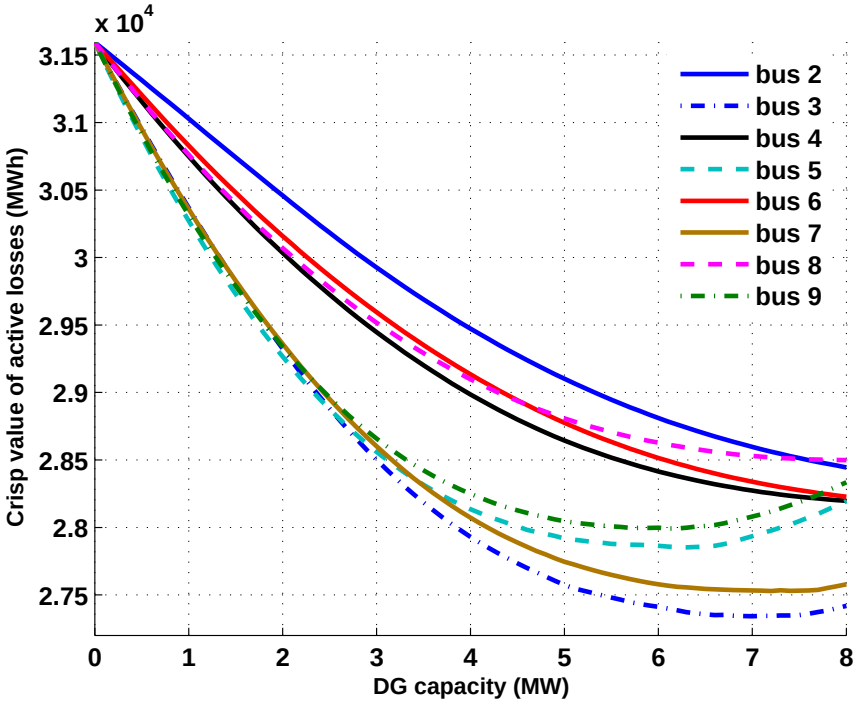

Figure 6.11: The DG penetration level impact on active losses in single DG scenario-Case I

on Trep is shown in Fig.6.12. As it can be seen in Fig.6.12, the existence of DG units in some buses highly affects (reduces) the load repression (like bus 2,3), while the presence of DG units in some buses (like 4,5,6,7) has no impact on load repression index. It is because of the topology of the network that the installed capacity of DG units can not help to reduce the load repression.

It is clear from the analysis that not only the size of DG unit affects the active losses and total load repression but also the location of DG units plays an important role.

6.3.2.11 Case II: A real 574-bus urban network

The second case is a 20-kV, 574-node distribution system, depicted in Fig.6.1, which is extracted from a real French urban network. This system has 573 sections with total length of 52.188km, and 180 load points. This network is fed through one substation. These data have been extracted from reports of Electricité de France (EDF) [145] and

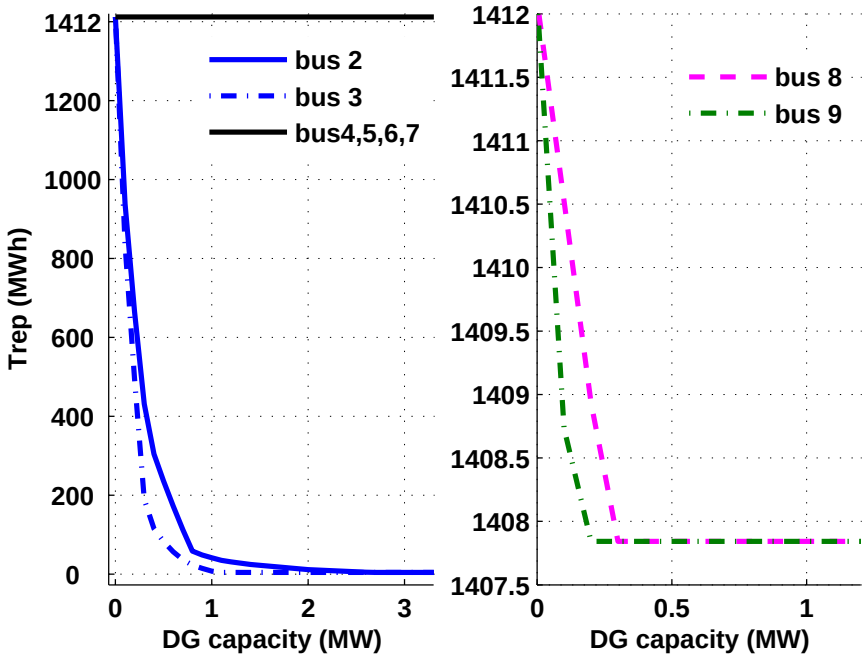

Figure 6.12: The DG penetration level impact on load repression in single DG scenario– Case I

more details can be found in [127]. All DG units are assumed to operate with constant power factor equal to 0.9 lag. The forecasted values of the DG capacities and their associated uncertainties are given in Table. 6.13. The other simulation data is the same as case I.

6.3.2.12 Calculating the technical indices

For the given network configuration, the introduced indices are calculated as follows: the yearly load repression, i.e. $Yrep_t$, is calculated under different uncertainties of demand level factors and the results are given in Table. 6.18. The limits of fuzzy loss variation, the crisp values of active losses and total load repression for the given configuration of the network are calculated for different demand level uncertainties are given in Table. 6.17.

The scope of this study has been limited to the uncertainties which are inherently possibilistic. It is of interest to know how it can be modified to investigate the impact of renewable energy resources (with probabilistic description) of distribution network performance. In [107], a mixed possibilistic-probabilistic method is proposed to deal with active

Table 6.17: The Trep and active losses under different uncertainties of demand level factors in Case-II

U_{dlf}	$\tilde{P}_{loss}(MWh)$				$(\tilde{P}_{loss})^*$	Trep
%	$\underline{P}_{loss}^{\alpha=0}$	$\underline{P}_{loss}^{\alpha=1}$	$\overline{P}_{loss}^{\alpha=1}$	$\overline{P}_{loss}^{\alpha=0}$	(MWh)	(MWh)
0	7348.0	7595.6	8331.0	8585.2	7965.1	0.0
5	7554.3	8041.0	8688.1	8895.0	8286.4	0.0
10	8182.2	8879.8	9761.7	10429.1	9312.1	4.0
15	8793.7	8967.9	9457.3	10248.1	9392.3	5.3
20	9044.1	9926.9	10619.6	10681.7	10040.0	7.6
25	9742.7	9788.8	9899.3	9937.1	9842.0	9.4
30	10470.8	11253.4	11967.6	12547.6	11552.0	11.8
35	10579.8	11284.3	12403.1	12469.7	11671.0	16.6
40	10703.2	11213.0	11748.5	11881.5	11375.0	20.9

Table 6.18: The yearly load repression under different uncertainties of demand level factors in Case-II

U_{dlf}	$Yrep_t(MWh)$				
%	$t=1$	$t=2$	$t=3$	$t=4$	$t=5$
$0 \rightarrow 5$	0	0	0	0	0
10	0	0	1.15	1.33	1.56
15	0.20	0.21	1.19	1.37	2.35
20	0.24	0.32	1.58	2.19	3.28
25	0.27	0.46	1.68	3.15	3.87
30	0.40	0.52	2.51	4.35	4.04
35	0.46	0.64	3.56	6.54	5.39
40	0.54	0.87	3.76	7.78	7.95

losses in presence of both renewable and non-renewable DG technologies. It can also be applied to model the impact of renewable DG technologies on load repression index. The contributions of the proposed evaluation method can be summarized as follows:

- The information gathered in the process (namely the load repression and active losses) is useful for regulators and DNOs and can be used to support the analysis of different expansion plans and also as an economical or technical signal to encourage or penalize DG investment in a given bus or DG technology or even size or operating schedule of the DG units.

- The mathematical formulation allows to define the load repression as an objective function to be minimized in robust distribution planning procedure.

- It is specially helpful in situation where there is not enough historic measured data

about the uncertain parameters or the uncertainty of the parameters can not described using a probability distribution function. This ability, make it possible to design strategies that satisfy the requirements of the regulatory bodies and the real concerns of the DNOs.

6.3.3 Fuzzy-probabilistic(Monte Carlo) problem formulation

The idea of using mixed possibilistic-probabilistic uncertainty modeling is useful when there exists some parameters that no statistical information is available about them and some parameters which are described stochastically using a PDF.

6.3.3.1 Problem Formulation

The assumptions for modeling the two types of uncertainties, constraints and the objective functions are described as follows:

6.3.3.2 Uncertainty Modeling

As already explained, the uncertain parameters are divided into two groups: possibilistic and probabilistic. In possibilistic uncertainty group the value load in each bus, DG generation which are not stochastic (controllable with decisions of their owners). The second group contains the stochastic generation of wind turbines which is probabilistically modeled. The description of the parameters of each group is as follows:
Possibilistic Parameters:

- Load: It is modeled as described in (6.23)
- DG generation pattern : The amount of energy which a controllable DG unit injects into the network is uncertain and usually depends on the decisions of DG owner so the DNO can not have a PDF of it if there is not much historic data about it. The output power of a controllable DG unit is modeled using a membership function as follows:

$$P_{h,i}^{dg} \in C_i^{dg} \times (\zeta_{\min}, \zeta_L, \zeta_U, \zeta_{\max}) \tag{6.34}$$

  Where, C_i^{dg} is the capacity of DG unit installed in bus i and $P_{dl,i}^{dg}$ is the active power of a DG unit in bus i in demand level dl.

6.3.3.3 Power Flow Constraints

The power flow equations must be satisfied in each demand level dl and year t, is as follows:

$$\begin{aligned}
\tilde{P}^{net}_{i,t,dl} &= -\tilde{P}^{D}_{i,t,dl} + \tilde{P}^{dg}_{i,t,dl} + \sum_{wind=1}^{N_{wind}} P^{wind}_{dl,i} \\
\tilde{Q}^{net}_{i,t,dl} &= -\tilde{Q}^{D}_{i,t,dl} + \tilde{Q}^{dg}_{i,t,dl} \\
\tilde{P}^{net}_{i,t,dl} &= \tilde{V}_{i,t,dl} \sum Y_{ij} \tilde{V}_{j,t,dl} \times cos(\tilde{\delta}_{i,t,dl} - \tilde{\delta}_{j,t,dl} - \theta_{ij}) \\
\tilde{Q}^{net}_{i,t,dl} &= \tilde{V}_{i,t,dl} \sum Y_{ij} \tilde{V}_{j,t,dl} \times sin(\tilde{\delta}_{i,t,dl} - \tilde{\delta}_{j,t,dl} - \theta_{ij})
\end{aligned} \tag{6.35}$$

where $\tilde{P}^{net}_{i,t,dl}$ and $\tilde{Q}^{net}_{i,t,dl}$ are the net active and reactive power injected to the network in bus i, in demand level dl and year t, respectively. $\tilde{P}^{D}_{i,t,dl}, \tilde{Q}^{D}_{i,t,dl}$ are the active and reactive demand in bus i, in demand level dl and year t, respectively.

6.3.3.4 Operating Limits of DG units

The operating limits of a DG units should be satisfied as described in (5.9).

6.3.3.5 Voltage Profile

This constraint is explained in (6.40)

6.3.3.6 Thermal Limits of feeders and substation

This constraint is explained in (6.41)

6.3.3.7 Active Losses

The total active loss of the network is equal to the sum of all active power injected to each bus, as follows:

$$Loss = \sum_{dl=1}^{N_{dl}} (\sum_{i=1}^{N_b} P_{dl,i}^{net} + P_{dl}^{grid}) \times \tau_{dl} \tag{6.36}$$

$$Loss \in (loss_{\min}, loss_L, loss_U, loss_{\max})$$

$$\alpha = 0$$

$$loss_{\min} = \min Loss$$

$$loss_{\max} = \max Loss$$

$$\alpha = 1$$

$$loss_L = \min Loss$$

$$loss_U = \max Loss$$

Subject to :

$$Constraints$$

Where, τ_{dl} is the duration of demand level h and N_{dl} is the number of demand levels.

6.3.3.8 Simulation Results

The proposed methodology is applied to a 574-bus realistic distribution network which is shown in Fig.6.1. This network consists of a 20 kV substation with capacity limit, i.e. $\overline{S}_{tr} = 20MVA$ and 573 feeders with 180 load points. The average load and power factor at each load point are 55.5 kW and 0.9285, respectively. There are six DG units present in the network where four of them are dispatchable (by non-DNO entities) and two of them are wind turbines. The DG capacities and their location in the network are given in Table.6.20. The shape and scale factors of the Weibull PDF of wind speed and the other simulation parameters are given in Table.6.19. It is assumed that there are 24 demand levels in each year with equal duration of $\tau_{dl} = 365hr$.

The proposed algorithm is applied to the introduced network and the total active losses

are obtained. The total active losses of the network can be presented in two ways: the first method is representing it by a trapezoidal fuzzy number in which each parameter of the membership function is a probabilistic quantity and has a PDF or histogram. In Fig.6.13, the probability distribution function of four parameters are shown. These parameters, i.e. $(Loss_{min}, Loss_L, Loss_U, Loss_{max})$, describe the total losses in the network.

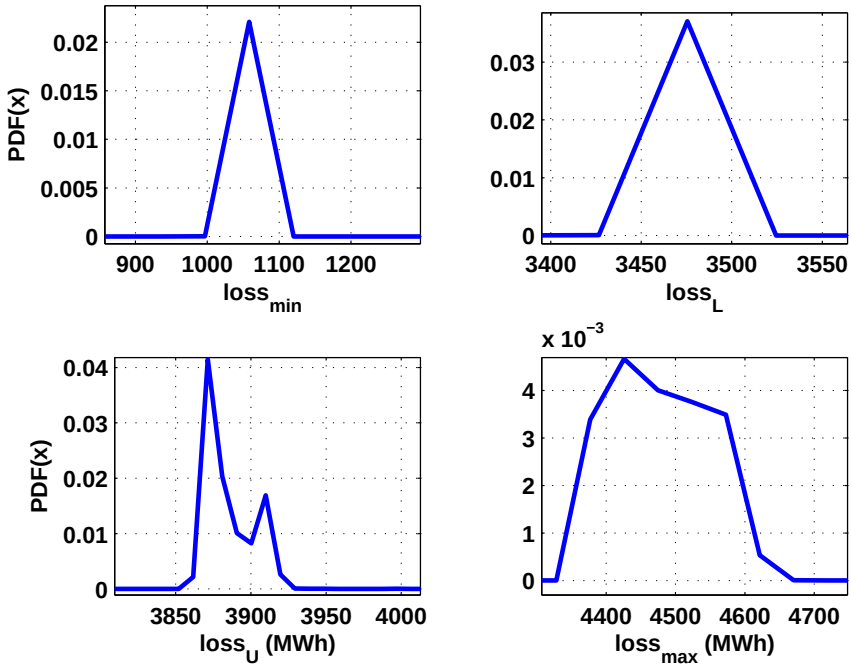

Figure 6.13: Probability distribution functions of total loss membership function

The histogram of variation of each parameter is shown in Fig.6.14, describes the distribution of samples in the total Monte Carlo experiments which has been 20000 experiments in this study.

The second method for representing the total active loss is calculating the crisp value of active loss using (4.16) in each Monte Carlo experiment and then obtaining the distribution of this quantity as shown in Fig.6.15.

The cumulative distribution function of crisp value of total losses is also shown in Fig.6.16. For example if DNO wants to know the probability of having more than a specific loss in their network. For example, that might be a question that what is the probability of having more than 3100 MWh loss in the network? Referring to Fig.6.16, the probability that total loss exceeds 3100 MWh, is equal to 0.4388.

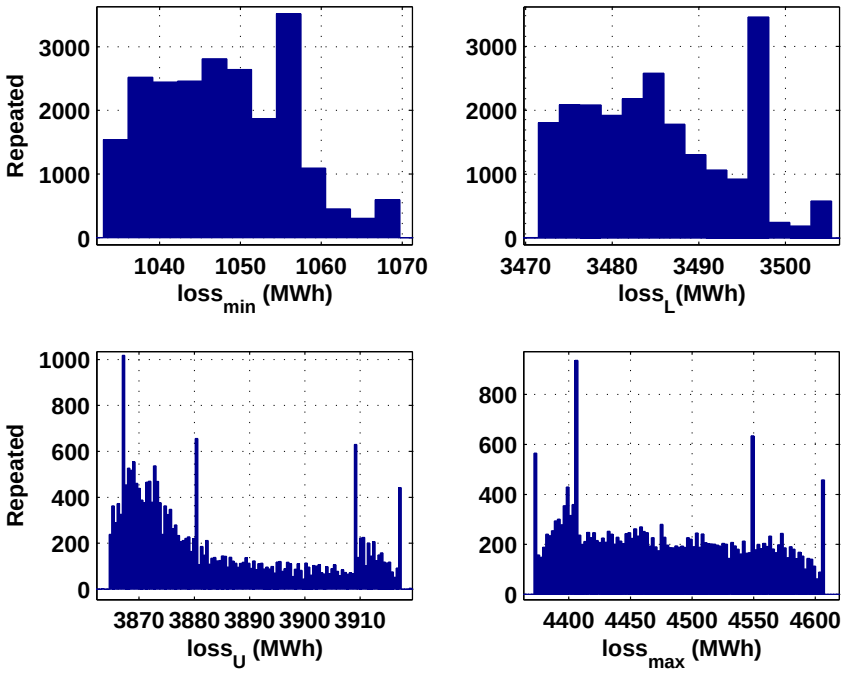

Figure 6.14: Histogram of total loss membership function parameters

The developed hybrid tool attempts to overcome limitations in evaluating the network losses when different sources of uncertainty exist. Specially when renewable and conventional DG units are present in the network. This hybrid approach makes the DNO enable to evaluate active losses when there are stochastic generations and also controllable DG units in the network. The simulation results can help the DNO to have estimation about the amount of money he should pay for compensation of active losses. Although the proposed analysis is offline and the running time of the algorithm is not of major concern but the computation burden of the proposed algorithm can be reduced using load flow techniques developed for radial distribution networks and also the variance reduction methods proposed for reducing the number of necessary Monte Carlo experiments. This will highly increase the speed of the proposed algorithm.

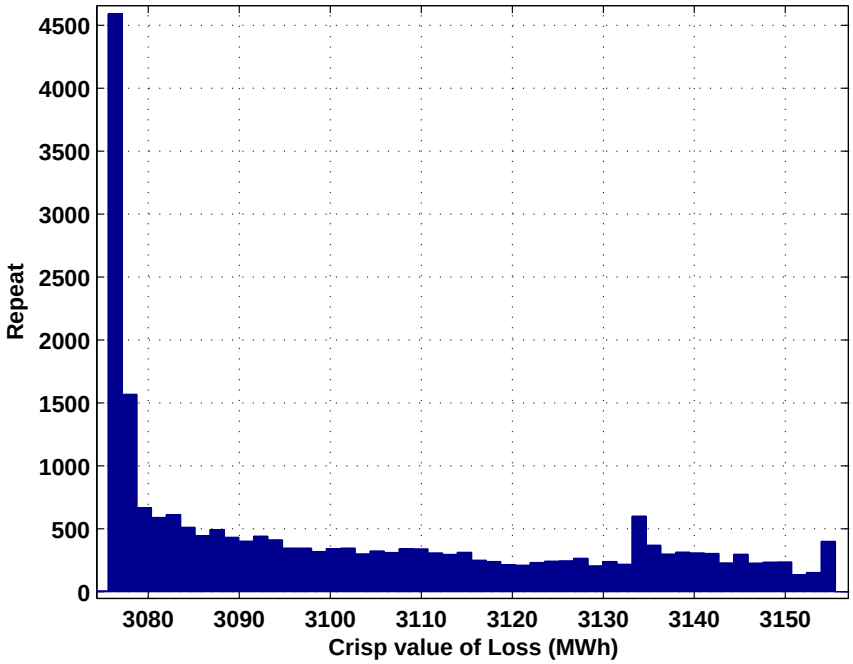

Figure 6.15: Histogram of crisp value of total losses

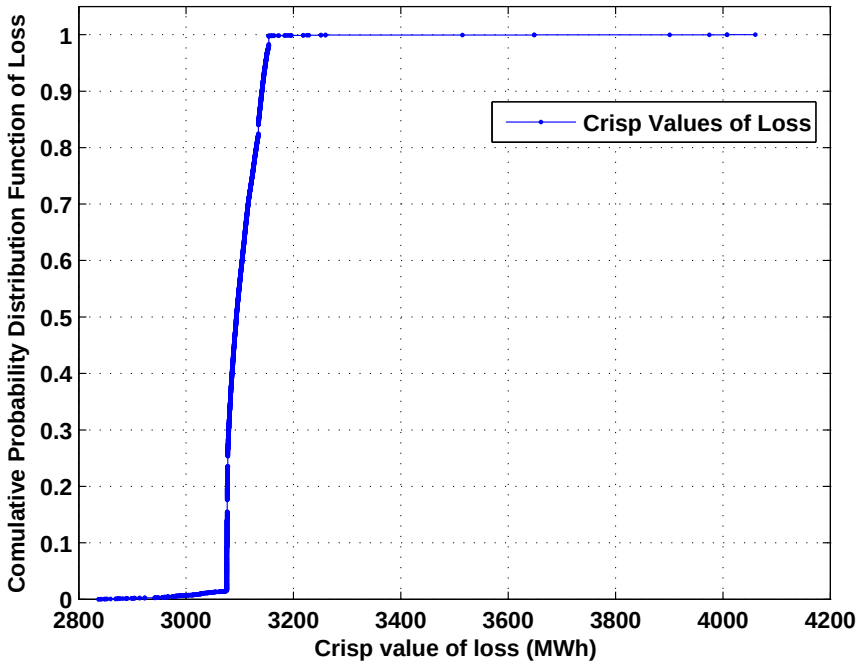

Figure 6.16: Cumulative distribution function of crisp value of total losses

Table 6.19: Data used in the study

Parameter	Unit	Value
c		8.78
k		1.75
V_{max}	Pu	1.05
V_{min}	Pu	0.95
v_{in}^{c}	m/s	3
v_{rated}	m/s	13
v_{out}^{c}	m/s	25
D_{min}		0.85
D_L		0.925
D_U		1.075
D_{max}		1.150
ζ_{min}		0
ζ_L		0.9
ζ_U		1
ζ_{max}		1
N_{dl}		24

Table 6.20: DG capacities and locations

DG Technology	Bus (i)	DG Capacity (MVA)
Gas Turbine	15	0.5
	163	0.5
	283	1
	495	3.5
Wind Turbine	426	0.5
	344	0.5

6.3.4 Fuzzy-probabilistic (Scenario based) problem formulation

6.3.4.1 Problem formulation

The calculation of technical indices at presence of different uncertainties is formulated in this section. The assumptions and technical constraints are described as follows:

6.3.4.2 Assumptions

The following assumptions are employed in problem formulation:

- Connection of a DG unit to a bus is modeled as a negative PQ load with a fix power factor. [64]
- The DNO is not authorized to invest in DG units. He can only forecast the decisions of DGOs regarding the operation/investment of DG units

6.3.4.3 Uncertainty modeling

The uncertainties of electrical loads, power generation of renewable and conventional DG units and investment decisions of DGOs are modeled in this section, as follows:

6.3.4.4 Electric load

In this section, it assumed that the load is modeled using a Fuzzy Trapezoidal Number (FTN) (see Fig.4.1). Assuming a predicted value of load, i.e. $S^D_{i,f}$, and a demand growth rate of ϵ_D, the demand in bus i, in year t can be calculated as:

$$\tilde{S}^D_{i,t} = (1 - D_u, 1 - \frac{D_u}{2}, 1 + \frac{D_u}{2}, 1 + D_u) \times S^D_{i,f} \times (1 + \epsilon_D)^t \tag{6.37}$$

6.3.4.5 Wind speed and wind turbine power generation

The generation schedule of a wind turbine is described in (5.3) and (5.4). The curve of a typical wind turbine is depicted in Fig. 2.1. Using the technique described in [109], the

PDF of wind speed is divided into twelve states. In each state, the generated power and the probability of falling into this state is calculated as (5.5).

6.3.4.6 Operating/Investment decisions of DGOs

In a liberalized electricity market the DNO can not oblige the DGO to invest in a given bus or operate its DG units as DNO desires. Another problem is that the behaviors of DGOs regarding the operation/investment of DG units can not be modeled using conventional probabilistic tools. This is mainly because there is no PDF available about the decisions of DGOs. If the DG technology is wind turbine then the generated power of each wind turbine depends only on the weather condition and if it is a conventional DG technology like Gas turbine then the DGO decides about its operating schedule. In this work, a fuzzy method is proposed for describing the investment decision of DGOs as follows:

Fuzzy installed capacity : the installed capacity of non-renewable DG units/wind turbines are modeled as described in (6.24).

Fuzzy DG generation: In this section, the apparent power of non-renewable DG units are modeled as a FTN, namely $\tilde{S}^{dg}_{i,t,s}$, as described in (6.24).

The active power of wind turbines depends on both wind speed and also the investment decision of DGOs as described below:

$$\tilde{P}^{w}_{i,t,s} = \sum_{\acute{t}=1}^{t} \tilde{\xi}^{w}_{i,\acute{t}} \times P^{w}_{i}(v_s) \tag{6.38}$$

$$wp_s = \frac{P^{w}_{i}(v_s)}{P^{w}_{i,r}}$$

6.3.4.7 Constraints

6.3.4.8 Power flow constraints

The flow equations that shall be satisfied for each configuration and states are:

$$\begin{aligned}
\tilde{P}^{net}_{i,t,s} &= -\tilde{P}^{D}_{i,t} + \sum_{dg/w} \tilde{P}^{dg/w}_{i,t,s} \\
\tilde{Q}^{net}_{i,t,s} &= -\tilde{Q}^{D}_{i,t} + \sum_{dg/w} \tilde{Q}^{dg/w}_{i,t,s} \\
\tilde{P}^{net}_{i,t,s} &= \tilde{V}_{i,t,s} \sum Y_{ij} \tilde{V}_{j,t,s} cos(\tilde{\delta}_{i,t,s} - \tilde{\delta}_{j,t,s} - \theta_{ij}) \\
\tilde{Q}^{net}_{i,t,s} &= \tilde{V}_{i,t,s} \sum Y_{ij} \tilde{V}_{j,t,s} sin(\tilde{\delta}_{i,t,s} - \tilde{\delta}_{j,t,s} - \theta_{ij})
\end{aligned} \tag{6.39}$$

6.3.4.9 Voltage profile

The voltage magnitude of each bus should be kept between the safe operation limits.

$$V_{\min} \leq \tilde{V}_{i,t,s} \leq V_{\max} \tag{6.40}$$

where $V_{\min}$ and $V_{\max}$ are the minimum and maximum safe operating limits of voltage, respectively.

6.3.4.10 Thermal limit of feeders and substation

To maintain the security of the feeders and substations, the flow of current/energy passing through them should be kept below their thermal limit, $I^{\ell}_{\max}/S^{grid}_{max}$, as follows:

$$\begin{aligned}
\tilde{I}_{\ell,t,s} &\leq I^{\ell}_{\max} \\
\tilde{S}^{grid}_{t,s} &\leq S^{grid}_{max}
\end{aligned} \tag{6.41}$$

where $\tilde{I}_{\ell,t,s}$ is the fuzzy current magnitude of feeder ℓ in state s and year t; $\tilde{S}^{grid}_{t,s}$ is the fuzzy apparent power passing through substation's transformer in state s and year t.

6.3.4.11 Evaluation Indices

Two indices are computed in this section namely active losses and technical risk as follows:

Active loss The total active loss in the network is calculate as follows:

$$\tilde{loss} = \sum_{i=1}^{N_b} \sum_{t=1}^{T} \sum_{s \in \Omega_s} \pi_s \times \tilde{P}_{i,t,s}^{net} \times 8760 \tag{6.42}$$
$$OF = (\tilde{loss})^*$$

Technical risk The possibility of occurrence of under/over-voltage in the load nodes is assumed as technical risk. The technical voltage risk in node i and year t, is calculated as follows [33]:

$$VR_{i,t,s} = \frac{A_1 + A_3}{A_1 + A_2 + A_3} \tag{6.43}$$

where $A_{1\to3}$ are depicted in Fig.6.17. The average value of $VR_{i,t,s}$ over all buses of the

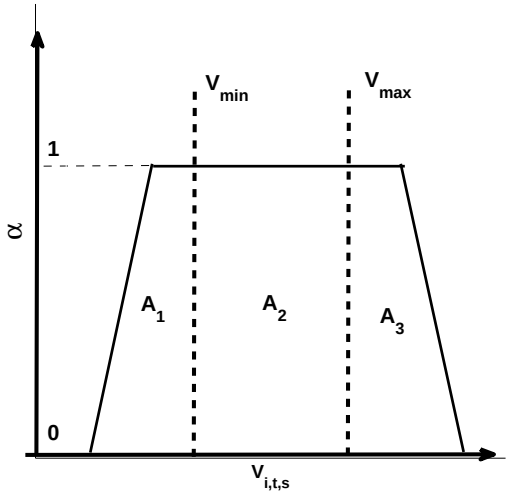

Figure 6.17: Technical risk of over/under voltage in bus i

network and states, can provide information about the overall voltage condition in year t. Additionally, the severity of over/under voltage should be also taken into account. To

do this, an index named Trisk is proposed in this thesis as follows:

$$Trisk = w_{sev} \times \max_{i,t}(\sum_{\Omega_s} \pi_s \times VR_{i,t,s}) + w_{avg} \times \sum_{t=1}^{T} \sum_{i=1}^{N_b} \sum_{\Omega_s} \pi_s \times \frac{VR_{i,t,s}}{T \times N_b} \tag{6.44}$$

where w_{sev} and w_{avg} are the weighting factors specified by DNO.

6.3.4.12 Simulation results

The presented solution algorithm was implemented in GAMS [147]. Two DG technology options, namely, Wind Turbine (WT) and Gas Turbine (GT) are considered here. The mean wind speed in the region is assumed to be $6.07 m/s$. The other characteristics of wind turbine are given in Table 5.1. The weighting factors w_1, w_2 are assumed to be 0.3 and 0.7, respectively. The demand growth rate, i.e. ϵ_D, is 2% for both cases.

Using the technique described in section 6.3.4.5, 12 states are determined for each wind turbine which are given in Table 5.2. The proposed methodology is applied to two distribution systems to demonstrate its abilities. The first case is a 9-node distribution test system and the second one is a large scale real 201-node distribution network. The evaluation horizon, i.e. T, is assumed to be 10 years. The uncertainty factor of demand, i.e. D_u is assumed to be 5% in bothe cases. V_{max} and V_{min} are considered to be 1.05 and 0.95 Pu, respectively.

Case I: 9-node test distribution network This case is a 11-kV, 9-bus distribution network which is shown in Fig.6.6. This network is fed through one substation and has 8 aggregated load points. The technical characteristics of the network can be found in [33]. The predicted values of DG capacities are given in Table 6.21. The technical risk of the given network when no DG unit (neither non-renewable nor wind turbines) exists in the network is 0.640 and the crisp value of active loss is 175296.84 MWh. Three different scenarios were created and assessed to demonstrate the proposed value, namely:

Scen 1. Non-renewable DG units

Scen 2. Renewable wind turbines

Scen 3. Mixed non-renewable and renewable DG units

Scen 1. Non-renewable DG units In this scenario, no wind turbine is considered in the assessment. With this assumption, there is no stochastic variable in the model. It is assumed that just one GT with the size of 5 MVA is installed in the network. The installation year as well as the DG location is changed to analyze its impact. In Fig.6.18 and Fig.6.19 the variation of crisp active loss and technical risk versus the change in installation year is depicted. Each graph corresponds to a specific node in the network.

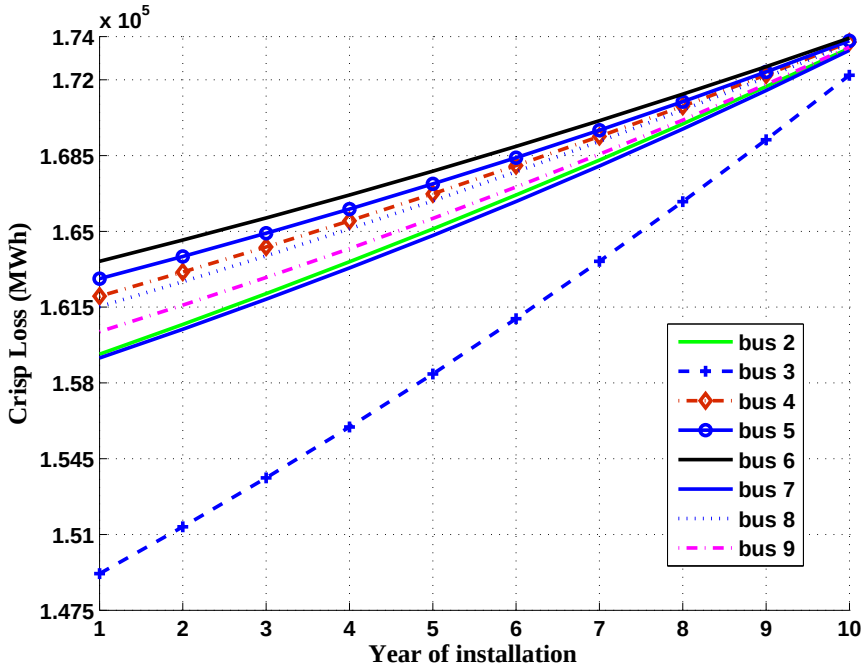

Figure 6.18: The variation of crisp active loss with variation in node and year of DG installation

The simulation result shows that the power injection by DG units (with the specified size) reduces both active loss and technical risk. However the magnitude of this reduction highly depends on where and when this DG will be connected to the network. As the installation year gets closer to the beginning of the evaluation horizon, the technical risk and the active losses are more reduced. Another aspect is the location of this unit. It can be concluded from Fig.6.18 that bus no 3 is the best location for loss reduction because regardless of the installation year, it shows more reduction in active loss compared to

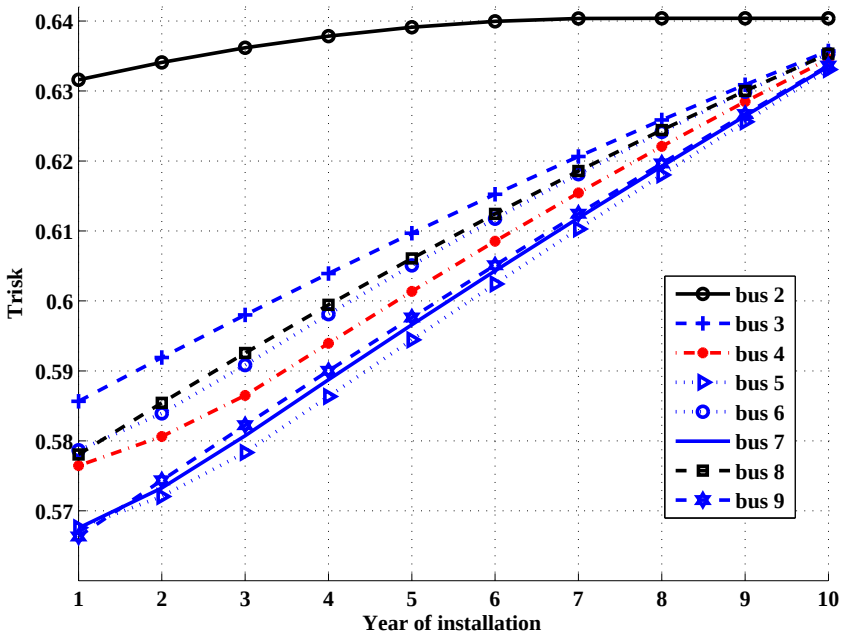

Figure 6.19: The variation of technical risk with variation in node and year of DG installation

other nodes of the network. From technical point of view bus no 5 has lower technical risk compared to other nodes as shown in Fig.6.19. The penetration level of WT units also changes the technical indices. In this study, it is assumed that the size of each DG units is 0.5 MVA. To analyze the impact of DG penetration level, the number of installed DG unit in each bus is varied and the technical risk and active loss are calculated. The variation of technical risk and active loss are depicted in Fig. 6.20 and Fig. 6.21, respectively.

It is important to recognize the impact of DG penetration and also the order in which the DG units will be connected to the distribution network, on the technical risks. In order to investigate this impact, the DG units on various locations are connected to the network. The size of DG units is also changed from 1 MW to 15 MW. First, it is assumed that a DG unit is connected to bus "X" and then it is connected to the bus "Y" and finally two DG units are connected to bus "X" and "Y" simultaneously. It is assumed that the second DG will have the same size of the first DG. In each case, the technical risk index is calculated. For the given 9-node network, $8 \times 7 \times 15 = 840$ simulation analysis are performed to explore all combination of buses and DG sizes (it is assumed all buses of the network are candidate for DG installation except the slack node and the second DG

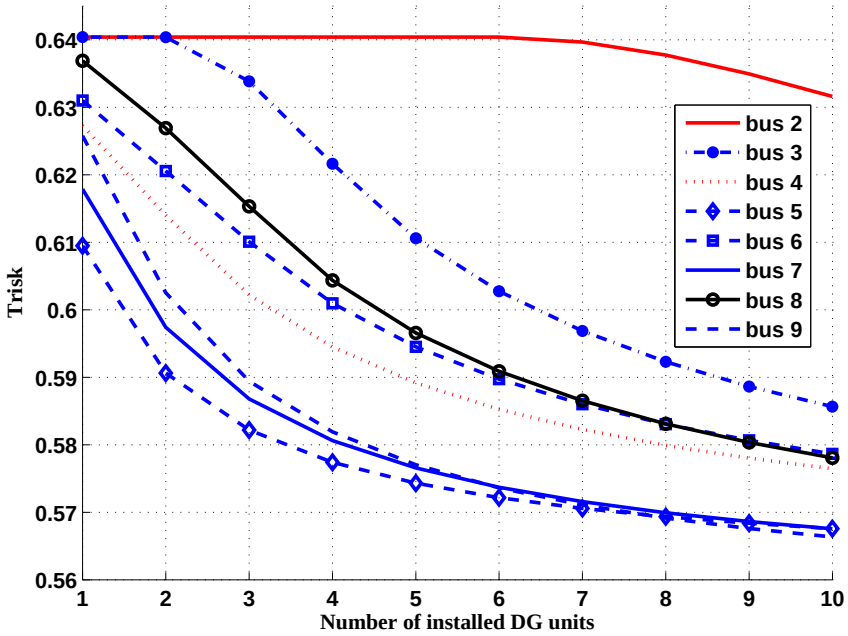

Figure 6.20: The variation of technical risk with variation in number of installed DG

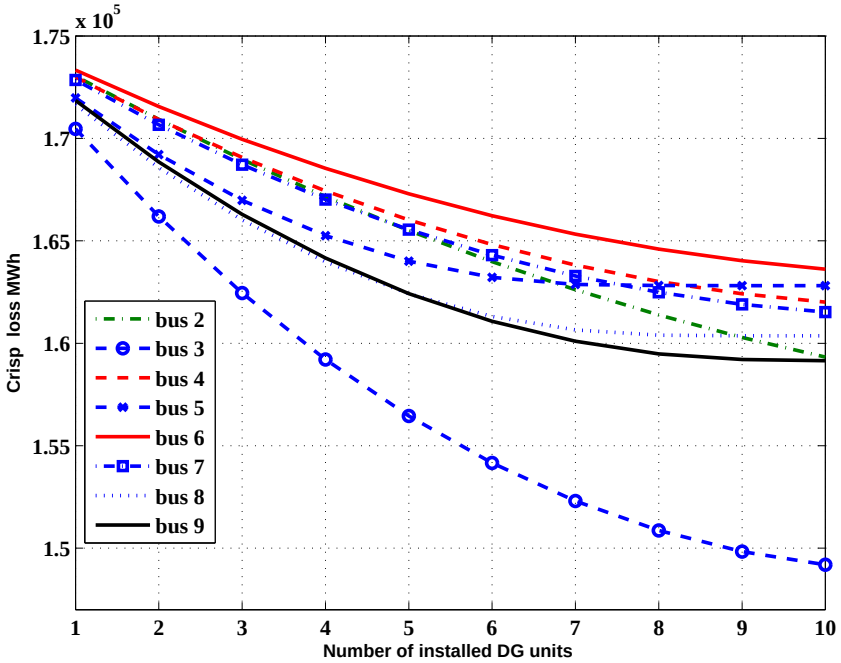

Figure 6.21: The variation of crisp loss with variation in number of installed DG

will be installed in a bus other than the first bus). In most cases, when both of the DG units are connected, the technical risk is lower than the single DG case. In three cases, as depicted in Fig.6.22, Fig.6.23,Fig.6.24, installing the second DG would increase the technical risk. For example as indicated in Fig 6.22, the technical risk in case of single DG (just in bus "X" or "Y") has a decreasing pattern when the DG size is less than 14MW. In case of two DG units (both of them are installed, one in bus "X" and the other one in bus "Y"), the technical risk decreases until DG capacity reaches to 9 MW. After the 9MW threshold, the technical risk will increase. Comparing the values of technical risk between these three cases, it can be concluded from Fig. 6.22 that if the fist bus is bus #4, then connecting another DG in bus 5 will decrease the technical risk. It is true until the size of the second DG (in bus #5) is below the 11 MW. On the other hand, if there exists a DG unit in bus "Y", installing a second DG in bus "X" will decrease the technical risk until the capacity of the second DG is below the 10 MW.

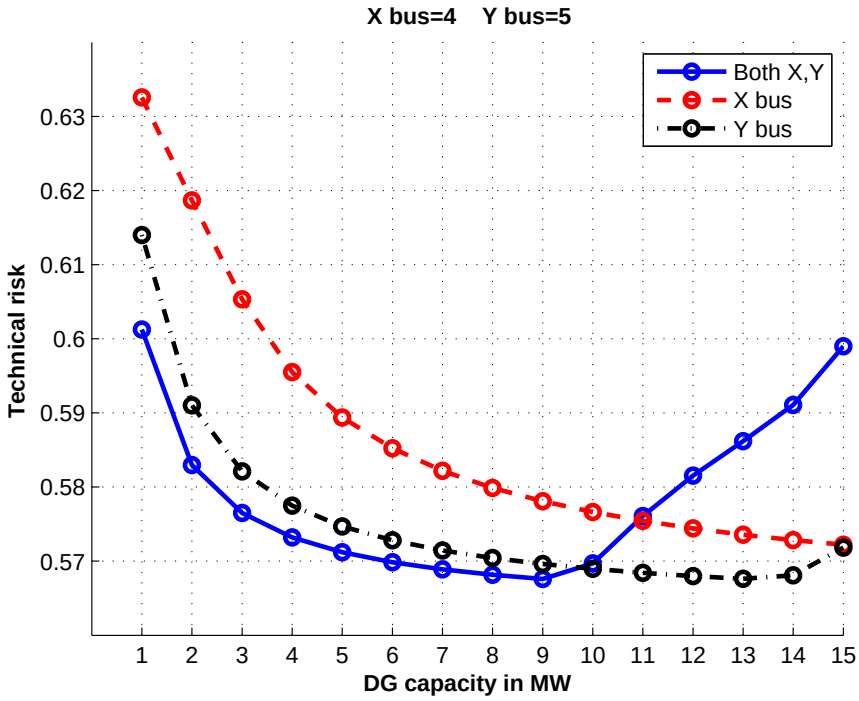

Figure 6.22: The comparison between the technical risk due to order of DG connection in bus 4,5

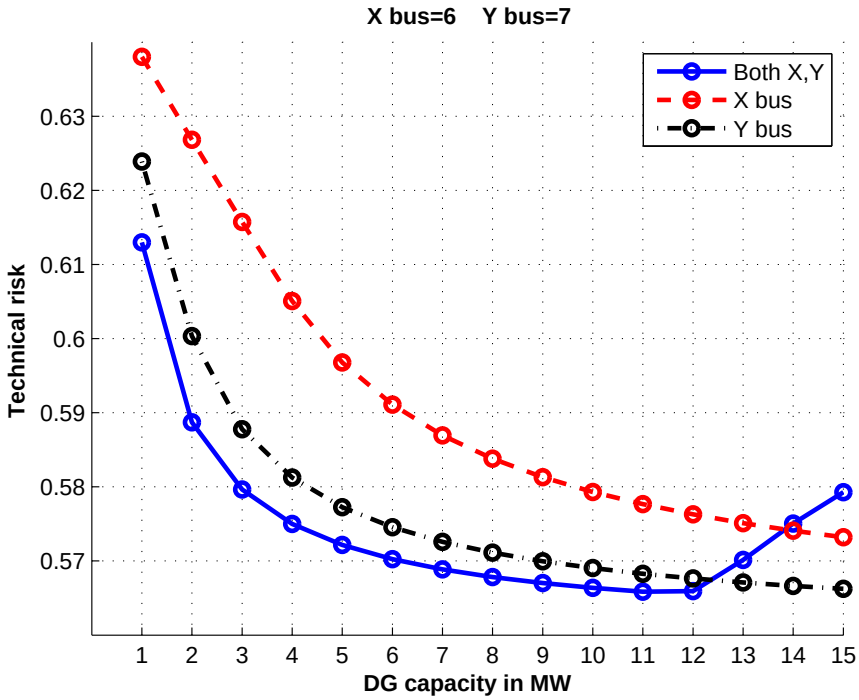

Figure 6.23: The comparison between the technical risk due to order of DG connection in bus 6,7

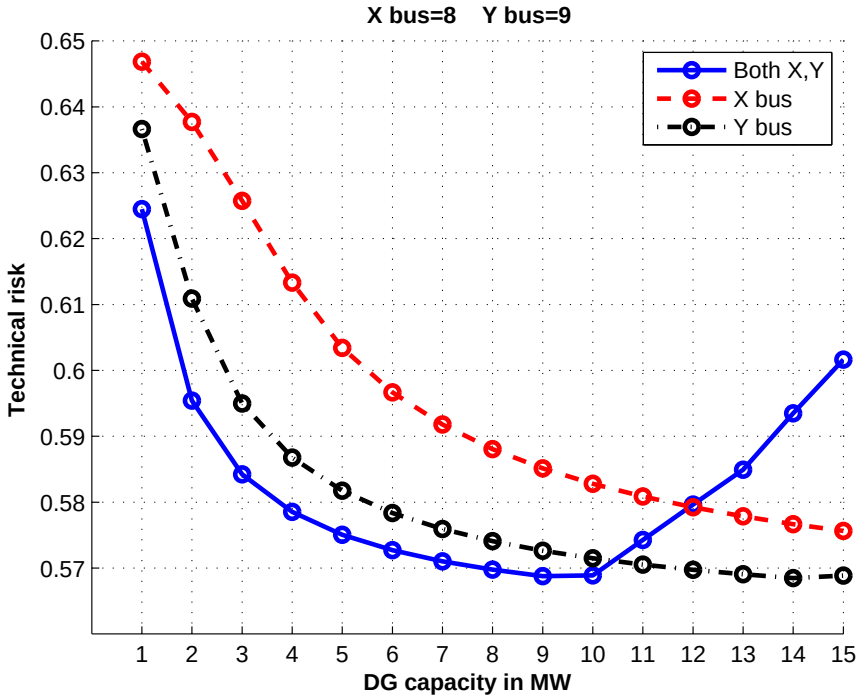

Figure 6.24: The comparison between the technical risk due to order of DG connection in bus 8,9

Scen 2. Renewable DG units (wind turbine) In this scenario, just wind turbine is considered in the assessment. The size of wind turbine is assume to be 5 MVA and just one wind turbine is installed in the network. In Fig.6.25 and Fig.6.26 the variation of crisp active loss and technical risk versus the installation year is depicted. Each graph corresponds to a specific node in the network.

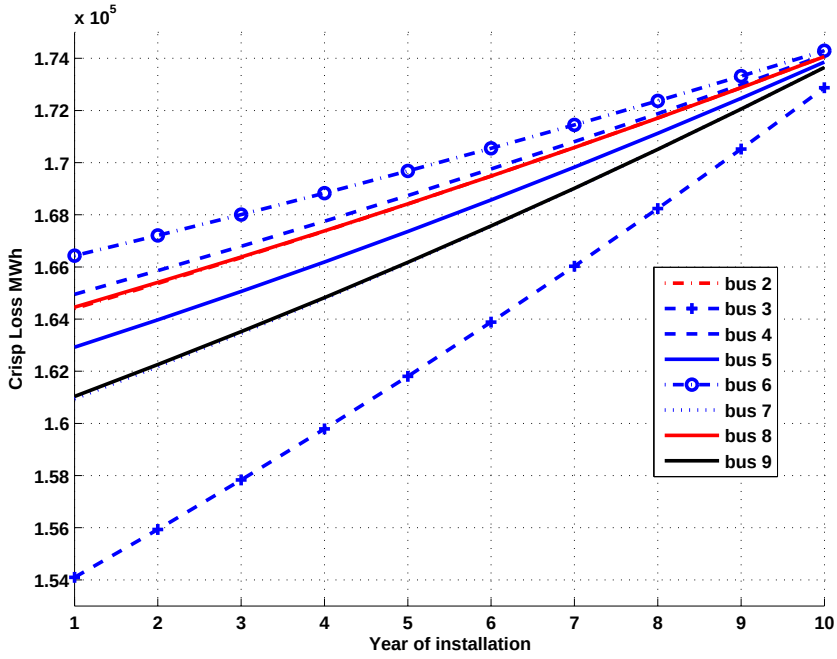

Figure 6.25: The variation of crisp active loss with variation in node and year of wind turbine installation

Fig. 6.25 shows that WT installation in node 3 leads to more active loss reduction compared to all other buses of the network. Fig. 6.26 states that node 5 is the best location for technical risk reduction in the network since it has the least Trisk compared to all other buses of the network. The penetration level of DG units also changes the technical indices. In this study it is assumed that the size of each wind turbine is 0.5 MVA. To analyze the impact of wind turbine penetration level, the number of installed wind turbine in each bus is varied and the technical risk and active loss are given in Fig. 6.27 and Fig. fig:penetwt, respectively.

Scen 3. Mixed non-renewable and renewable DG units In this scenario, both non-renewable and wind turbine units are present in the network. The location and

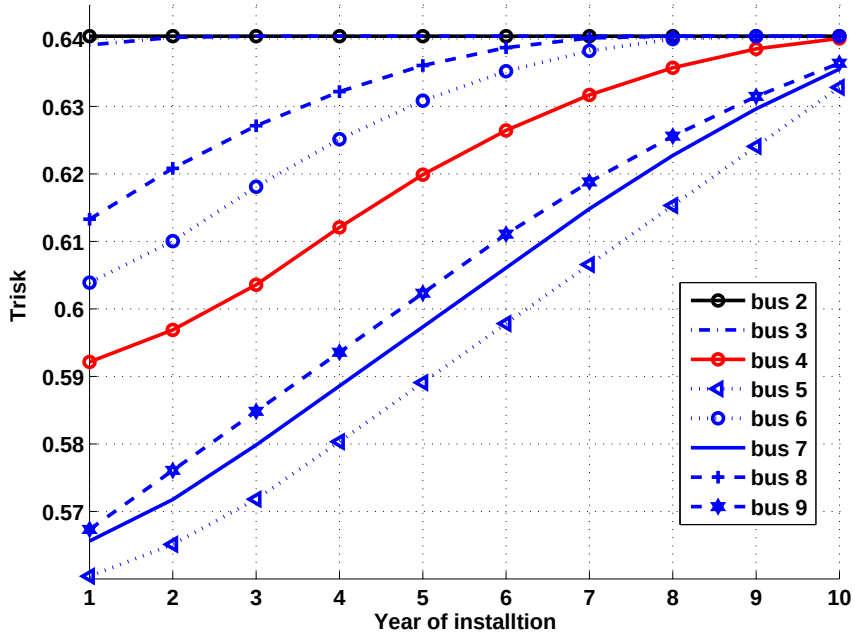

Figure 6.26: The variation of technical risk with variation in node and year of wind turbine installation

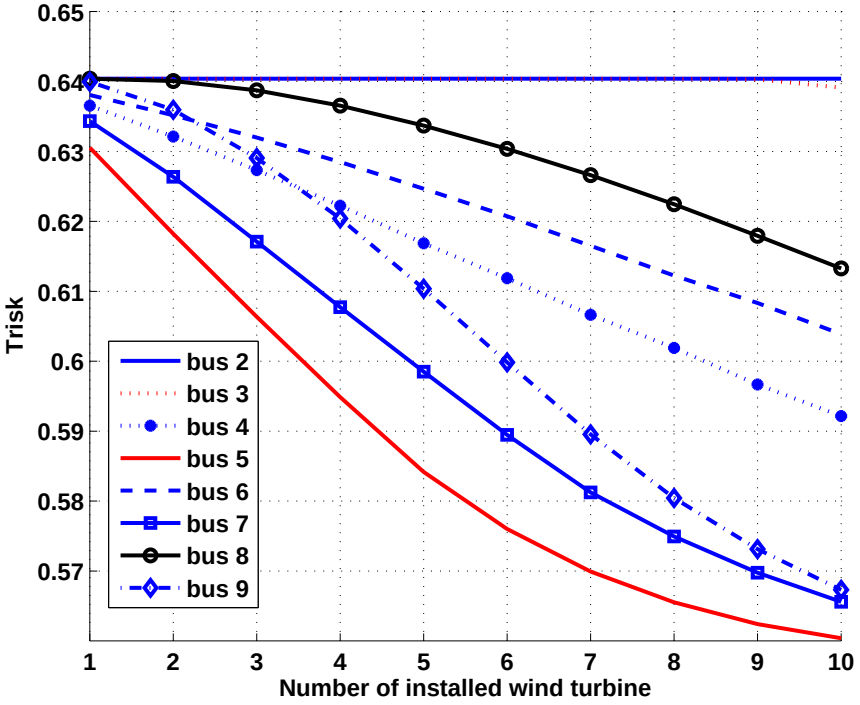

Figure 6.27: The variation of technical risk with variation in number of installed WT

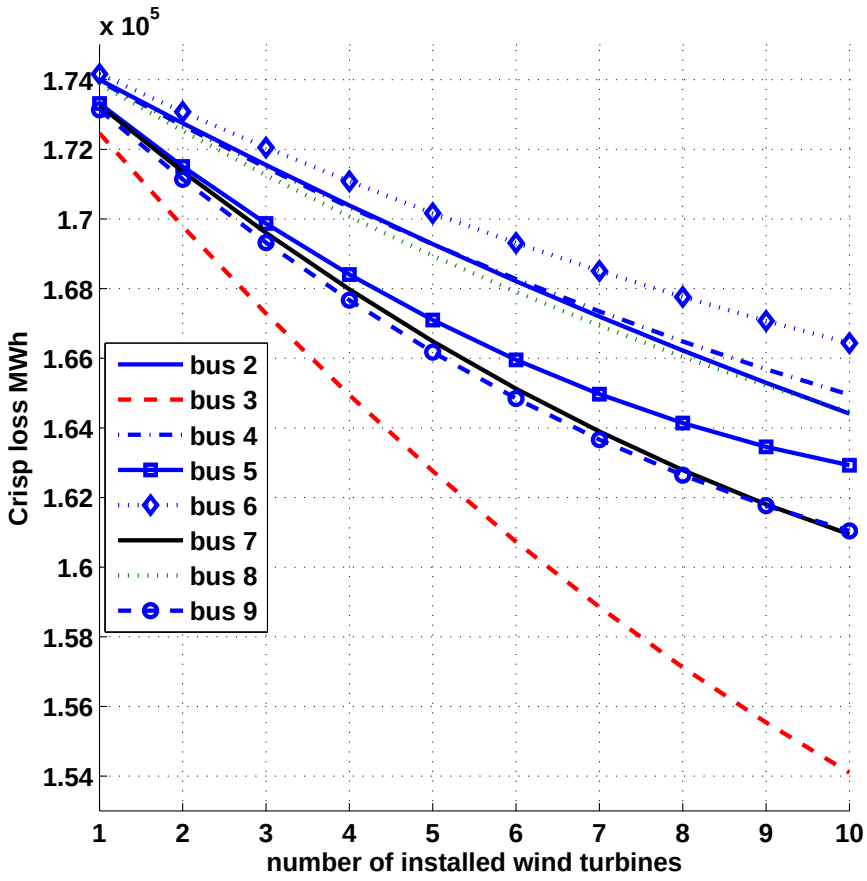

Figure 6.28: The variation of crisp loss with variation in number of installed WT

year of installation are given in Table. 6.21. The technical risk is 0.518 and active loss is equal to 130134.4962 MWh. The variation of $\sum_{\Omega_s} \pi_s \times VR_{i,t,s}$ is given in Table. 6.22.

Table 6.21: Predicted values of capacities to be installed in Case-I

DG tech	bus	No of installed	year	Cap	$\zeta_{\min}^{dg/w}$	$\zeta_{L}^{dg/w}$	$\zeta_{U}^{dg/w}$	$\zeta_{\max}^{dg/w}$
WT_1	5	8	2	0.5	0.3	0.9	1.05	1.1
WT_2	8	1	3	0.5	0.7	0.8	1	1.15
WT_3	3	2	4	0.5	0.1	0.6	1.1	1.2
GT_1	2	3	1	0.5	0	0.9	1.05	1.1
GT_2	9	1	5	0.2	0	0	1	1.15
GT_3	5	4	3	0.4	0.1	0.6	1.1	1.2

Table 6.22: The expected value of $VR_{i,t,s}$ over the states in scenario 3 of case I

	Bus			
t	3	5	7	9
1	0.603	0.541	0.703	0.179
2	0.642	0.199	0.922	0.210
3	0.682	0.376	1	0.117
4	0.448	0.551	1	0.149
5	0.484	0.724	1	0.182
6	0.520	0.894	1	0.214
7	0.557	1	1	0.248
8	0.594	1	1	0.281
9	0.631	1	1	0.315
10	0.668	1	1	0.350

Case II: A real 201-node distribution network The proposed methodology is applied to a large 201-node 10 kV distribution system which is shown in Fig.5.4. The technical data of this network can be found in [115]. The DG locations and capacities are described in Table. 6.24. The technical risk of the network is 0.6367 and the crisp value of active loss is 189477 MWh. The variation of average, maximum and minimum value of the technical risk throughout the network is depicted in Fig. 6.29. The minimum average risk is in bus 201 with the average risk of 0.3257 and the worst risk occurs in bus 146 with the average risk of 0.9526 over the evaluation horizon.

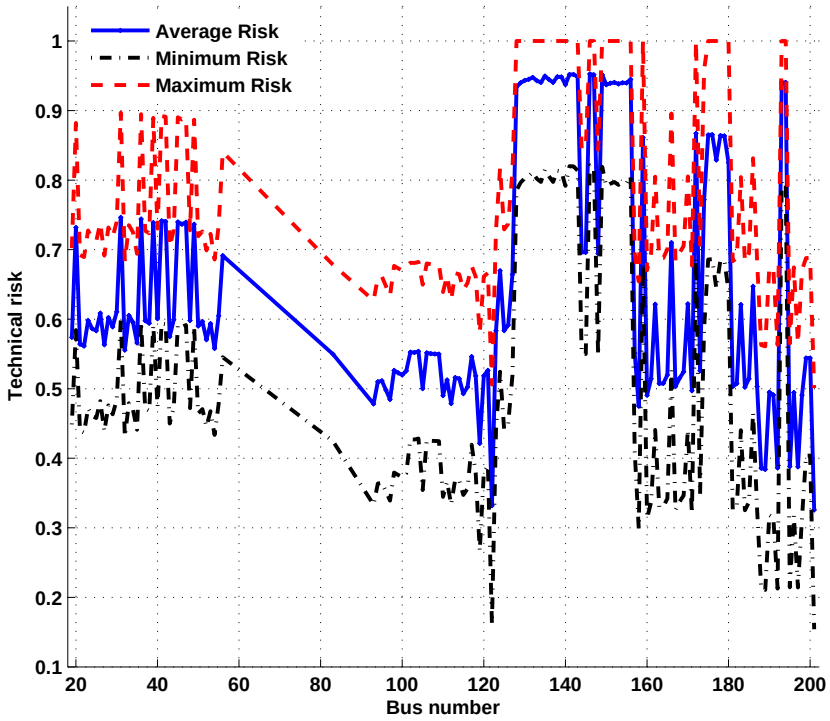

Figure 6.29: The variation of the technical risk throughout the network in case II

The yearly variation of $VR_{i,t,s}$ over some selected buses are described in Table 6.24.

If the number of scenarios (states) are too high that the computational burden becomes a matter of concern, the scenario reduction method can be used. The purpose of scenario reduction is selection of a set, i.e. Ω_S, with the cardinality of N_{Ω_S}, from the original set, i.e. Ω_J [101]. This procedure should be done in a way that makes a trade off between the loss of the information and decreasing the computational burden. The details of this procedure can be found in [102].

Table 6.23: Predicted values of capacities to be installed in case II

DG tech	bus	number of installed units	year
WT_1	93	8	1
WT_2	128	4	1
WT_3	158	6	1
GT_1	32	7	1
GT_2	69	4	1
GT_3	83	6	1

Table 6.24: The expected value of $VR_{i,t,s}$ over the scenarios in case II

	Bus									
t	201	189	158	105	52	186	166	174	159	128
1	0.154	0.211	0.299	0.354	0.446	0.466	0.527	0.587	0.681	0.786
2	0.191	0.248	0.337	0.386	0.473	0.506	0.567	0.628	0.722	0.827
3	0.229	0.286	0.376	0.418	0.500	0.545	0.607	0.668	0.764	0.869
4	0.267	0.325	0.415	0.450	0.527	0.586	0.648	0.709	0.805	0.911
5	0.305	0.363	0.454	0.483	0.555	0.626	0.689	0.750	0.847	0.953
6	0.344	0.402	0.494	0.515	0.584	0.667	0.730	0.792	0.889	0.994
7	0.383	0.442	0.533	0.549	0.612	0.708	0.771	0.833	0.931	1.000
8	0.422	0.481	0.573	0.582	0.641	0.749	0.812	0.875	0.973	1.000
9	0.461	0.521	0.614	0.616	0.670	0.790	0.854	0.917	1.000	1.000
10	0.501	0.561	0.654	0.650	0.699	0.831	0.896	0.959	1.000	1.000

The application of the proposed method can be defined as minimizing the evaluated indices. This can be done using the reinforcement strategies, capacitor installation, distribution network reconfiguration and etc. Knowing the impacts of DGO's decisions on technical performance of the distribution networks can help the regulators as an economic signals to reward/penalize their actions.Another application of the proposed method for DNO would be evaluating the DGO's proposal for new DG connection and analyzing its impact on the technical performance of the network. It may influence the DG connection permission that can be granted by DNO to DGO.

6.4 Conclusions

This chapter presents a long-term dynamic multi-objective model for planning of distribution networks regarding the benefits of DNO and DGOs in section 6.2. The proposed model simultaneously optimizes two objectives, namely the benefits of DNO and DGO and determines the optimal schemes of sizing, placement and specially the dynamics (i.e., timing) of investments on distributed generation units and network reinforcements over the planning period. The proposed model also considers the uncertainty of electric load, electricity price and wind turbine power generation using the point estimate method. The effect of benefit sharing is investigated for steering the decisions of DGOs. An efficient two-stage heuristic method is proposed to solve the formulated planning problem and tested on a real large scale distribution network. In section 6.3, three different methods of uncertainty handling in DG impact assessment on operating of distribution networks are described.

CHAPTER 7

Conclusion and Future Work

7.1 Conclusions

DG is a promising option for distribution network operators to meet the requirements of his costumers. The presence of DG units specially the renewable technologies would introduce volatility and intermittence, which would affect the operation and planning of distribution networks. The integration of DG units in distribution networks is more beneficial when the optimal decisions related to location, size and operations of them are centrally made by the DNO. Thus, we have presented in this dissertation a stochastic optimization algorithm for the expansion planning of distribution networks with the integration of renewable and non-renewable DG technologies. The model described in Chapter 5, is a comprehensive dynamic multi-objective model for DG integration in distribution networks. The proposed two-step algorithm finds the non-dominated solutions by simultaneous minimization of active losses, costs and emissions in the first stage and uses a fuzzy satisfying method to select the best solution from the candidate set in the second stage. In Chapter 6, it is assumed that the DNO is not authorized to invest in DG units and he should just screen and guide(through incentives) the activities of DG developers. In this chapter, a long-term dynamic multi-objective model for planning of distribution networks regarding the benefits of DNO and DGOs as described in section 6.2. The proposed model simultaneously optimizes two objectives, namely the benefits of DNO and DGO and determines the optimal schemes of sizing, placement and specially the dynamics (i.e., timing) of investments on distributed generation units and network reinforcements over the planning period. The proposed model also considers the uncertainty of electric load, electricity price and wind turbine power generation using the point

estimate method. The effect of benefit sharing is investigated for steering the decisions of DGOs. An efficient two-stage heuristic method is proposed to solve the formulated planning problem and tested on a real large scale distribution network. In section 6.3, three different methods of uncertainty handling in DG impact assessment on operating of distribution networks are described.

7.2 Main contributions of thesis

The main contributions of the research presented in this thesis are as follows:

(a) A new hybrid heuristic GA and Immune Algorithm is developed to find the Pareto optimal fronts in multi objective problem formulation.

(b) A comprehensive multi-objective planning model for integration of DG units in distribution networks have been proposed. This model simultaneously optimizes the DG and distribution network investment decisions by determining the optimal timing, sizing and locating the DG units and also the reinforcement strategies of distribution network. It can also handle the uncertainties of input data.

(c) A new possibilistic framework is proposed for evaluating the impacts of DG units on distribution network performance. The model considers possibilistic modeling of the uncertainties associated to loads and decisions of DG investors including their installed capacity and operating schedule. The proposed technical indices demonstrate the ability of the given distribution network in load supply and also its efficiency at presence of DG units. The proposed model is useful for basic engineering design and as a diagnostic tool for DNOs in evaluating their decisions in network reinforcement or reconfiguration of distribution network at presence of uncertainties associated to DG units and load values.

(d) Two evaluation tools are proposed for DNOs which helps them to deal with the effect of stochastic (probabilistic) and fuzzy (possibilistic) uncertainties of renewable and conventional DG technologies on distribution networks, simultaneously. The first method uses the fuzzy principles and Monte Carlo Simulation method for handling

the uncertainties. The second method have the same principles for non-stochastic uncertainties while used the scenario modeling for probabilistic uncertain parameters. This will effectively reduce the computational burden needed for such analysis.

(e) A comprehensive model is developed which multi-objectively considers the benefits of DNO and DG owners and provides a win-win strategy for both parties. This model includes the timing of investment for network and DG units in the problem formulation. The uncertainties of electricity price, electric loads and generation of wind turbines are modeled using a two point estimate method (2PEM).

7.3 Recommendations for Future Work

Further work can be conducted based on the proposed framework of this thesis. The possible directions of future research are presented below:

- The impact of DG units on reliability of distribution networks can be investigated.
- The possibility of optimal distribution network investment can be investigated using the introduced load repression index.
- It may be useful to examine the role of smart grids at presence of DG units in the planning procedure, network reconfiguration and voltage control.
- The load repression index used in Chapter 6.3.2 can be extended to include the DG generation abilities. This would be beneficial to design a distribution network that can provide a better service for DG developers.
- The optimal reconfiguration and capacitor placement in distribution network in conjunction with the proposed method can be investigated.
- The impacts of load modeling on planning/operational issues can be analyzed.

References

[1] T. Ackermann, G. Andersson, and L. Soder, "Distributed generation: a definition," *Electric Power Systems Research*, vol. 57, no. 3, pp. 195 – 204, 2001.

[2] ENA, "Distributed generation connection guide, ver. 3," Energy Networks Associations, Tech. Rep., Nov 2010.

[3] N. Hadjsaid, L. Le-Thanh, R. Caire, B. Raison, F. Blache, B. Sta? andhl, and R. Gustavsson, "Integrated ict framework for distribution network with decentralized energy resources: Prototype, design and development," in *Power and Energy Society General Meeting, 2010 IEEE*, july 2010, pp. 1 –4.

[4] EREC, *Renewable Energy in Europe- Markets, Trends and Technologies, 2nd Edition.* USA: EUROPEAN RENEWABLE ENERGY COUNCIL (EREC), 2010.

[5] T. Burton, D. Sharpe, N. Jenkins, and E. Bossanyi, *Wind Energy handbook.* USA: JOHNWILEY and SONS, LTD, 2001.

[6] G. Boyle, *Renewable Energy.* Oxford Univ. Press, 2004.

[7] M. Jafarian and A. Ranjbar, "Fuzzy modeling techniques and artificial neural networks to estimate annual energy output of a wind turbine," *Renewable Energy*, vol. In Press, Corrected Proof, pp. –, 2010.

[8] R. Foster, M. Ghassemi, and A. Cota, *Solar Energy: Renewable Energy And The Environment.* USA: Crc Press, 2009.

[9] Y. Atwa, E. El-Saadany, M. Salama, and R. Seethapathy, "Optimal renewable resources mix for distribution system energy loss minimization," *IEEE Transactions on Power Systems*, vol. 25, no. 1, pp. 360 –370, feb. 2010.

[10] M. H. Nehrir and C. Wang, *Modeling and Control of Fuel Cells: Distributed Generation Applications.* USA: IEEE Press Series on Power Engineering, 2009.

[11] J. Wood, *Local Energy: Distributed generation of heat and power.* California: The Institution of Engineering and Technology, 2010.

[12] M. P. Boyce, *Gas Turbine Engineering Handbook, Third Edition.* USA: Gulf professional publishing, 2002.

[13] B. F.Kolanowski, *Guide to Microturbines.* Marcel Dekker, Inc, 2004.

[14] capstoneturbine, http://www.capstoneturbine.com/prodsol/products/, accesed March 2011.

[15] M. Meckler and L. B. Hyman, *Sustainable On-Site CHP Systems: Design, Construction, and Operations.* New York: McGraw-Hill, 2010.

[16] K. Divya and J. ?stergaard, "Battery energy storage technology for power systems–an overview," *Electric Power Systems Research*, vol. 79, no. 4, pp. 511 – 520, 2009.

[17] P. Hu, R. Karki, and R. Billinton, "Reliability evaluation of generating systems containing wind power and energy storage," *Generation, Transmission Distribution, IET*, vol. 3, no. 8, pp. 783 –791, august 2009.

[18] R. Zito, *Energy Storage: A New Approach*. USA: WILEY, 2010.

[19] F. A. FARRET and M. G. SIMOES, *Integration Of Alternative Sources OF Energy*. USA: JOHN WILEY and SONS, 2006.

[20] Y. Yuan, Q. Li, and W. Wang, "Optimal operation strategy of energy storage unit in wind power integration based on stochastic programming," *Renewable Power Generation, IET*, vol. 5, no. 2, pp. 194 –201, march 2011.

[21] A. Abedini and H. Nikkhajoei, "Dynamic model and control of a wind-turbine generator with energy storage," *Renewable Power Generation, IET*, vol. 5, no. 1, pp. 67 –78, january 2011.

[22] C. Abbey and G. Joos, "A stochastic optimization approach to rating of energy storage systems in wind-diesel isolated grids," *IEEE Transactions on Power Systems,*, vol. 24, no. 1, pp. 418 –426, feb. 2009.

[23] F. Chacra, P. Bastard, G. Fleury, and R. Clavreul, "Impact of energy storage costs on economical performance in a distribution substation," *IEEE Transactions on Power Systems,*, vol. 20, no. 2, pp. 684 – 691, may 2005.

[24] M. Ross, R. Hidalgo, C. Abbey, and G. Joo? ands, "Energy storage system scheduling for an isolated microgrid," *Renewable Power Generation, IET*, vol. 5, no. 2, pp. 117 –123, march 2011.

[25] A. J. Duque, E. D. Castronuovo, I. Sanchez, and J. Usaola, "Optimal operation of a pumped-storage hydro plant that compensates the imbalances of a wind power producer," *Electric Power Systems Research*, vol. In Press, Corrected Proof, pp. –, 2011.

[26] Y. Atwa and E. El-Saadany, "Optimal allocation of ess in distribution systems with a high penetration of wind energy," *IEEE Transactions on Power Systems,*, vol. 25, no. 4, pp. 1815 –1822, nov. 2010.

[27] E. F. Fuchs and M. A. Masoum, *Power Conversion of Renewable Energy Systems*. USA: Springer, 2010.

[28] B. Bolund, H. Bernhoff, and M. Leijon, "Flywheel energy and power storage systems," *Renewable and Sustainable Energy Reviews*, vol. 11, no. 2, pp. 235 – 258, 2007.

[29] P. Hoffmann, *Tomorrows Energy Hydrogen, Fuel Cells, and the Prospects for a Cleaner Planet*. USA: The MIT press, 2001.

[30] I. Dincer and M. A. Rosen, *Thermal energy storage systems and applications, second edition*. USA: Wiley, 2011.

[31] N. Hadjsaid, J.-F. Canard, and F. Dumas, "Dispersed generation impact on distribution networks," *Computer Applications in Power, IEEE*, vol. 12, no. 2, pp. 22 –28, apr 1999.

[32] R. Singh and S. Goswami, "Optimum allocation of distributed generations based on nodal pricing for profit, loss reduction, and voltage improvement including voltage rise issue," *International Journal of Electrical Power and Energy Systems*, vol. 32, no. 6, pp. 637 – 644, 2010.

[33] M.-R. Haghifam, H. Falaghi, and O. Malik, "Risk-based distributed generation placement," *Generation, Transmission and Distribution, IET*, vol. 2, no. 2, pp. 252–260, March 2008.

[34] S.-H. Lee and J.-W. Park, "Selection of optimal location and size of multiple distributed generations by using kalman filter algorithm," *IEEE Transactions on Power Systems*, vol. 24, no. 3, pp. 1393–1400, Aug. 2009.

[35] A. Kumar and W. Gao, "Optimal distributed generation location using mixed integer non-linear programming in hybrid electricity markets," *Generation, Transmission Distribution, IET*, vol. 4, no. 2, pp. 281 –298, february 2010.

[36] P. Siano, L. Ochoa, G. Harrison, and A. Piccolo, "Assessing the strategic benefits of distributed generation ownership for dnos," *Generation, Transmission and Distribution, IET*, vol. 3, no. 3, pp. 225–236, March 2009.

[37] P. M. Costa and M. A. Matos, "Avoided losses on lv networks as a result of microgeneration," *Electric Power Systems Research*, vol. 79, no. 4, pp. 629–634, April 2009.

[38] T. Gzela and M. H. Hocaoglu, "An analytical method for the sizing and siting of distributed generators in radial systems," *Electric Power Systems Research*, vol. 79, no. 6, pp. 912–918, June 2009.

[39] N. Khalesi, N. Rezaei, and M.-R. Haghifam, "Dg allocation with application of dynamic programming for loss reduction and reliability improvement," *International Journal of Electrical Power and Energy Systems*, vol. 33, no. 2, pp. 288 – 295, 2011.

[40] T. Gozel and M. H. Hocaoglu, "An analytical method for the sizing and siting of distributed generators in radial systems," *Electric Power Systems Research*, vol. 79, no. 6, pp. 912 – 918, 2009.

[41] G. Harrison, A. Piccolo, P. Siano, and A. Wallace, "Exploring the tradeoffs between incentives for distributed generation developers and dnos," *IEEE Transactions on Power Systems*, vol. 22, no. 2, pp. 821–828, May 2007.

[42] M. Akorede, H. Hizam, I. Aris, and M. Ab Kadir, "Effective method for optimal allocation of distributed generation units in meshed electric power systems," *Generation, Transmission Distribution, IET*, vol. 5, no. 2, pp. 276 –287, 2011.

[43] A. Piccolo and P. Siano, "Evaluating the impact of network investment deferral on distributed generation expansion," *IEEE Transactions on Power Systems*, vol. 24, no. 3, pp. 1559–1567, Aug. 2009.

[44] A. A. El-Ela, S. Allam, and M. Shatla, "Maximal optimal benefits of distributed generation using genetic algorithms," *Elec. Power Sys. Res.,*, vol. 80, no. 7, pp. 869 – 877, 2010.

[45] B. Renders, L. Vandevelde, L. Degroote, K. Stockman, and M. Bollen, "Distributed generation and the voltage profile on distribution feeders during voltage dips," *Elec. Power Sys. Res.,*, vol. 80, no. 12, pp. 1452 – 1458, 2010.

[46] A. Zangeneh, S. Jadid, and A. Rahimi-Kian, "Promotion strategy of clean technologies in distributed generation expansion planning," *Renewable Energy*, vol. 34, no. 12, pp. 2765 – 2773, 2009.

[47] ——, "A fuzzy environmental-technical-economic model for distributed generation planning," *Energy*, vol. 36, no. 5, pp. 3437 – 3445, 2011.

[48] H. Hedayati, S. Nabaviniaki, and A. Akbarimajd, "A method for placement of dg units in distribution networks," *IEEE Transactions on Power Delivery,*, vol. 23, no. 3, pp. 1620–1628, July 2008.

[49] L. Wang and C. Singh, "Reliability-constrained optimum placement of reclosers and distributed generators in distribution networks using an ant colony system algorithm," *Systems, Man, and Cybernetics, Part C: Applications and Reviews, IEEE Transactions on*, vol. 38, no. 6, pp. 757 –764, 2008.

[50] ——, "Population-based intelligent search in reliability evaluation of generation systems with wind power penetration," *IEEE Transactions on Power Systems,*, vol. 23, no. 3, pp. 1336 –1345, 2008.

[51] D. T.-C. Wang, L. F. Ochoa, and G. P. Harrison, "Dg impact on investment deferral: Network planning and security of supply," *IEEE Transactions on Power Systems,*, vol. 25, no. 2, pp. 1134 –1141, may 2010.

[52] T. T. H. Pham, Y. Besanger, and N. Hadjsaid, "New challenges in power system restoration with large scale of dispersed generation insertion," *IEEE Transactions on Power Systems,*, vol. 24, no. 1, pp. 398 –406, feb. 2009.

[53] A. Algarni and K. Bhattacharya, "Disco operation considering dg units and their goodness factors," *IEEE Transactions on Power Systems*, vol. 24, no. 4, pp. 1831 –1840, nov. 2009.

[54] Y.-K. Wu, C.-Y. Lee, L.-C. Liu, and S.-H. Tsai, "Study of reconfiguration for the distribution system with distributed generators," *IEEE Transactions on Power Delivery,*, vol. 25, no. 3, pp. 1678 –1685, 2010.

[55] K. Zare, A. J. Conejo, M. Carrin, and M. P. Moghaddam, "Multi-market energy procurement for a large consumer using a risk-aversion procedure," *Electr. Power Syst. Res.*, vol. 80, no. 1, pp. 63 – 70, 2010.

[56] K. Zare, M. P. Moghaddam, and M. K. S. E. Eslami, "Electricity procurement for large consumers based on information gap decision theory," *Energy Policy*, vol. 38, no. 1, pp. 234 – 242, 2010.

[57] H. Khodr, M. R. Silva, Z. Vale, and C. Ramos, "A probabilistic methodology for distributed generation location in isolated electrical service area," *Electric Power Systems Research*, vol. 80, no. 4, pp. 390 – 399, 2010.

[58] G. Koutroumpezis and A. Safigianni, "Optimum allocation of the maximum possible distributed generation penetration in a distribution network," *Elec. Power Sys. Res.,*, vol. 80, no. 12, pp. 1421 – 1427, 2010.

[59] S. Ghosh, S. Ghoshal, and S. Ghosh, "Optimal sizing and placement of distributed generation in a network system," *International Journal of Electrical Power and Energy Systems*, vol. 32, no. 8, pp. 849 – 856, 2010.

[60] H. Khan and M. A. Choudhry, "Implementation of distributed generation (idg) algorithm for performance enhancement of distribution feeder under extreme load growth," *International Journal of Electrical Power and Energy Systems*, vol. 32, no. 9, pp. 985 – 997, 2010.

[61] A. Barin, L. F. Pozzatti, L. N. Canha, R. Q. Machado, A. R. Abaide, and G. Arend, "Multi-objective analysis of impacts of distributed generation placement on the operational characteristics of networks for distribution system planning," *International Journal of Electrical Power and Energy Systems*, vol. 32, no. 10, pp. 1157 – 1164, 2010.

[62] G. Celli and F. Pilo, "Optimal distributed generation allocation in mv distribution networks," in *Power Industry Computer Application*, 2001, pp. 81–86.

[63] J.-H. Teng, Y.-H. Liu, C.-Y. Chen, and C.-F. Chen, "Value-based distributed generator placements for service quality improvements," *Electrical power energy systems*, vol. 29, no. 3, pp. 268–274, March 2007.

[64] L. Ochoa, A. Padilha-Feltrin, and G. Harrison, "Evaluating distributed generation impacts with a multiobjective index," *IEEE Transactions on Power Delivery*, vol. 21, no. 3, pp. 1452–1458, July 2006.

[65] G. Celli, E. Ghiani, S. Mocci, and F. Pilo, "A multiobjective evolutionary algorithm for the sizing and siting of distributed generation," *IEEE Transactions on Power Systems*, vol. 20, no. 2, pp. 750–757, May 2005.

[66] W. El-Khattam, K. Bhattacharya, Y. Hegazy, and M. Salama, "Optimal investment planning for distributed generation in a competitive electricity market," *IEEE Transactions on Power Systems*, vol. 19, no. 3, pp. 1674–1684, Aug. 2004.

[67] H. Khodr, Z. Vale, and C. Ramos, "A benders decomposition and fuzzy multicriteria approach for distribution networks remuneration considering dg," *IEEE Transactions on Power Systems*, vol. 24, no. 2, pp. 1091–1101, May 2009.

[68] D. Singh and K. S. Verma, "Multiobjective optimization for dg planning with load models," *IEEE Transactions on Power Systems*, vol. 24, no. 1, pp. 427–436, Feb. 2009.

[69] K.-H. Kim, K.-B. Song, S.-K. Joo, Y.-J. Lee, and J.-O. Kim, "Multiobjective distributed generation placement using fuzzy goal programming with genetic algorithm," *European Transactions on Electrical Power*, vol. 18, no. 3, pp. 217–230, 2008.

[70] R. Jabr and B. Pal, "Ordinal optimisation approach for locating and sizing of distributed generation," *Generation, Transmission and Distribution, IET*, vol. 3, no. 8, pp. 713–723, August 2009.

[71] W. El-Khattam, Y. Hegazy, and M. Salama, "An integrated distributed generation optimization model for distribution system planning," *IEEE Transactions on Power Systems*, vol. 20, no. 2, pp. 1158–1165, May 2005.

[72] A. Alarcon-Rodriguez, E. Haesen, G. Ault, J. Driesen, and R. Belmans2, "Multiobjective planning framework for stochastic and controllable distributed energy resources," *IET Renewable Power Generation*, vol. 3, no. 2, pp. 227–238, June 2009.

[73] A. Zangeneh, S. Jadid, and A. Rahimi-Kian, "Normal boundary intersection and benefit-cost ratio for distributed generation planning," *European Transactions on Electrical Power*, pp. 1430–1440, 2009.

[74] S. Favuzza, G. Graditi, M. Ippolito, and E. Sanseverino, "Optimal electrical distribution systems reinforcement planning using gas micro turbines by dynamic ant colony search algorithm," *IEEE Transactions on Power Systems*, vol. 22, no. 2, pp. 580–587, May 2007.

[75] P. M. Costa and M. A. Matos, "Avoided losses on lv networks as a result of microgeneration," *Electric Power Systems Research*, vol. 79, no. 4, pp. 629 – 634, 2009.

[76] M. Zangiabadi, R. Feuillet, H. Lesani, N. Hadj-Said, and J. T. Kval?y, "Assessing the performance and benefits of customer distributed generation developers under uncertainties," *Energy*, vol. 36, no. 3, pp. 1703 – 1712, 2011.

[77] M. Matos and E. Gouveia, "The fuzzy power flow revisited," *IEEE Transactions on Power Systems*, vol. 23, no. 1, pp. 213–218, Feb. 2008.

[78] E. M. Gouveia and M. A. Matos, "Symmetric ac fuzzy power flow model," *European Journal of Operational Research*, vol. 197, no. 3, pp. 1012 – 1018, 2009.

[79] W. El-Khattam, Y. Hegazy, and M. Salama, "Investigating distributed generation systems performance using monte carlo simulation," *IEEE Transactions on Power Systems*, vol. 21, no. 2, pp. 524–532, May 2006.

[80] K. Zare, M. P. Moghaddam, and M. K. S. E. Eslami, "Demand bidding construction for a large consumer through a hybrid igdt-probability methodology," *Energy*, vol. 35, no. 7, pp. 2999 – 3007, 2010.

[81] C. Kahraman, *Fuzzy Multi-Criteria Decision Making: Theory and Applications with Recent Developments*. Springer, 2008.

[82] K. Deb, *Multi Objective Optimization Using Evolutionary Algorithms*. USA: JOHN WILEY and SONS, 2003.

[83] F. Mendoza, J. Bernal-Agustin, and J. Dominguez-Navarro, "Nsga and spea applied to multiobjective design of power distribution systems," *IEEE Transactions on Power Systems*, vol. 21, no. 4, pp. 1938 –1945, Nov. 2006.

[84] A. Bhattacharya and P. Chattopadhyay, "A modified particle swarm optimization for solving the non-convex economic dispatch," vol. 01, May 2009, pp. 78 –81.

[85] F. Glover and M. Laguna, *Tabu Search*. USA: Springer, 1998.

[86] J. Farmer, N. Packard, and A. Perelson, "The immune system, adaptation and machine learning," *Physica*, vol. D, no. 22, pp. 187–204, October 1986.

[87] J. Dreo, A. Petrowski, P. Siarry, and E. Taillard, *Metaheuristics for Hard Optimization*. Springer, 2003.

[88] F. Dario and M. Claudio, *Bio-Inspired Artificial Intelligence: Theories Methods and Technologies*. The MIT Press, 2008.

[89] L. C. Jain, V. Palade, and D. Srinivasan, *Advances in Evolutionary Computing for System Design*. Springer, 2007.

[90] M. Basu, "Dynamic economic emission dispatch using evolutionary programming and fuzzy satisfying method," *International Journal of Emerging Electric Power Systems*, vol. 8, no. 4, March 2007.

[91] P. Maghouli, S. Hosseini, M. Buygi, and M. Shahidehpour, "A multi-objective framework for transmission expansion planning in deregulated environments," *IEEE Transactions on Power Systems*, vol. 24, no. 2, pp. 1051 –1061, May 2009.

[92] J. Pan and S. Rahman, "Multi-attribute utility analysis with imprecise information: an enhanced decision support technique for the evaluation of electric generation expansion strategies," *Electric Power Systems Research*, vol. 46, no. 2, pp. 101 – 109, 1998.

[93] F. A. Lootsma, *Multi-Criteria Decision Analysis via Ratio and Difference Judgement (Applied Optimization)*. USA: Springer, 1999.

[94] R. Garg, V. Agrawal, and V. Gupta, "Coding, evaluation and selection of thermal power plants - a madm approach," *International Journal of Electrical Power and Energy Systems*, vol. 29, no. 9, pp. 657 – 668, 2007.

[95] L. Xuebin, "Study of multi-objective optimization and multi-attribute decision-making for economic and environmental power dispatch," *Electric Power Systems Research*, vol. 79, no. 5, pp. 789 – 795, 2009.

[96] H. Aalami, M. P. Moghaddam, and G. Yousefi, "Modeling and prioritizing demand response programs in power markets," *Electric Power Systems Research*, vol. 80, no. 4, pp. 426 – 435, 2010.

[97] A. Agalgaonkar, S. Kulkarni, and S. Khaparde, "Evaluation of configuration plans for dgs in developing countries using advanced planning techniques," *IEEE Transactions on Power Systems*, vol. 21, no. 2, pp. 973–981, May 2006.

[98] A. Zangeneh, S. Jadid, and A. Rahimi-Kian, "A hierarchical decision making model for the prioritization of distributed generation technologies: A case study for iran," *Energy Policy*, vol. 37, no. 12, pp. 5752 – 5763, 2009.

[99] M. H. Kalos and P. A. Whitlock, *Monte Carlo Methods*. WILEY-VCH Verlag GmbH and Co. KGaA, 2004.

[100] H. P. Hong, "An efficient point estimate method for probabilistic analysis," *Reliability Engineering and System Safety*, vol. 59, no. 3, pp. 261 – 267, 1998.

[101] J. Morales, S. Pineda, A. Conejo, and M. Carrion, "Scenario reduction for futures market trading in electricity markets," *IEEE Trans. on Power Sys.,*, vol. 24, no. 2, pp. 878 –888, May 2009.

[102] A. J. Conejo, M. Carrion, and J. M. Morales, *Decision Making Under Uncertainty in Electricity Markets*. New York: Springer, 2010.

[103] S. Pineda and A. Conejo, "Scenario reduction for risk-averse electricity trading," *Generation, Transmission Distribution, IET*, vol. 4, no. 6, pp. 694 –705, 2010.

[104] H. Heitsch and W. Ro"misch, "Scenario reduction algorithms in stochastic programming," *Computational Optimization and Applications*, vol. 24, pp. 187–206, 2003.

[105] H. Zhang and D. Liu, Eds., *Fuzzy Modeling and Fuzzy Control*. Birkhuser, 2006.

[106] T. Ross, Ed., *Fuzzy logic with engineering applications*. Wiley, 2004.

[107] A. Soroudi and M. Ehsan, "A possibilistic-probabilistic tool for evaluating the impact of stochastic renewable and controllable power generation on energy losses in distribution networks–a case study," *Renewable and Sustainable Energy Reviews*, vol. 15, no. 1, pp. 794 – 800, 2011.

[108] Y. B. Haim, *Info-Gap Decision Theory (Second Edition)*. California: Academic Press, 2006.

[109] Y. Atwa and E. El-Saadany, "Probabilistic approach for optimal allocation of wind-based distributed generation in distribution systems," *Renewable Power Generation, IET*, vol. 5, no. 1, pp. 79 –88, 2011.

[110] M. Dilek, F. de Leon, R. Broadwater, and S. Lee, "A robust multiphase power flow for general distribution networks," *Power Systems, IEEE Transactions on*, vol. 25, no. 2, pp. 760 –768, may 2010.

[111] W. H. Kersting, *Distribution System Modeling and Analysis, Second Edition (Electric Power Engineering Series)*, 2nd ed. CRC Press, Nov. 2006.

[112] R. Jabr, "Radial distribution load flow using conic programming," *IEEE Transactions on Power Systems*, vol. 21, no. 3, pp. 1458–1459, 2006.

[113] A. Soroudi and M. Ehsan, "A distribution network expansion planning model considering distributed generation options and techo-economical issues," *Energy*, vol. 35, no. 8, pp. 3364 – 3374, 2010.

[114] K. Abdul-Rahman and S. Shahidehpour, "A fuzzy-based optimal reactive power control," *IEEE Transactions on Power Systems*, vol. 8, no. 2, pp. 662–670, May 1993.

[115] P. M. D. O. D. Jesus, "Remuneration of distributed generation: A holistic approach," Ph.D. dissertation, Porto Portugal, 2007.

[116] A. Conejo, J. Fernandez-Gonzalez, and N. Alguacil, "Energy procurement for large consumers in electricity markets," *Generation, Transmission and Distribution, IEE Proceedings-*, vol. 152, no. 3, pp. 357 – 364, may 2005.

[117] EPRI, "Distributed energy resources emissions survey and technology characterization," Electric Power Research Institute, Tech. Rep., Nov 2004.

[118] CBO, "Prospects for distributed electricity generation," congress of the United States congressional budget office, Tech. Rep., Sep 2003.

[119] A. Soroudi, M. Ehsan, and H. Zareipour, "A practical eco-environmental distribution network planning model including fuel cells and non-renewable distributed energy resources," *Renewable Energy*, vol. 36, no. 1, pp. 179 – 188, 2011.

[120] A. Soroudi and M. Ehsan, "Efficient immune-ga method for dnos in sizing and placement of distributed generation units," *European Transactions on Electrical Power*, vol. 21, no. 3, pp. 1361–1375, 2011.

[121] ——, "Multi-objective planning model for integration of distributed generations in deregulated power systems," *Iranian Journal of Science and Technology, Transaction B: Engineering*, vol. 34, no. 3, pp. 307–324, 2010.

[122] A. Kusiak and Z. Zhang, "Short-horizon prediction of wind power: A data-driven approach," *IEEE Transactions on Energy Conversion*, vol. 25, no. 4, pp. 1112 –1122, 2010.

[123] R. Jabr and B. Pal, "Intermittent wind generation in optimal power flow dispatching," *Generation, Transmission Distribution, IET*, vol. 3, no. 1, pp. 66 –74, 2009.

[124] F. Nogales, J. Contreras, A. Conejo, and R. Espinola, "Forecasting next-day electricity prices by time series models," *IEEE Transactions on Power Systems,*, vol. 17, no. 2, pp. 342 –348, May 2002.

[125] A. Conejo, F. Nogales, and J. Arroyo, "Price-taker bidding strategy under price uncertainty," *IEEE Transactions on Power Systems,*, vol. 17, no. 4, pp. 1081 – 1088, Nov. 2002.

[126] J. Morales, L. Baringo, A. Conejo, and R. Minguez, "Probabilistic power flow with correlated wind sources," *Generation, Transmission Distribution, IET*, vol. 4, no. 5, pp. 641 –651, May 2010.

[127] B. Berseneff, "Reglage de la tension dans les reseaux de distribution du futur/ volt var control in future distribution networks," Ph.D. dissertation, Grenoble, France, 2010.

[128] T. MathWorks, http://www.mathworks.com.

[129] N. Sadati, T. Amraee, and A. Ranjbar, "A global particle swarm-based-simulated annealing optimization technique for under-voltage load shedding problem," *Applied Soft Computing*, vol. 9, no. 2, pp. 652 – 657, 2009.

[130] M. AlHajri and M. El-Hawary, "Exploiting the radial distribution structure in developing a fast and flexible radial power flow for unbalanced three-phase networks," *IEEE Transactions on Power Delivery*, vol. 25, no. 1, pp. 378 –389, 2010.

[131] G. Chang, S. Chu, and H. Wang, "An improved backward/forward sweep load flow algorithm for radial distribution systems," *IEEE Transactions on Power Systems,*, vol. 22, no. 2, pp. 882 –884, May 2007.

[132] B. Borkowska, "Probabilistic load flow," *IEEE Transactions on Power Apparatus and Systems,*, vol. PAS-93, no. 3, pp. 752 –759, May 1974.

[133] R. Allan, C. Grigg, D. Newey, and R. Simmons, "Probabilistic power-flow techniques extended and applied to operational decision making," *Electrical Engineers, Proceedings of the Institution of*, vol. 123, no. 12, pp. 1317 –1324, 1976.

[134] R. Allan and M. Al-Shakarchi, "Probabilistic a.c. load flow," *Electrical Engineers, Proceedings of the Institution of*, vol. 123, no. 6, pp. 531 –536, 1976.

[135] A. Leite da Silva and V. Arienti, "Probabilistic load flow by a multilinear simulation algorithm," *Generation, Transmission and Distribution, IEE Proceedings C*, vol. 137, no. 4, pp. 276 –282, Jul. 1990.

[136] A. Schellenberg, W. Rosehart, and J. Aguado, "Cumulant-based probabilistic optimal power flow (p-opf) with gaussian and gamma distributions," *IEEE Transactions on Power Systems,*, vol. 20, no. 2, pp. 773 – 781, May 2005.

[137] A. Tamtum, A. Schellenberg, and W. Rosehart, "Enhancements to the cumulant method for probabilistic optimal power flow studies," *IEEE Transactions on Power Systems,*, vol. 24, no. 4, pp. 1739 –1746, 2009.

[138] P. Zhang and S. Lee, "Probabilistic load flow computation using the method of combined cumulants and gram-charlier expansion," *IEEE Transactions on Power Systems*, vol. 19, no. 1, pp. 676 – 682, 2004.

[139] C. Su, "Stochastic evaluation of voltages in distribution networks with distributed generation using detailed distribution operation models," *IEEE Transactions on Power Systems*, vol. 25, no. 2, pp. 786 –795, may 2010.

[140] J. Morales and J. Perez-Ruiz, "Point estimate schemes to solve the probabilistic power flow," *IEEE Transactions on Power Systems,*, vol. 22, no. 4, pp. 1594 –1601, 2007.

[141] P. Caramia, G. Carpinelli, M. Pagano, and P. Varilone, "Probabilistic three-phase load flow for unbalanced electrical distribution systems with wind farms," *Renewable Power Generation, IET*, vol. 1, no. 2, pp. 115 –122, 2007.

[142] S. Wong, K. Bhattacharya, and J. Fuller, "Electric power distribution system design and planning in a deregulated environment," *Generation, Transmission Distribution, IET*, vol. 3, no. 12, pp. 1061 –1078, december 2009.

[143] J. Usaola, "Probabilistic load flow in systems with wind generation," *Generation, Transmission Distribution, IET*, vol. 3, no. 12, pp. 1031 –1041, 2009.

[144] J. Morales, L. Baringo, A. Conejo, and R. Minguez, "Probabilistic power flow with correlated wind sources," *Generation, Transmission Distribution, IET*, vol. 4, no. 5, pp. 641 –651, May 2010.

[145] Electricite de France (EDF), online: http://www.edf.com, accessed Dec 2010.

[146] E. M. Gouveia and M. A. Matos, "Symmetric ac fuzzy power flow model," *European Journal of Operational Research*, vol. 197, no. 3, pp. 1012 – 1018, 2009.

[147] GAMS, "The general algebraic modeling system," Online, Tech. Rep., Feb 2005.